

INTERNATIONAL JOURNAL
of
COMPUTERS, COMMUNICATIONS & CONTROL

Year: 2006 Volume: I Number: 4

CCC Publications

www.journal.univagora.ro

EDITORIAL ORGANIZATION

Editor-in-Chief

Prof. Florin-Gheorghe Filip, *Member of the Romanian Academy*
Romanian Academy, 125, Calea Victoriei
010071 BUCHAREST-1, Romania, ffilip@acad.ro

Executive Editor

Dr. Ioan Dziţac
AGORA University
idzitac@univagora.ro

Managing Editor

Prof. Mişu-Jan Manolescu
AGORA University
rektorat@univagora.ro

Editorial secretary

Horea Oros
horos@uoradea.ro

Publisher & Editorial Office

CCC Publications, AGORA University
Piata Tineretului 8, Oradea, jud. Bihor, Romania, Zip Code 410526
Tel: +40 259 427 398, Fax: +40 259 434 925, E-mail: ccc@univagora.ro
Website: www.journal.univagora.ro
ISSN 1841-9836 (print version), 1841-9844 (online version)

EDITORIAL BOARD

Prof. Pierre Borne

Ecole Centrale de Lille
Cit  Scientifique-BP 48
Villeneuve d'Ascq Cedex, F 59651, France
p.borne@ec-lille.fr

Prof. Antonio Di Nola

Department of Mathematics and Information Sciences
Universit  degli Studi di Salerno
Salerno, Via Ponte Don Melillo 84084 Fisciano, Italy
dinola@cds.unina.it

Prof. Constantin Gaiandric

Institute of Mathematics of
Moldavian Academy of Sciences
Kishinev, 277028, Academiei 5, Republic of Moldova
gaiandric@math.md

Prof. Kaoru Hirota

Hirota Lab. Dept. C.I. & S.S.
Tokyo Institute of Technology,
G3-49, 4259 Nagatsuta, Midori-ku, 226-8502, Japan
hirota@hrt.dis.titech.ac.jp

Prof. Shimon Y. Nof

School of Industrial Engineering
Purdue University
Grissom Hall, West Lafayette, IN 47907, U.S.A.
nof@purdue.edu

Prof. Mario de J. P rez Jim nez

Dept. of CS and Artificial Intelligence
University of Seville
Sevilla, Avda. Reina Mercedes s/n, 41012, Spain
marper@us.es

Prof. Dr. Petre Dini

Cisco
170 West Tasman Drive
San Jose, CA 95134, USA
pdini@cisco.com

Prof.  mer Egecioglu

Department of Computer Science
University of California
Santa Barbara, CA 93106-5110, U.S.A
omer@cs.ucsb.edu

Prof. Xiao-Shan Gao

Academy of Mathematics and System Sciences
Academia Sinica
Beijing 100080, China
xgao@mmrc.iss.ac.cn

Prof. George Metakides

University of Patras
University Campus
Patras 26 504, Greece
george@metakides.net

Dr. Gheorghe P un

Institute of Mathematics
of the Romanian Academy
Bucharest, PO Box 1-764, 70700, Romania
gpaun@us.es

Prof. Dana Petcu

Computer Science Department
Western University of Timisoara
V.Parvan 4, 300223 Timisoara, Romania
petcu@info.uvt.ro

Prof. Radu Popescu-Zeletin

Fraunhofer Institute for Open Communication Systems
Technical University Berlin
Germany
rpz@cs.tu-berlin.de

Prof. Athanasios D. Styliadis

Alexander Institute of Technology
Thessaloniki
Agiou Panteleimona 24, 551 33, Thessaloniki, Greece
styl@it.teithe.gr

Prof. Horia-Nicolai Teodorescu

Faculty of Electronics and Telecommunications
Technical University "Gh. Asachi" Iasi
Iasi, Bd. Carol I 11, 700506, Romania
hteodor@etc.tuiasi.ro

Prof. Imre J. Rudas

Institute of Intelligent Engineering Systems
Budapest Tech
Budapest, Bécsi út 96/B, H-1034, Hungary
rudas@bmf.hu

Dr. Gheorghe Tecuci

Center for Artificial Intelligence
George Mason University
University Drive 4440, VA 22030-4444, U.S.A.
tecuci@gmu.edu

Dr. Dan Tufiş

Research Institute for Artificial Intelligence
of the Romanian Academy
Bucharest, "13 Septembrie" 13, 050711, Romania
tufis@racai.ro

CCC Publications, powered by AGORA University Publishing House, currently publishes the "International Journal of Computers, Communications & Control" and its scope is to publish scientific literature (journals, books, monographs and conference proceedings) in the field of Computers, Communications and Control.

Copyright © 2006 by CCC Publications

Contents - Special issue on CESA

Preface	
By Pierre Borne	7
New Discrete Tanaka Sugeno Kang Fuzzy Systems Characterization and Stability Domain	
By Mohamed Benrejeb, Dhaou Soudani, Anis Sakly, Pierre Borne	9
On Guaranteed Global Exponential Stability Of Polynomial Singularly Perturbed Control Systems	
By Hajer Bouzaouache, Naceur Benhadj Braiek	21
Numerical Aspects and Performances of Trajectory Planning Methods of Flexible Axes	
By Jean-Yves Dieulot, Issam Thimoumi, Frédéric Colas, Richard Béarée	35
The Fast Fourier and Hilbert-Huang Transforms: A Comparison	
By Denis Donnelly	45
An Iterative Method for the Design Process of Mode Handling Model	
By Nadia Hamani, Nathalie Dangoumau, Etienne Craye	53
Time Disturbances and Filtering of Sensors Signals in Tolerant Multi-product Job-shops with Time Constraints	
By Nabil Jerbi, Simon Collart Dutilleul, Etienne Craye, Mohamed Benrejeb	61
Switching LPV Controllers for a Variable Speed Pitch Regulated Wind Turbine	
By Fabien Lescher, Jing-Yun Zhao, Pierre Borne	73
Realization of Embedded Multimedia System Based On Dual-Core Processor OMAP5910	
By Peng Li, Yu Lu, Shen Li, Hongxing Wei	85
Obstacle Detection in Cluttered Traffic Environment Based on Candidate Generation and Classification	
By Qing Li, F.C. Sun	93
Computation on the Optimal Control of Networked Control Systems with Multiple Switching Modes Over High Speed Local Area Networks	
By Gang Zheng, Wenli Zeng, Fanjiang Xu	101
Ant Colony with Dynamic Local Search for the Time Scheduling of Transport Networks	
By Salah Zidi, Salah Maouche, Slim Hammadi	110

**Generic Modeling and Configuration Management in
Product Lifecycle Management**

By Souheil Zina, Muriel Lombard, Luc Lossent, Charles Henriot

126

Author index

139

Preface

Over the last decades, it has become a strong need for exchange on common computational and algorithmic tools between researchers working in different application backgrounds. Under this situation, the first CESA conference (CESA96) was successfully held in Lille, France in July 1996.

The Multiconference on “Computational Engineering in Systems Applications” (CESA2006), was co-sponsored by IMACS (the International Association for Mathematics and Computers in Simulation) and IEEE Systems Man and Cybernetics (IEEE/SMC) Society, and has been held on 4-6 October 2006 in Beijing, China. Its aim was to bring together scholars and practitioners from academia and industries to exchange the latest development in theories, and applications of computational techniques. This Conference was co-chaired by Professor Pierre Borne (Ecole Centrale de Lille, France) and Professor Bo Zhang (Tsinghua University, China). In addition to the plenary lectures presented by Professor James M. Tien (Rensselaer Polytechnic Institute, USA), Professor Tianyou Chai (Northeastern University, China), Professor Florin G. Filip (Vice President of the Romanian Academy), Professor Jianwei Zhang (University of Hamburg, Germany) and Professor Toshio Fukuda (Nagoya University, Japan), 388 communications have been selected and accepted for presentation.

The papers presented in this special issue correspond to enlarged and improved papers which have been selected among the best communications presented during the conference.

Guest editor
Professor Pierre Borne
Chairman of CESA2006

Ecole Centrale de Lille, Cité scientifique
Laboratoire d'Automatique, Génie Informatique et Signal
BP 48, 59651 Villeneuve d'Ascq Cedex, France
E-mail: pierre.borne@ec-lille.fr

New Discrete Tanaka Sugeno Kang Fuzzy Systems Characterization and Stability Domain

Mohamed Benrejeb, Dhaou Soudani, Anis Sakly, Pierre Borne

Abstract: In this paper, an analytical approach to characterize discrete Tanaka Sugeno Kang (TSK) fuzzy systems is presented. This characterization concerns the choice of the adequate conjunctive operator between input variables of discrete TSK fuzzy models, t-norm, and its impact on stability domain estimation. This new approach is based on stability conditions issued from vector norms corresponding to a vector-Lyapunov function. In particular, second order discrete TSK models are considered and this work concludes that Zadeh's t-norm, logic product min, gives the largest estimation of stability domain.

Keywords: Discrete nonlinear systems, discrete TSK fuzzy model, t-norm, stability domain, vector norm, arrow form matrix.

1 Introduction

Fuzzy control of systems presents a major interest in several applications including industrial ones. However, closed loop system properties are not easily understood and the design of the fuzzy system is generally based on intuitive approaches.

Different fuzzy control strategies exist. In particular, TSK fuzzy approach permits the description and the control of a system by defining different models related via a rule base.

The stability of TSK systems has been one of the central issues and is subject of many works either in the continuous case or in the discrete one. To do this, different approaches are considered mainly based on Lyapunov functions [5, 10, 12]. In particular, the Linear Matrix Inequality (LMI) formulation is used [11] and, according to the considered system, permits the stability problem resolution. In our previous work [1], the used approach is led through the convergence of a regular vector norm [3]. The vector norm approach, based on the comparison and overevaluating principle, has a major advantage that it deals with a very large class of systems, since no restrictive assumption is made on the matrices of state equations. So, in [1], the approach estimates the stability domain of continuous TSK fuzzy systems and its dependence on the choice of the conjunctive operator between inputs.

In this way, many authors have presented and analyzed several of these operators defined by t-norms and so said t-operators [4, 6, 7]. In particular, in [6], six t-norms are used to represent this connective operator in the inverse pendulum control. In another work [9], are used the same t-norms to study their impact on fuzzy control performances of a second order process by defining a performance criterion based on error measurement of the closed loop system. However, then exist other operators to represent this connective such as mean operators developed in [14].

Except [1], all these studies don't treat the influence of the choice of the conjunctive operator between inputs on the stability conditions obtained and often only *prod* or *min* operators are used without theoretical argumentation and just for simplification reasons.

Therefore, in this way the study will be considered and constitutes a generalization of [1] in the discrete case seeing the soft implementation nature of this control strategy.

By exploiting conditions or hypothesis obtained from stability analysis of discrete TSK fuzzy systems based on vector norms approach, the influence of the choice of t-norm is studied. Similarly to [1], only second order TSK fuzzy models are considered for simplification reason.

In the next section, is presented the structure of discrete TSK fuzzy models. In section 3, several definitions dealing with t-norm notion as well as its properties are given. In section 4, sufficient stability conditions of these TSK systems based on vector norms approach are presented. Then, the study of the

impact of the choice of t-norm on the proposed stability conditions will be considered in section 5. In particular, second order TSK fuzzy models are considered. A DC motor is studied in section 6 as an application example validating this study. Finally, some concluding remarks are pointed out.

2 TSK discrete models description

An r -order TSK discrete fuzzy model of an n -order nonlinear system to be controlled is given by a rule base where the i^{th} rule is in the form:

$$R_i : \text{IF } x_1 \text{ is } G_1^i \text{ AND } x_2 \text{ is } G_2^i \text{ AND } \dots \text{ AND } x_n \text{ is } G_n^i \\ \text{THEN } \begin{cases} x(k+1) = A_i x(k) + B_i u(k) \\ y(k) = C_i x(k) \end{cases} \quad i = 1, 2, \dots, r \quad (1)$$

where G_j^i , $j=1,2,\dots,n$, is the i^{th} fuzzy set of the state vector x_j .

The state vector $x \in \mathfrak{R}^n$, the control input $u \in \mathfrak{R}$ and the matrices A_i , B_i and C_i are of appropriate dimensions.

According to the Parallel Distributed Compensation (PDC) concept [13], the rule base R'_i of the fuzzy controller stabilizing the former system is in the form:

$$R'_i : \text{IF } x_1 \text{ is } G_1^i \text{ AND } x_2 \text{ is } G_2^i \text{ AND } \dots \text{ AND } x_n \text{ is } G_n^i \\ \text{THEN } u(k) = -K_i x(k) \quad i = 1, 2, \dots, r \quad (2)$$

with $K_i = [k_i^1, k_i^2, \dots, k_i^n]$.

By substituting u in the equation (1) above, it comes:

$$x(k+1) = \sum_{i=1}^r \sum_{j=1}^r h_i h_j (A_i - B_i K_j) x(k) \quad (3)$$

with:

$$h_i = w_i / \sum_{i=1}^r w_i \quad (4)$$

$$w_i = T(G_1^i(x_1), G_2^i(x_2), \dots, G_n^i(x_n)) \quad (5)$$

and T a t-norm.

When linear models of the system to be controlled are considered in the controllable form given by:

$$A_i = \begin{bmatrix} 0 & 1 & \dots & 0 \\ \vdots & \ddots & \ddots & \vdots \\ 0 & \dots & 0 & 1 \\ -a_i^1 & \dots & -a_i^{n-1} & -a_i^n \end{bmatrix} \quad \text{and } B_i = B = \begin{bmatrix} 0 \\ \vdots \\ 0 \\ 1 \end{bmatrix} \quad (6)$$

relation (3) becomes:

$$\begin{aligned} x(k+1) &= \sum_{i=1}^r \sum_{j=1}^r h_i h_j (A_i - B_i K_j) x(k) \\ &= \sum_{i=1}^r \sum_{j=1}^r h_i h_j (A_i - B K_j) x(k) \\ &= \sum_{i=1}^r \sum_{j=1}^r h_i h_j A_i x(k) - \sum_{i=1}^r \sum_{j=1}^r h_i h_j B K_j x(k) \\ &= \sum_{i=1}^r h_i \sum_{j=1}^r h_j A_i x(k) - \sum_{j=1}^r h_j \sum_{i=1}^r h_i B K_j x(k) \\ &= \sum_{i=1}^r h_i A_i x(k) - \sum_{j=1}^r h_j B K_j x(k) \end{aligned}$$

then finally:

$$x(k+1) = \sum_{i=1}^r h_i(A_i - BK_i)x(k) \tag{7}$$

3 T-norms

An important task to be performed in the design of TSK fuzzy systems is the choice of the conjunctive operator materializing the connective *AND* between input variables in the rule base and so corresponding to the intersection operation between fuzzy subsets relatively to different inputs.

Often, this operator is defined by a t-norm T , whose definition and proprieties are presented as follows.

Definition 1. A triangular norm (t-norm) is a function $T:[0,1] \times [0,1] \rightarrow [0,1]$ verifying for every u, v, w and t of $[0,1]$:

- i) $T(u,v) = T(v,u)$ (commutativity)
 - ii) $T(u,T(v,w)) = T(T(u,v),w)$ (associativity)
 - iii) $T(u,v) \leq T(w,t)$ si $u \leq w$ et $v \leq t$ (monotonicity)
 - iv) $T(u, 1) = u$ (oneidentity)
- (8)

min operator is the largest of all possible t-norms, $T(u,v) \leq \min(u,v)$.

The intersection operation between fuzzy subsets is defined by a t-norm T such as:

$$C = A \cap B, \text{ then } \forall x \in X \mu_C(x) = T(\mu_A(x), \mu_B(x)) \tag{9}$$

The commonly encountered t-norms are given in table 1.

Table 1: Main t-norms

t-norm	Name
$\min(u, v)$	Zadeh (logical operators)
uv	Bandler (probabilistic operators)
$\max(u + v - 1, 0)$	Lukasiewicz (bounded operators)
$\begin{cases} u & \text{if } v = 1 \\ v & \text{if } u = 1 \\ 0 & \text{otherwise} \end{cases}$	Weber (drastic operators)

Definition 2. A t-norm T is said archimedean if and only if $T(u, v)$ is continuous and $T(u, u) < u$ for each u of $]0,1[$. Moreover, T is said strict archimedean if and only if $T(u, v) < T(w, t)$ as soon as $u < w$ and $v < t$.

Any function $T:[0,1] \times [0,1] \rightarrow [0,1]$ is an archimedean t-norm if and only if it exists a continuous decreasing function $f: [0,1] \rightarrow [0, +\infty[$ such that $f(1)=0$ satisfying :

$$T(u,v) = f^{-1*}(f(u) + f(v)) \tag{10}$$

where f^{-1*} is the pseudo-inverse of f such as $f^{-1*} = \begin{cases} f^{-1}(w) & \text{if } w \in [0, f(0)[\\ 0 & \text{if } w \in [f(0), +\infty[\end{cases}$.

Besides, T is strict if and only if $f(0) = +\infty$.
 f is said the additive generator of the t-norm T .

The additive generators associated to main parameterized archimedean t-norms are presented in table 2 [14].

Table 2: Main parametrized t-norms and their additive generators

t-norm	Generator $f(u)$	Parameter	Name
$\frac{uv}{\gamma + (1-\gamma)(u+v-uv)}$	$\frac{1}{\gamma} \text{Log} \left[\frac{\gamma + (1-\gamma)u}{u} \right]$ Strict Archimedean	$\gamma > 0$	Hamacher
$\frac{1}{\left[\left(\frac{1}{u}\right)^p + \left(\frac{1}{v}\right)^p - 1 \right]^{\frac{1}{p}}}$	$\frac{1}{(1+u)^{\frac{1}{p}}}$ Strict Archimedean	$p > 0$	Schweizer & Sklar
$\frac{1}{1 + \left[\left(\frac{1}{u} - 1\right)^\lambda + \left(\frac{1}{v} - 1\right)^\lambda \right]^{\frac{1}{\lambda}}}$	$\frac{1}{1 + u^{\frac{1}{\lambda}}}$ Strict Archimedean	$\lambda > 0$	Dombi
$1 - \min \left[1, \left((1-u)^\omega + (1-v)^\omega \right)^{\frac{1}{\omega}} \right]$	$(1-u)^\omega$ Archimedean no strict	$\omega > 0$	Yager
$\frac{uv}{\max(u,v,\alpha)}$	No archimedean	$\alpha \in [0,1]$	Dubois & Prade

4 New stability conditions

In [2], a change of base of (6) under the arrow form give:

$$x(k+1) = \sum_{i=1}^r h_i M_i x(k) \quad (11)$$

where M_i is a matrix in the arrow form and P is the corresponding passage matrix:

$$M_i = P^{-1}(A_i - BK_i)P \quad (12)$$

$$M_i = \begin{bmatrix} \alpha_1 & 0 & \cdots & 0 & \beta_1 \\ 0 & \ddots & \ddots & \vdots & \vdots \\ \vdots & \ddots & \ddots & 0 & \vdots \\ 0 & \cdots & 0 & \alpha_{n-1} & \beta_{n-1} \\ \gamma_i^1 & \cdots & \cdots & \gamma_i^{n-1} & \gamma_i^n \end{bmatrix} \text{ and } P = \begin{bmatrix} 1 & 1 & \cdots & 1 & 0 \\ \alpha_1 & \alpha_2 & \cdots & \alpha_{n-1} & 0 \\ \alpha_1^2 & \alpha_2^2 & \cdots & \alpha_{n-1}^2 & \vdots \\ \vdots & \vdots & \cdots & \vdots & 0 \\ \alpha_1^{n-1} & \alpha_2^{n-1} & \cdots & \alpha_{n-1}^{n-1} & 1 \end{bmatrix} \quad (13)$$

with:

$$\begin{aligned} \beta_j &= \prod_{\substack{q=1 \\ q \neq j}}^{n-1} (\alpha_j - \alpha_q)^{-1} \quad \forall j = 1, 2, \dots, n-1 \\ \left\{ \begin{array}{l} \gamma_i^j = -P_i(\alpha_j) \quad \forall j = 1, 2, \dots, n-1 \\ P_i(\lambda) = \lambda^n + \sum_{q=0}^{n-1} (a_i^{q+1} + k_i^{q+1}) \lambda^q \\ \gamma_i^n = -(a_i^n + k_i^n) - \sum_{j=1}^{n-1} \alpha_j \end{array} \right. \quad (14) \end{aligned}$$

The application of the classical Borne-Gentina criterion [3] leads to the following theorem.

Theorem 3. *The discrete system described by (7) is asymptotically stable if there exist $0 < \alpha_j < 1$, $\alpha_j \neq \alpha_k$, $\forall j \neq k$, such as $\forall x \in S$:*

$$\begin{aligned} \text{i)} \quad & 1 - |\alpha_j| > 0 \quad \forall j = 1, 2, \dots, n-1 \\ \text{ii)} \quad & 1 - \left| \sum_{i=1}^r h_i \gamma_i^n \right| - \sum_{j=1}^{n-1} \left| \sum_{i=1}^r h_i \gamma_i^j \beta_j \right| (1 - |\alpha_j|)^{-1} > 0 \end{aligned} \quad (15)$$

If $S = \mathfrak{R}^n$, the stability is global.

Furthermore, if there exist $\alpha_j, j = 1, 2, \dots, n-1$, such as :

$$\begin{aligned} \text{i)} \quad & 0 < \alpha_j < 1 \quad j = 1, 2, \dots, n-1 \\ \text{ii)} \quad & \sum_{i=1}^r h_i \gamma_i^n > 0 \\ \text{iii)} \quad & \sum_{i=1}^r h_i \gamma_i^j \beta_j > 0 \quad j = 1, 2, \dots, n-1 \end{aligned} \quad (16)$$

then the previous theorem can be simplified to the following corollary.

Corollary 4. *The discrete system described by (7) is asymptotically stable if there exist $0 < \alpha_j < 1$, $\alpha_j \neq \alpha_k$, $\forall j \neq k$, such as $\forall x \in S$:*

$$BPH < 0 \quad (17)$$

where matrices $B \in \mathfrak{R}^{n \times n}$, $P \in \mathfrak{R}^{n \times r}$ and $H \in \mathfrak{R}^{r \times 1}$ are such as :

$$B = \begin{bmatrix} \beta_1 & 0 & \cdots & 0 \\ 0 & \ddots & \ddots & \vdots \\ \vdots & \cdots & \beta_{n-1} & 0 \\ 0 & \cdots & 0 & -1 \end{bmatrix}, P = \begin{bmatrix} P_1(\alpha_1) & \cdots & P_r(\alpha_1) \\ \vdots & \cdots & \vdots \\ P_1(\alpha_{n-1}) & \cdots & P_r(\alpha_{n-1}) \\ P_1(1) & \cdots & P_r(1) \end{bmatrix} \text{ and } H = \begin{bmatrix} h_1 \\ \vdots \\ h_r \end{bmatrix} \quad (18)$$

If $S = \mathfrak{R}^n$, the stability is global.

According to the choice of the coefficients α_j , different conditions on the parameters h_i can be obtained.

5 T-norm influence on the proposed stability conditions

Let us consider the following classical fuzzy partition of a second order TSK model given by figure 1, with:

$$\mu_i = G_i^1(x_i) \quad i = 1, 2, \dots, n \quad (19)$$

and:

$$G_i^1(x_i) = \min(1, \max(0, \frac{L_i - x_i}{2L_i})) \text{ and } G_i^2(x_i) = 1 - G_i^1(x_i) \quad (20)$$

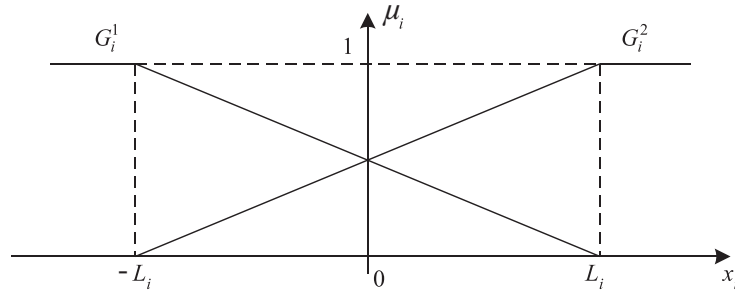


Figure 1: Fuzzy partition of state variables for $r=2$

Then, the whole fuzzy state space considered is the open subset $\Omega =]-L_1, L_1[\times]-L_2, L_2[\times \dots \times]-L_n, L_n[$. So, the notion of global stability, whenever used in the literature on fuzzy control, refers to local stability within a such domain [8].

For second order TSK model, i.e. $r=2$, then $h_2 = 1 - h_1$ and:

$$h_1 = \frac{w_1}{w_1 + w_2} = \frac{T(\mu_1, \mu_2, \dots, \mu_n)}{T(\mu_1, \mu_2, \dots, \mu_n) + T(1 - \mu_1, 1 - \mu_2, \dots, 1 - \mu_n)} \quad (21)$$

where T is a t-norm. **Propositions** [1]

1. Let $\mu_1, \mu_2, \dots, \mu_n$ and $\mu_{max} \in [0, 1]$ such as $\mu_1 \leq \mu_{max}, \mu_2 \leq \mu_{max}, \dots,$ and $\mu_n \leq \mu_{max}$.

Then, we obtain:

$$h_1(\mu_1, \mu_2, \dots, \mu_n) \leq h_1(\mu_{max}, \mu_{max}, \dots, \mu_{max}) \quad (22)$$

This proposition allows the determination of the domain S by its characteristic point M in figure 2.

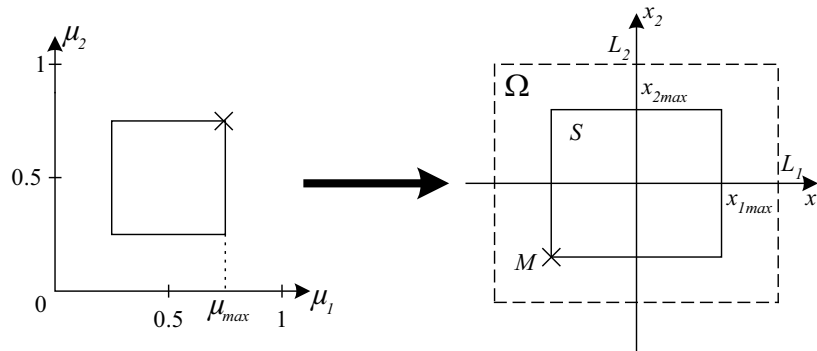


Figure 2: Correspondence between the state space variables domain and the membership values domain

2. Let us note $\varphi_n(\mu) = T(\mu_1, \mu_2, \dots, \mu_n)$ when $\mu_1 = \mu_2 = \dots = \mu_n = \mu$. φ_n is an increasing function on $[0, 1]$ with $\varphi_n(0) = 0$ and $\varphi_n(1) = 1$.

If the following conditions are satisfied :

- i) φ_n is continuous
 - ii) $\forall \mu > 0, \varphi_n(\mu) \neq 0$
 - iii) $\forall \mu_1, \mu_2 \in]0, 1]$ with $\mu_2 > \mu_1, \frac{\varphi_n(\mu_2)}{\mu_2} \geq \frac{\varphi_n(\mu_1)}{\mu_1}$
- (23)

then we have:

$$\begin{cases} h_1(\mu, \mu, \dots, \mu) \geq \mu & \text{if } \mu \geq 0.5 \\ h_1(\mu, \mu, \dots, \mu) \leq \mu & \text{if } \mu \leq 0.5 \end{cases} \quad (24)$$

This proposition means that for a given μ , the smallest coefficient h_1 is obtained with the t-norm of Zadeh, the logic product *min*; and so for the condition (22) we obtain the largest rectangular form domain S with this t-norm by taking $\mu_{max} = c$.

3. Conditions (23) of the proposition 2 are satisfied for each strict archimedean t-norm such as $\varphi_n(\mu)$ is derivable on $]0, 1]$.

The proposed approach is illustrated by considering the following parameterized t-norms:

- the Hamacher one: $T(\mu_1, \mu_2) = \frac{\mu_1 \mu_2}{\gamma + (1-\gamma)(\mu_1 + \mu_2 - \mu_1 \mu_2)}$ for $\gamma > 0$,
- the Yager one: $T(\mu_1, \mu_2) = 1 - \min(1, ((1 - \mu_1)^\omega + (1 - \mu_2)^\omega)^{\frac{1}{\omega}})$ for $\omega > 0$,
- and the Dubois one: $T(\mu_1, \mu_2) = \frac{\mu_1 \mu_2}{\max(\mu_1, \mu_2, \alpha)}$ for $\alpha \in [0, 1]$.

6 Application example

As an example, let consider in figure 3 the case of a DC motor with two linear models $G_1(p)$ and $G_2(p)$ with $\delta_1 = 0.5$ and $\delta_2 = 1$.

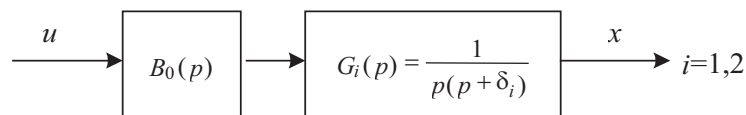


Figure 3: DC motor discrete models

$B_0(p) = \frac{1 - e^{-T_e p}}{p}$ is a zero order holder and $T_e = 0.2s$ is the sampling time.

The discrete models of the DC motor are given by the following z-transmittances:

$$G_i(z) = \frac{N_i(z)}{(z-1)(z-\psi_i)} \quad i = 1, 2$$

with $\psi_i = e^{-\delta_i T_e}$ and $N_i(z) = \frac{\delta_i T_e + e^{-\delta_i T_e} - 1}{\delta_i^2} z + \frac{1 - e^{-\delta_i T_e} (1 + \delta_i T_e)}{\delta_i^2}$.

The two discrete DC linear models are considered in the following controllable form:

$$A_1 = \begin{bmatrix} 0 & 1 \\ -0.905 & 1.905 \end{bmatrix}, \quad A_2 = \begin{bmatrix} 0 & 1 \\ -0.819 & 1.819 \end{bmatrix} \quad \text{and} \quad B = \begin{bmatrix} 0 \\ 1 \end{bmatrix}$$

We suppose that for particular constraints the choice of K_i is imposed such that the pole placement is different for the two models by taking:

$$K_1 = \begin{bmatrix} -0.7 & 1.2 \end{bmatrix} \text{ and } K_2 = \begin{bmatrix} -1.1 & 1.2 \end{bmatrix}$$

According to [3], the minimal overvaluing matrix relatively to the regular vector norm p :

$$p(x) = [|x_1|, |x_2|]^T$$

is such as:

$$M(\cdot) = \begin{bmatrix} |\alpha| & 1 \\ |\gamma_1| & |\gamma_2| \end{bmatrix}$$

with

$$\begin{aligned} \gamma_1 &= (0.486 - 0.086\alpha)h_1 + \alpha^2 - 0.619\alpha - 0.281 \\ \gamma_2 &= 0.086h_1 + 0.619 - \alpha \end{aligned}$$

Then, stability conditions deduced from the corollary are:

- i) $0 < \alpha < 1$
- ii) $0.086h_1 + 0.619 - \alpha > 0$
- iii) $(0.486 - 0.086\alpha)h_1 + \alpha^2 - 0.619\alpha - 0.281 < 0$
- iv) $0.4h_1 + 0.1 > 0$

When i) is satisfied, relations ii) and iv) are too. Then condition iii) leads to the following inequality

$$h_1 < -\frac{\alpha^2 - 0.619\alpha - 0.281}{0.486 - 0.086\alpha} = c$$

When $0.5 < c < 1$, let S a neighborhood of the equilibrium point 0, included in Ω , $\Omega =]-1, 1[\times]-1, 1[$, that verifies a such condition. S is an overvaluing domain of the fuzzy system and an estimation of a symmetrical domain S with respect to 0 imposes:

$$1 - c < h_1 < c.$$

Now, consider the study of the impact of the t-norm T on the width of the neighborhood S of the equilibrium point 0, and then the determination of the largest stability domain D included in S verifying the previous condition.

For $\alpha = 0.345$, we obtain the maximal value of c , $c=0.82$. Thus, the overvaluing matrix $M(\cdot)$ is constant:

$$M(\cdot) = M = \begin{bmatrix} \alpha & 1 \\ 0 & \alpha \end{bmatrix}$$

which is triangular and not irreducible. However, for $c = 0.80$, this irreducibility is skirted and for $\alpha = 0.345$, its comes the following overvaluing matrix

$$M = \begin{bmatrix} 0.345 & 1 \\ 0.01 & 0.343 \end{bmatrix}$$

which is irreducible, whose principal eigenvalue is $\lambda_m = 0.446$, the corresponding vector is:

$$u_m = [9.88 \ 1]^T$$

and the largest estimated stability domain D is such as

$$D = \{x \in S / p^T(x)u_m = 9.88|x_1| + |x_2| \leq x_{\max}\}$$

where S is the square form domain and x_{\max} is its width. S depends on the condition $h_1 < c$ with $c = 0.8$ and so on the t-norm T .

Table 3: μ_{max} and x_{max} corresponding to different t-norms

t-norm	μ_{max}	x_{max}
Zadeh	0.80	0.60
Bandler	0.67	0.34
Hamacher ($\gamma = 0$)	0.75	0.50
Hamacher ($\gamma = \infty$)	0.58	0.16
Yager ($\omega = 2$)	0.62	0.24
Dubois ($\alpha = 0.5$)	0.70	0.40

For $n = 2$, table 3 gives μ_{max} , corresponding to the membership values domain, and x_{max} , corresponding to the square form domain S , with respect to different t-norms.

The results obtained in table 3 shows that for $n = 2$, the greatest value of μ_{max} and so the largest domain S is obtained specifically for the logic product *min*.

Figure 4 presents an estimation of the largest stability domain D respectively for Zadeh and Bandler t-norms.

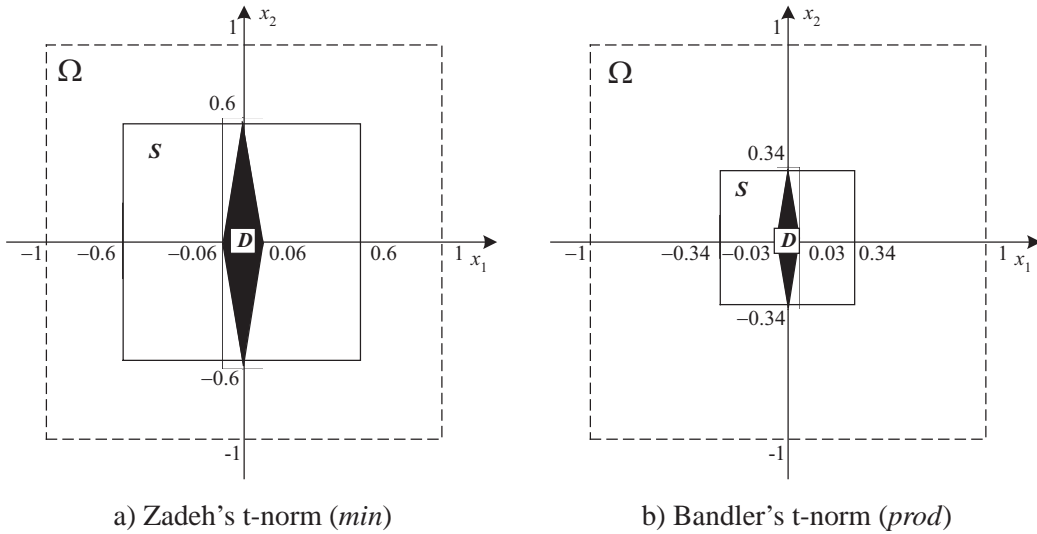


Figure 4: Stability domains obtained for two different t-norms

7 Conclusion

In this paper, we are interested in the stability study of discrete TSK fuzzy systems and the correspondent domain estimation relatively to the used conjunctive operator, materialized by a t-norm. The stability approach is based on vector norms. When second order TSK models are considered, a mathematical study permits to conclude that Zadeh's t-norm, *min* operator, yields to the largest stability domain. A DC motor with two discrete models is considered as an illustrative example and the estimated stability domains for different t-norms confirm the former result.

However, it suits to remark that this study can be generalized for r -order TSK models, in the two

cases continuous and discrete, with r greater than 2 and then we must distinguish between the two cases, r odd or even. For two cases, the stability study can be led in different symmetrical rectangular zones surrounding the equilibrium point, from the smallest to the largest.

References

- [1] Benrejeb M., Sakly A., Ben Othman K. and Borne P.: Choice of Conjunctive Operator of TSK Fuzzy Systems and Stability Domain Study. To appear in MATCOM (MATHematics and COMputers and simulation Journal).
- [2] Benrejeb M., Borne P. and Laurent F. : Sur une application de la représentation en flèche à l'analyse des processus. RAIRO Automatique, 16 (2). (1982) 133-146.
- [3] Borne P., Richard J. P. and Radhy N. E. : Stabilité, stabilisation, régulation : approche par les normes vectorielles, Systèmes non linéaires, tome 2 : stabilité-stabilisation. coordonné par Fossard A. J. et Normand-Cyrot D., Responsable du tome : Borne P., 45-90. Editions Masson, Paris (1993).
- [4] Butkiewicz B.S. : Control Error of Fuzzy System with Different Reasoning and Defuzzification Methods. 7th International Fuzzy Systems Association World Congress (IFSA) , III. Praga, Czech (1997).
- [5] Cao S. G., Rees N. W. and Feng G. : Quadratic stability analysis and design of continuous-time fuzzy control systems. Int. J. Syst. Sci., 27(2). (1996) 193-203.
- [6] Cardenas E., Castillo J.C., Cordon O., Herrera F. and Peregrin A. : Applicability of T-norms in Fuzzy Control. Busefal, 61. (1995) 28-37.
- [7] Gupta M.M. and Qi J. : Design of Fuzzy Logic Controllers Based on Generalized T-operators. Fuzzy Sets and Systems, 40. (1991) 473-489.
- [8] Palm R., Driankov D. and Hellendoorn H. : Model Based Fuzzy Control. Springer-Verlag, Berlin Heidelberg (1997).
- [9] Sakly A., Ben Othman K. and Benrejeb M. : Sur le Choix de l'Opérateur de Conjonction en Commande Floue Basé sur la Robustesse de Critères de Performances. 2^{ème} Conférence Internationale JTEA, Tome 1, Sousse Nord (2002).
- [10] Sugeno M. : On stability of fuzzy systems expressed by fuzzy rules with singleton consequences. IEEE Transactions on Fuzzy Systems, 7(2). (1999) 201-223.
- [11] Tanaka K., Ikeda T. and Wang H.O. : Fuzzy Regulators and Fuzzy Observers : Relaxed Stability Conditions and LMI-based Designs. IEEE Transactions on Fuzzy Systems, 6(2). (1998) 1-16.
- [12] Tanaka K. and Sugeno M. : Stability analysis and design of fuzzy control systems. Fuzzy sets and systems, 45. (1992) 135-156.
- [13] Tanaka K. and Sano M. : A Robust Stabilization Problem of Fuzzy Control Systems and its Application to Backing up Control of a Truck-Trailer. IEEE Transactions on Fuzzy Systems, II. (1994) 119-134.
- [14] Yager R. R. and Filev D. P. : Essentials of Fuzzy Modeling and Control. John Wiley & Sons, Inc., USA (1994).

Mohamed BENREJEB¹, Dhaou SOUDANI¹, Anis SAKLY¹, Pierre BORNE²

¹Ecole Nationale d'Ingénieurs de Tunis
Unité de Recherche LARA-Automatique
BP 37, Le Belvédère, 1002 Tunis, Tunisie

²Ecole Centrale de Lille, Cité scientifique
Laboratoire d'Automatique, Génie Informatique et Signal
BP 48, 59651 Villeneuve d'Ascq Cedex, France

E-mail: mohamed.benrejeb@enit.rnu.tn, dhaou.soudani@enit.rnu.tn,
sakly_anis@yahoo.fr, pierre.borne@ec-lille.fr

Received: November 10, 2006

On Guaranteed Global Exponential Stability Of Polynomial Singularly Perturbed Control Systems

Hajer Bouzaouache, Naceur Benhadj Braiek

Abstract: The problem of global exponential stability for a class of nonlinear singularly perturbed systems is examined in this paper. The stability analysis is based on the use of basic results of integral manifold of nonlinear singularly perturbed systems, the composite Lyapunov method and the notations and properties of Tensoriel algebra. Some of the derived results are presented as linear matrix inequalities (LMIs) feasibility tests. Moreover, we pointed out that if the global exponential stability of the reduced order subsystem is established this is equivalent to guarantee the global exponential stability of the original high order closed loop system. An upper bound ε_1 of the small parameter ε , can also be determined up to which established stability conditions via LMI's are maintained verified. A numerical example is given to illustrate the proposed approach.

Keywords: Nonlinear singularly perturbed system, Integral manifold, Lyapunov stability, Kronecker product, Linear matrix inequalities (LMIs).

1 Introduction

Stability analysis and control of nonlinear singularly perturbed systems have been widely studied in the literature [2], [6], [7], [12], [13]. In a two time scale framework, the stability study of the controlled systems using the Lyapunov stability method [15] and the integral manifold approach as a means for the control of nonlinear systems based on the singular perturbation method have been developed in recent years [10], [11], [14], [16], [17]. The approaches proposed in this direction, differ by imposing different conditions on the smoothness properties of the used functions, different assumptions and different classes of Lyapunov functions.

In this paper, we are concerned with the global exponential stability of polynomial singularly perturbed systems when the chosen design manifold is an exact integral one. Further extension of some previous results [11], [17] are suggested and leads to effective global exponential stability conditions via LMIs [8] which can be easily verified when using LMI toolbox of Matlab.

The contribution of the present paper is based, on one hand, on the use of the Lyapunov method which is a powerful tool for combined controller design and stability analysis, the definition of appropriate Lyapunov functions for the reduced systems and the corrected system via the integral manifold approach and on the other hand, on the notations and properties of the tensoriel product [9].

Our paper is organized as follows: in section 2 we present the considered description of the studied systems which allows important algebraic manipulations and some results from the literature on integral manifolds for nonlinear singularly perturbed systems. Some useful notations and needed assumptions are introduced in section 3. Exploiting the stability statements about singularly perturbed systems possessing integral manifolds and using the composite Lyapunov technique, we propose in section 4 an appropriate control law that insures the existence of an attractive integral manifold and furthermore insures stability of the studied systems when the dynamics are restrictive to the integral manifold. The stability results proving the global exponential stability of polynomial singularly perturbed systems are also given and presented as linear matrix inequalities feasibility tests. Finally an illustrative example is treated and some conclusions are drawn.

2 Studied systems and integral manifolds

The class of systems to be considered in this paper are described by the following state equations:

$$\begin{cases} \dot{x} = f(x, z) & \text{(a)} \\ \varepsilon \dot{z} = g(x, z) + l(x, z)u & \text{(b)} \end{cases} \quad (1)$$

where $x \in \mathbb{R}^{n_1}$ is the state of the slow subsystem (1-a), $z \in \mathbb{R}^{n_2}$ is the state of the fast subsystem, $u \in \mathbb{R}^p$ is the input control. ε is a small positive parameter. f , g and l are analytic vector fields which are sufficiently many times continuously differentiable functions of their arguments. Using the Kronecker power of vectors, these functions can be written in the polynomial form as [7]:

$$\begin{cases} f(x, z, \varepsilon) = \sum_{i=1}^r \sum_{j=1}^{i+1} F_{ij} x^{[i+1-j]} \otimes z^{[j-1]} \\ g(x, z) = \sum_{i=1}^r \sum_{j=1}^{i+1} G_{ij} x^{[i+1-j]} \otimes z^{[j-1]} \\ l(x, z) = \sum_{i=1}^r \sum_{j=1}^{i+1} L_{ij} (I_m \otimes (x^{[i+1-j]} \otimes z^{[j-1]})) \end{cases} \quad (2)$$

In general the stability of the reduced order subsystems for a class of nonlinear singularly perturbed systems cannot guarantee the stability of the original full order system even with the additional stability of the boundary layer subsystem but when an attractive manifold is designed, the stability problem of the original system reduces to a stability problem of a low dimensional system on the manifold. Subsequently, in the context of control system design, our goal is to find an appropriate control law that insures the existence of an attractive integral manifold and furthermore insures stability of the studied systems (1) when the dynamics are restrictive to the integral manifold.

The basic ideas of exploiting the integral manifold method are:

- If an integral manifold Σ of systems described by (1) is established, so that if the initial states start on Σ , the trajectory of the system remains on Σ thereafter.
- When restricted to the integral manifold Σ , the dynamics of the system should insure stability of the equilibrium.
- The integral manifold should be attractive so that if the initial conditions are off Σ , the solution trajectory asymptotically converges to Σ .

According to these important issues of the integral manifold method, let's present the definition, and the properties of integral manifold of nonlinear systems.

Definition 1. [16] *The set $\Sigma \subset \mathbb{R} \times \mathbb{R}^n$ is said to be an integral manifold (invariant manifold) for the differential equation: $\dot{X} = N(t, X)$, $X, N \in \mathbb{R}^n$ if for $(t_0, X_0) \in \Sigma$, the solution $(t, X(t))$, $X(t_0) = X_0$, is in Σ for $t \in \mathbb{R}$. If $(t, X(t)) \in \Sigma$ for only a finite interval of time, then Σ is said to be a local integral manifold.*

Lemma 1. [11] *Consider the following system:*

$$\begin{cases} \dot{x} = f(t, x, y, \varepsilon) \\ \varepsilon \dot{y} = g(t, x, y, \varepsilon) \end{cases} \quad (3)$$

$x, f \in \mathbb{R}^n, y, g \in \mathbb{R}^m, t \in \mathbb{R}, \varepsilon$ a small parameter. And suppose the following hypotheses hold:

- The algebraic equation $g(t, x, y, 0) = 0$ has an isolated solution $y = h_0(t, x)$, $\forall t \in \mathbb{R}, \forall x \in \mathbf{B}_x$
- The functions f , g , and h_0 are twice continuously differentiable ($\in C^2$) $\forall t \in \mathbb{R}, \forall x \in \mathbf{B}_x, \forall \varepsilon \in [0, \varepsilon_0]$ and for $\|y - h_0(t, x)\| \leq \bar{\varphi}_y$ where ε_0 and $\bar{\varphi}_y$ are positive real constants.

– The eigenvalues $\lambda_i = \lambda_i(t, x), i = 1, 2, \dots, m$ of the matrix $Z(t, x) := \left(\frac{\partial g}{\partial y} \right) (t, x, h_0(t, x), 0)$ satisfy the inequality

$$\operatorname{Re}[\lambda_i] \leq -2\beta < 0 \quad \forall t \in \mathbb{R}, \forall x \in B_x \quad (4)$$

Then there exists $\varepsilon \leq \varepsilon_1$ such that $\forall \varepsilon \in [0, \varepsilon_1)$, the singularly perturbed system (3) has an m -dimensional local integral manifold

$$\Sigma_\varepsilon : y = h_0(t, x) + H(t, x, \varepsilon) = h(t, x, \varepsilon) \quad (5)$$

where $h(t, x, \varepsilon)$ is defined for all $x \in B_x$ and $\varepsilon \leq \varepsilon_1$ and is continuously differentiable ($\in C^1$)

The function $h(t, x, \varepsilon) \in C^1$ satisfies the so-called manifold equation :

$$\varepsilon \frac{\partial h}{\partial t} + \varepsilon \frac{\partial h}{\partial x} f(t, x, h, \varepsilon) g(t, x, h, \varepsilon) \quad (6)$$

which is obtained by substituting y by h in equation (3).

On this manifold, the flow of systems (3) is governed by the n -dimensional reduced system

$$\dot{x} = f(t, x, h(t, x, \varepsilon), \varepsilon) \quad (7)$$

Furthermore, if for $x \in B_x$ and p integer we have $f(t, x, y, \varepsilon) \in C^{p+1}, g(t, x, y, \varepsilon) \in C^{p+2}$ and $h_0(t, x) \in C^{p+2}$ then $h \in C^p$

3 Useful notations and assumptions

In our study we make use of the following lemma 2 and Assumptions 1-2. The lemma 2 is concerned with a Kronecker transformation of vectors. More properties of the Kronecker product are given in the Appendix.

Lemma 2. [6] Given $X = \begin{pmatrix} x \\ z \end{pmatrix} \in \mathbb{R}^n; x \in \mathbb{R}^{n_1}, z \in \mathbb{R}^{n_2}$ and $n = n_1 + n_2$ there exists a matrix $\widehat{M}^{(i)} \in \mathbb{R}^{n_i \times n_i}$ making possible a transformation which introduces the change of coordinates that forms the new following Kronecker power of vector:

$$\widehat{\begin{pmatrix} x \\ z \end{pmatrix}}^{[i]} = \begin{bmatrix} x^{[i]} \\ \vdots \\ x^{[i-j]} \otimes z^{[j]} \\ \vdots \\ z^{[i]} \end{bmatrix} \in \mathbb{R}^{n_i}$$

such that

$$X^{[i]} = \begin{pmatrix} x \\ z \end{pmatrix}^{[i]} = \widehat{M}^{(i)} \widehat{\begin{pmatrix} x \\ z \end{pmatrix}}^{[i]} \quad (8)$$

with

$$\begin{cases} \widehat{M}^{(i)} = \begin{pmatrix} (i) & (i-1) \\ M & \otimes I_n \end{pmatrix} U V & \left| \begin{array}{l} 1 \leq j \leq (i-1) \\ n_i = \sum_{j=0}^i n_1^{i-j} n_2^j \end{array} \right. \\ \widehat{M}^{(1)} = I_n & \end{cases} \quad (9)$$

$$\nabla_t V_1(t, x) + (\nabla_x V_1(t, x))^T f(t, x, 0, 0) \leq -2\gamma_1 V_1 \quad (14)$$

where $\alpha_1, \alpha_2, \alpha_3$, and γ_1 are positive constants.

Assumption 2. *There exists a continuously differentiable function $V_2(t, z) : \mathbb{R} \times \mathbb{R}^{n_2} \rightarrow \mathbb{R}^+$ such that the following inequalities hold:*

$$\forall t \in \mathbb{R}, z \in \mathbb{R}^{n_2}$$

$$\beta_1 \|z\|^2 \leq V_2(t, z) \leq \beta_2 \|z\|^2 \quad (15)$$

$$\frac{dV_2(t, z)}{dt} \leq -\frac{2}{\varepsilon} \gamma_2 V_2(t, z) \quad (16)$$

$$(17)$$

where β_1, β_2 and γ_2 are positive constants.

4 Main results

Given the system (1), (2), we have to determine an adequate feedback control u that, starting from any initial states, will attract exponentially the trajectories of the closed loop system along the chosen design manifold to the equilibrium point at the origin.

In what follows, we assume that hypothesis of lemma 1 are satisfied, and hence the singularly perturbed system (1) has an n_2 dimensional integral manifold:

$$z = h_0(x) \quad (18)$$

satisfying the equation (1-b). The flow of system (1), on this manifold, is governed by the n_1 dimensional reduced system:

$$\dot{x} = f(t, x, h_0(t, x, \varepsilon), \varepsilon) \quad (19)$$

This result can be reached by the design of a desired control u satisfying:

$$l(x, z)u = -g(x, z) + A(z - h_0) + \varepsilon \frac{dh_0(x)}{dx} f(x, z) \quad (20)$$

where A is a Hurwitz matrix. Specifically, we choose the design manifold in this paper to be equal to $z = h_0(x) = 0$. Then, the control in equation (20) becomes:

$$l(x, z)u = -g(x, z) + Az \quad (21)$$

and the nonlinear singularly perturbed system (1) can be written as:

$$\begin{cases} \dot{x} = \sum_{i=1}^r \sum_{j=1}^{i+1} F_{ij} x^{[i+1-j]} \otimes z^{[j-1]} & \text{(a)} \\ \varepsilon \dot{z} = Az & \text{(b)} \end{cases} \quad (22)$$

It is then clear, that the fast subsystem and the fast states of the system (22) are attracted toward the manifold as quickly as desired by the choice of the Hurwitz matrix A .

The reduced order system of (22) is obtained by setting $\varepsilon = 0$ as:

$$\dot{x} = f(x, 0) = \sum_{i=1}^r F_{ii} x^{[i]} \quad (23)$$

The boundary layer system is given, in the fast time scale $\tau \frac{t}{\varepsilon}$, by:

$$\frac{dz^*(\tau)}{d\tau} = Az^*(\tau) \quad (24)$$

Now to study the stability of the system (22), let's consider that the reduced order system (23) and the boundary layer system (24) have respectively $V_1(x)$ and $V_2(z)$ as quadratic Lyapunov candidate functions verifying Assumptions 1-2 and defined as follows :

$$V_1(x) = x^T P_1 x \quad (25)$$

$$V_2(z) = z^T P_2 z \quad (26)$$

where P_1, P_2 are symmetric positive definite matrices solutions of the following Lyapunov equations:

$$\dot{V}_1(x) \leq -x^T Q_1 x \quad (27)$$

$$\dot{V}_2(z) \leq -z^T Q_2 z \quad (28)$$

Q_1, Q_2 are also positive definite matrices.

Based on results of the stability theory [15] and others derived in previous work [1], [5], (27) and (28) are formulated as follows:

$$\tau_1^T (M_1^T P_1 + P_1 M_1) \tau_1 \leq -Q_1 \quad (29)$$

$$\left(\frac{A}{\varepsilon}\right)^T P_2 + P_2 \left(\frac{A}{\varepsilon}\right) \leq -Q_2 \quad (30)$$

where

$$P_1 = \begin{bmatrix} P_1 & & & 0 \\ & P_1 \otimes I_{n_1} & & \\ & & \ddots & \\ 0 & & & P_1 \otimes I_{n_1^{s-1}} \end{bmatrix} \quad (31)$$

and

$$M_1 = \begin{bmatrix} \lambda_{11}\Pi_{11} & \lambda_{12}\Pi_{12} & \cdots & \lambda_{1s}\Pi_{1s} \\ \vdots & \ddots & & \vdots \\ \vdots & & \ddots & \vdots \\ \lambda_{s1}\Pi_{s1} & \cdots & \cdots & \lambda_{ss}\Pi_{ss} \end{bmatrix} \quad (32)$$

with

$$\Pi_{k-j+1,j} = \begin{bmatrix} \text{mat}_{(n^{k-j}, n^j)} (F_{kk}^{1T}) \\ \text{mat}_{(n^{k-j}, n^j)} (F_{kk}^{2T}) \\ \vdots \\ \text{mat}_{(n^{k-j}, n^j)} (F_{kk}^{nT}) \end{bmatrix} \quad (33)$$

For the corrected system (22), we define the following Lyapunov functions:

$$V(x, z, \varepsilon) = X^T E_\varepsilon P X \quad (34)$$

where

$$X = \begin{bmatrix} x \\ z \end{bmatrix} \in \mathbb{R}^n; P = \begin{pmatrix} P_1 & 0 \\ 0 & P_2 \end{pmatrix} \quad \text{and} \quad E_\varepsilon = \begin{pmatrix} I_{n_1} & 0 \\ 0 & \varepsilon I_{n_2} \end{pmatrix} \quad (35)$$

The derivative of $V(x, z, \varepsilon)$ along the trajectories of (22) is given by:

$$\dot{V}(x, z, \varepsilon) = X^T E_\varepsilon P \dot{X} + \dot{X}^T E_\varepsilon P X \quad (36)$$

In the above equation, we need to explicit the derivative of the state vector X . So, we begin by writing the state equations (22) in the following form:

$$\dot{X} = \begin{pmatrix} \dot{x} \\ \dot{z} \end{pmatrix} = \sum_{i=1}^r \Lambda_i \widehat{\begin{pmatrix} x \\ z \end{pmatrix}}^{[i]} \quad (37)$$

with

$$\Lambda_1 = \begin{pmatrix} F_{11} & F_{12} \\ 0 & \frac{A}{\varepsilon} \end{pmatrix}$$

and for $i > 1$:

$$\Lambda_i = \begin{pmatrix} F_{i1} \cdots F_{ij} \cdots F_{i(i+1)} \\ O_{n_2 \times \alpha_i} \end{pmatrix} \quad (38)$$

Using the results given by the lemma 2, it follows from equation (37) that

$$\dot{X} = \sum_{i=1}^r \Lambda_i \overset{(i)}{M} + X^{[i]} \quad (39)$$

where $\overset{(i)+}{M}$ is the Moore-Penrose pseudo inverse of $\overset{(i)}{M}$ defined in (A.4).

The derivative of the composite Lyapunov function (34) is then written:

$$\dot{V}(x, z, \varepsilon) = 2 \sum_{k=1}^r X^T (E_\varepsilon P \Lambda_k \overset{(k)}{M} +) X^k \quad (40)$$

Using the property of the vec-function (1), we have:

$$\dot{V}(x, z, \varepsilon) = 2 \sum_{k=1}^r V_k^T X^{[k+1]} \quad (41)$$

where

$$V_k = \text{vec}(E_\varepsilon P \Lambda_k \overset{(k)}{M} +) \quad (42)$$

Knowing that all polynomials with even degree ($2s$) can be represented as a symmetric quadratic form. Thus, we assume in the following development that r is odd: $r = 2s - 1$, and it comes out:

$$V_k^T X^{[k+1]} = \sum_{j=g_k}^{h_k} \lambda_{k-j+1,j} X^{[k+1-j]} N_{k-j+1,j} X^{[j]} \quad (43)$$

where $\lambda_{k-j+1,j}$ are arbitrary reals verifying:

$$\sum_{j=g_k}^{h_k} \lambda_{k-j+1,j} = 1 \quad (44)$$

and for $k = 1, \dots, 2s - 1$:

$$g_k = \sup(0, k + 1 - s) \text{ and } h_k = \inf(s, k) \quad (45)$$

for $j = g_k, \dots, h_k$:

$$N_{k-j+1,j} = \underset{(n^{k-j+1}, n^j)}{\text{mat}} (V_k) \quad (46)$$

Applying the properties [1], one obtains:

$$N_{k-j+1,j} = \underset{(n^{k-j+1}, n^j)}{\text{mat}} \left(\text{vec}(E_\varepsilon P \Lambda_k \overset{(k)}{M} +) \right) = U_{n^{k-j} \times n} (E_\varepsilon P \otimes I_{n^{k-j}}) \cdot M_{k-j+1,j} \quad (47)$$

with

$$M_{k-j+1,j} = \begin{bmatrix} \text{mat}_{(n^{k-j},n^j)}(\mathbf{B}_k^{1T}) \\ \text{mat}_{(n^{k-j},n^j)}(\mathbf{B}_k^{2T}) \\ \vdots \\ \text{mat}_{(n^{k-j},n^j)}(\mathbf{B}_k^{nT}) \end{bmatrix} \text{ and } \mathbf{B}_k = \Lambda_k^{(k)} M + \quad (48)$$

where \mathbf{B}_k^i is the i -th row of the matrix \mathbf{B}_k :

$$\mathbf{B}_k = \begin{bmatrix} \mathbf{B}_k^1 \\ \mathbf{B}_k^2 \\ \vdots \\ \mathbf{B}_k^n \end{bmatrix} \quad (49)$$

By (47) and from the relation (48), we obtain:

$$\begin{aligned} & X^{[k-j+1]T} N_{k-j+1,j} X^{[j]} \\ &= X^{[k-j+1]T} U_{n^{k-j} \times n} (E_\varepsilon P \otimes I_{n^{k-j}}) M_{k-j+1,j} X^{[j]} \\ &= X^{[k-j+1]T} (E_\varepsilon P \otimes I_{n^{k-j}}) M_{k-j+1,j} X^{[j]} \end{aligned} \quad (50)$$

Consequently, we have:

$$V_k^T X^{[k+1]} = \sum_{j=g_k}^{h_k} \lambda_{k-j+1,j} X^{[k-j+1]T} N_{k-j+1,j} X^{[j]} = X^T (P_\varepsilon M_k) X \quad (51)$$

with

$$X = \begin{bmatrix} X \\ X^{[2]} \\ \vdots \\ X^{[s]} \end{bmatrix} \quad (52)$$

and

$$P_\varepsilon = \begin{bmatrix} E_\varepsilon P & & & 0 \\ & E_\varepsilon P \otimes I_n & & \\ & & \ddots & \\ 0 & & & E_\varepsilon P \otimes I_{n^{s-1}} \end{bmatrix} \quad (53)$$

Let's note that P_ε is a symmetric positive matrix, and $\dot{V}(X, \varepsilon)$ (41) can be written as:

$$\dot{V}(X, \varepsilon) = 2 \sum_{k=1}^{2s-1} V_k^T X^{[k+1]} = X^T (P_\varepsilon M_\varepsilon + M_\varepsilon^T P_\varepsilon) X \quad (54)$$

with

$$M_\varepsilon = \sum_{k=1}^{2s-1} M_k = \begin{bmatrix} \lambda_{11} M_{11} & \lambda_{12} M_{12} & \cdots & \lambda_{1s} M_{1s} \\ \vdots & \ddots & & \vdots \\ \vdots & & \ddots & \vdots \\ \lambda_{s1} M_{s1} & \cdots & \cdots & \lambda_{ss} M_{ss} \end{bmatrix} \quad (55)$$

When considering the non-redundant form, the vector X can be written as:

$$X = \tau \tilde{X} \quad (56)$$

where

$$\tau = \begin{bmatrix} T_1 & & 0 \\ & \ddots & \\ 0 & & T_s \end{bmatrix} \text{ and } \tilde{X} = \begin{bmatrix} \tilde{X} \\ \vdots \\ \tilde{X}^{[s]} \end{bmatrix} \quad (57)$$

>From (54) and (56) we easily obtain:

$$\dot{V}(X, \varepsilon) = \tilde{X}^T \tau^T (P_\varepsilon M_\varepsilon + M_\varepsilon^T P_\varepsilon) \tau \tilde{X} \quad (58)$$

Let us denote the largest eigenvalue of the matrix P_ε by $\lambda_{\max}(P_\varepsilon)$, the smallest eigenvalue of Q by $\lambda_{\min}(Q)$. Where the matrix Q verifies: $\dot{V}(X, \varepsilon) \leq -X^T Q X$. The positive definiteness of P_ε and Q implies that these scalars are all strictly positive. Since matrix theory shows that:

$$P_\varepsilon \leq \lambda_{\max}(P_\varepsilon)I; \lambda_{\min}(Q)I \leq Q \quad (59)$$

We have

$$X^T Q X \geq \frac{\lambda_{\min}(Q)}{\lambda_{\max}(P_\varepsilon)} X^T [\lambda_{\max}(P_\varepsilon)I] X \geq \frac{\lambda_{\min}(Q)}{\lambda_{\max}(P_\varepsilon)} X^T [\lambda_{\max}(E_\varepsilon P)I] X \quad (60)$$

Otherwise

$$X^T X \geq \|X\|^2 \text{ and } E_\varepsilon P \leq \lambda_{\max}(E_\varepsilon P)I \quad (61)$$

Hence, (54) will satisfies the following condition:

$$\dot{V}(X, \varepsilon) \leq -2\gamma V(X, \varepsilon) \text{ where } \gamma = \frac{1}{2} \cdot \frac{\lambda_{\min}(Q)}{\lambda_{\max}(P_\varepsilon)} \quad (62)$$

It comes out

$$V(X, \varepsilon) \leq V(X_0) e^{-2\gamma(t-t_0)} \quad (63)$$

Considering the previous developments, we state now our main result:

Theorem 1. Assume the following assumptions hold:

- (i) Lemma 1 satisfied
- (ii) Assumptions 1 - 2 are satisfied

The system (1) is globally exponentially stable (GES), if there is, for all $\varepsilon < \varepsilon_1$, $\varepsilon_1 > 0$ a feasible solution to the LMI :

$$\begin{cases} \varepsilon > 0 \\ \exists P_1^T = P_1 > 0 \\ \exists P_2^T = P_2 > 0 \\ \exists P^T = P > 0 \\ \left(\frac{\Delta}{\varepsilon}\right)^T P_2 + P_2 \left(\frac{\Delta}{\varepsilon}\right) \leq -Q_2 \\ \tau_1^T (M_1^T P_1 + P_1 M_1) \tau_1 \leq -Q_1 \\ \tau^T (M_\varepsilon^T P_\varepsilon + P_\varepsilon M_\varepsilon) \tau \leq -Q \end{cases} \quad (64)$$

M_1 , τ_1 and P_1 are given by (32), (57) and (31). M_ε , τ and P_ε are given by (55), (57) and (53). Moreover, the Lyapunov function that demonstrates the G.E.S is given by: $V(x) = X^T E_\varepsilon P_\varepsilon X$

Now, let's evaluate the convergence rate of the full order system (22). In view of (12), (15), and (27), we have for all $t \in \mathbb{R}$, $x \in \mathbb{R}^{n_1}$ and $z \in \mathbb{R}^{n_2}$:

$$V_1(x) \leq (\alpha_2 \|x_0\|^2 + \varepsilon \beta_2 \|z_0\|^2) e^{-2\gamma(t-t_0)} \quad (65)$$

>From (12) and (15) we have:

$$\|x\| \leq \left(\left(\sqrt{\frac{\alpha_2}{\alpha_1}} \|x_0\| \right)^2 + \left(\sqrt{\frac{\varepsilon \beta_2}{\alpha_1}} \|z_0\| \right)^2 \right)^{1/2} e^{-\gamma(t-t_0)} \leq \left(\sqrt{\frac{\alpha_2}{\alpha_1}} \|x_0\| + \sqrt{\frac{\varepsilon \beta_2}{\alpha_1}} \|z_0\| \right) e^{-\gamma(t-t_0)} \quad (66)$$

Identically, using (15) and (16), we obtain:

$$\beta_1 \|z^2\| \leq V_2(z) \leq \beta_2 \|z_0^2\| e^{-2(\gamma_2/\varepsilon)(t-t_0)} \quad (67)$$

then

$$\|z\| \leq \sqrt{\frac{\beta_2}{\beta_1}} \|z_0\| e^{-(\gamma_2/\varepsilon)(t-t_0)} \quad (68)$$

>From (66) and (68), we can write in the case $\gamma \leq (\gamma_2/\varepsilon)$ that

$$\|X\|^2 \leq 2\eta e^{-2\gamma(t-t_0)}$$

where

$$\eta = \max \left(\left(\sqrt{\frac{\alpha_2}{\alpha_1}} \|x_0\| + \sqrt{\frac{\varepsilon\beta_2}{\alpha_1}} \|z_0\| \right)^2, \left(\sqrt{\frac{\beta_2}{\beta_1}} \|z_0\| \right)^2 \right) \quad (69)$$

which implies that the norm $\|X\|$ of the state vector converges to zero exponentially, with a rate γ . The convergence rates of the reduced systems can be calculated:

$$\gamma_1 = \frac{1}{2} \cdot \frac{\lambda_{\min}(Q_1)}{\alpha_2}, \quad \gamma_2 = \frac{\lambda_{\min}(Q_2)}{2\beta_2}$$

>From above, we state the following second result:

Theorem 2. Assume the following assumptions hold:

(i) Lemma 1 satisfied

(ii) Assumptions 1 - 2 are satisfied

(iii) There exists a Lyapunov function $V(t, X, \varepsilon)$ that satisfies equation ((34))

Then the original nonlinear singularly perturbed system ((1)) is globally exponentially stable under the proposed control ((21)) and with the convergence rate γ ((63)).

Moreover, note that when we proves that the limit of γ as $\varepsilon \rightarrow 0$, tends to the convergence rate of the reduced order system. This implies that under the proposed control (21), the global exponential stability of the initial studied system is equivalent to that of the reduced order system.

5 Illustrative Example

To illustrate the previous derived results, we consider a third order nonlinear singularly perturbed system defined by the following equations:

$$\begin{cases} \dot{x}_1 = -x_1 + x_2 + 0.1x_1z \\ \dot{x}_2 = -x_1 - 0.09x_2 + 2z + 0.05x_1z \\ \varepsilon\dot{z} = 4x_1 - 4x_2 + z + 0.5x_1^2 - x_2^2 + 10u \end{cases}$$

This system can be described by the following model using the Kronecker product and the power of vectors which allowed important algebraic manipulations.

$$\begin{cases} \dot{x} = F_{11}x + F_{12}z + F_{21}x^{[2]} + F_{22}x \otimes z + F_{23}z^{[2]} \\ \varepsilon\dot{z} = G_{11}x + G_{12}z + G_{21}x^{[2]} + G_{22}x \otimes z + G_{23}z^{[2]} + Bu \end{cases}$$

where

$$F_{11} = \begin{bmatrix} -1 & 1 \\ -1 & -0.09 \end{bmatrix}, F_{12} = \begin{bmatrix} 0 \\ 2 \end{bmatrix}, G_{11} = [4 \quad -4], G_{12} = 1,$$

$$F_{21} = 0_{2 \times 4}, F_{22} = \begin{bmatrix} 0.1 & 0 \\ 0 & 0.5 \end{bmatrix}, F_{23} = 0_{2 \times 1}$$

$$G_{21} = [0.5 \quad 1 \quad 0], G_{22} = [0 \quad 0], G_{23} = 0, B = 10.$$

When implemented using the LMI toolbox of Matlab, the proposed LMI's conditions proves that the numerical studied system which is initially unstable can be globally exponentially stabilised by the given controller with the considered $A = -1$ for all $\varepsilon < \varepsilon_1 = 0.5$ in view of theorem 1:

$$u = -0.4x_1 + 0.4x_2 - 0.1z - 0.05x_1^2 + 0.1x_2^2$$

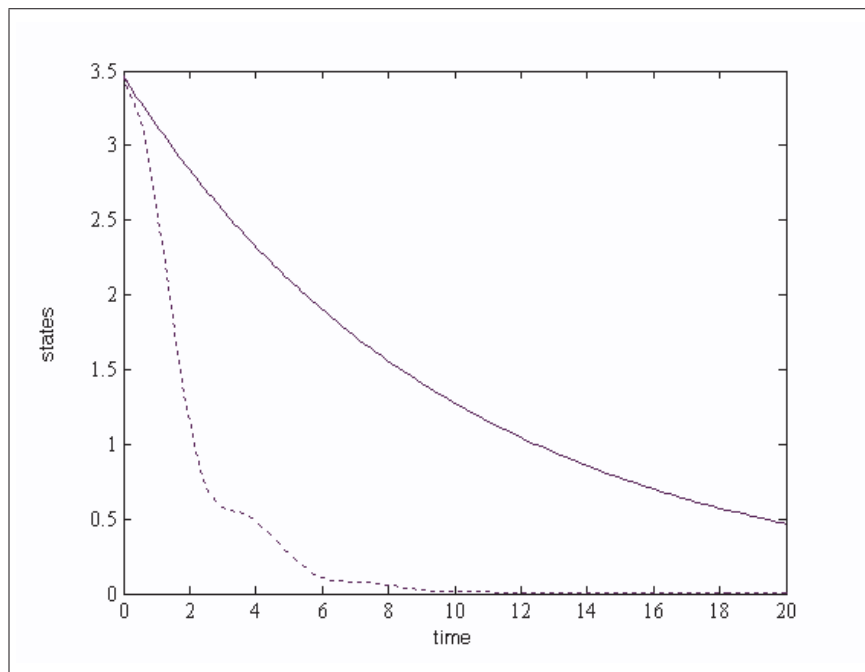


Figure 1: State trajectories of the controlled studied system

Hence for all $\varepsilon < \varepsilon_1 = 0.5$ and from any initial states, the trajectories of the system are steered to the origin along the integral manifold with the convergence rate 0.1 in view of (62). Indeed, it is shown in Fig. 1 that the state trajectories of the controlled system (---) are bounded by the function (—).

6 Conclusion

In this paper, the global exponential stabilisation for nonlinear singularly perturbed control systems is investigated. In the stability study, the composite Lyapunov method was applied and the global exponential stability of the equilibrium of the full control system was established for all $\varepsilon < \varepsilon_1$. The upper bound ε_1 for which the stability properties are guaranteed can be reached after a number of iterations on ε when resolving the proposed LMI's conditions via the LMI Toolbox of Matlab. A numerical example has been provided to illustrate the proposed results.

7 Appendix

Notations: The dimensions of the matrices used here are the following:

$A(p \times q), B(r \times s), C(s \times h), D(s \times h), E(n \times p),$

$P(n \times n), X(n \times 1) \in \mathbb{R}^m, Y(m \times 1) \in \mathbb{R}^m, Z(q \times 1) \in \mathbb{R}^q$

Let's consider the following notations:

I_n : $n \times n$ identity matrix;

$0_{n \times m}$: $n \times m$ zero matrix;

O zero matrix of convenient dimensions ;

A^T : transpose of matrix A ;

$A > 0$ ($A \geq 0$): symmetric positive definite (semi definite matrix A);

e_k : q dimensional unit vector which has 1 in the k th element and zero elsewhere.

(q)

The k th row of a matrix such as A is denoted A_k . and the k th column is denoted $A_{.k}$. The ik element of A will be denoted a_{ik} .

The Kronecker product of A and B is denoted $A \otimes B$ a $(p.r \times q.s)$ matrix, and the i -th Kronecker's power of A denoted $A^{[i]} = A \otimes A \otimes \dots \otimes A$ a $(p^i \times q^i)$ matrix.

The non-redundant j -power $\tilde{X}^{[j]}$ of the state vector X introduced in [9] is defined as:

$$\begin{aligned} \tilde{X}^{[1]} &= X^{[1]} = X \\ \left\{ \begin{array}{l} \forall j \geq 2 \quad \tilde{X}^{[j]} = [x_1^j, x_1^{j-1}x_2, \dots, x_1^{j-1}x_n, x_1^{j-2}x_2^2, \\ x_1^{j-2}x_2x_3, \dots, x_1^{j-2}x_2x_n, \\ \dots, x_1^{j-2}x_2^n, \dots, x_1^{j-3}x_2^3, \dots, x_n^j] \end{array} \right. \end{aligned} \quad (\text{A.1})$$

where the repeated components of the redundant j -power are omitted. Then we have the following relation:

$$\left\{ \begin{array}{l} \forall j \in \mathbb{N} \quad \exists! T_j \in \mathbb{R}^{n^j \times n^j}; \alpha_j = \binom{n+j-1}{j} \\ X^{[j]} = T_j \tilde{X}^{[j]} \end{array} \right. \quad (\text{A.2})$$

thus, one possible solution for the inversion can be written as:

$$\tilde{X}^{[j]} = T_j^+ X^{[j]} \quad (\text{A.3})$$

where T_j^+ is the Moore-Penrose pseudo inverse of T_j given by:

$$T_j^+ = \left(T_j^T T_j \right)^{-1} T_j^T \quad (\text{A.4})$$

and α_j stands for the binomial coefficients.

An important vector valued function of matrix denoted $vec(\cdot)$ was defined as [9]:

$$vec_{pq \times 1}(A) = \begin{bmatrix} A_{.1} \\ A_{.2} \\ \vdots \\ A_{.q} \end{bmatrix} \quad (\text{A.5})$$

A matrix valued function is a vector denoted $mat_{(n,m)}(\cdot)$ was defined in [1] as follows: If V is a vector of dimension $p = n \times n$ then $Mmat_{(n,m)}(V)$ is the $n \times m$ matrix verifying:

$$V = vec(M) \quad (\text{A.6})$$

Among the main properties of this product presented in [9], [1], we recall the following useful ones:

$$(A \otimes B)(C \otimes D) = (AC) \otimes (BD) \quad (\text{A.7})$$

$$(A \otimes B)^T = A^T \otimes B^T \quad (\text{A.8})$$

$$B \otimes A = U_{r \times p}(A \otimes B)U_{q \times s} \quad (\text{A.9})$$

$$X \otimes Y = U_{n \times m}(Y \otimes X) \quad (\text{A.10})$$

$$vec(EAC) = (C^T \otimes E) vec(A) \quad (\text{A.11})$$

$$vec(A^T) = U_{p \times q} vec(A) \quad (\text{A.12})$$

$$\forall i \leq k \quad X^{[k]} = U_{n^i \times n^{k-i}} X^{[k]} \quad (\text{A.13})$$

References

- [1] E. Benhadj Braiek , F. Rotella, M. Benrejeb, Algebraic criteria for global stability analysis of nonlinear systems, *SAMS Journal*, Vol.17, pp. 211-227, 1995.
- [2] P. Borne, J.C Gentina, On the stability of large nonlinear systems. Structured and simultaneous Lyapunov for system stability problem, *Joint. Aut. Cont. Conf., Austin, Texas*, 1974.
- [3] P. Borne, M. Benrejeb, On the stability of a class of interconnected systems. Application to the forced Working condition, *Actes 4th IFAC Symposium MTS, Fredericton, Canada*, 1977.
- [4] P. Borne and G. Dauphin-Tanguy, Singular perturbations, boundary layer problem, *Systems and Control Encyclopedia*, M.G.Singh Eds, Pergamon press, III I-2, 1987.
- [5] H. Bouzaouache, E. Benhadj Braiek, On the stability analysis of nonlinear systems using polynomial Lyapunov functions, *IMACS World Congress, Paris*, 2005.
- [6] H. Bouzaouache, Sur la représentation d'état des systèmes non linéaires singulièrement perturbés polynomiaux, *Conférence Tunisienne de Génie Electrique CTGE* ,pp. 420-424, 2004.
- [7] H. Bouzaouache, E. Benhadj Braiek, M. Benrejeb, A reduced optimal control for nonlinear singularly perturbed systems", *Systems Analysis Modelling Simulation Journal*.Vol 43, pp. 75-87, 2003.
- [8] S. Boyd, L. El Ghaoui and Feron E. Balakrishnan, Linear Matrix Inequalities in System and Control Theory, *SIAM, Philadelphia*,1994.
- [9] J. W. Brewer, Kronecker product and matrix calculus in system theory, *IEEE Trans.on Circ.Syst*, 25 , N°9, pp. 772-781, 1978.
- [10] C.C. Chen, Research on the feedback control of nonlinear singularly perturbed systems, PhD Thesis, *Inst. Electrical Eng., NatSun Yat Sen Univ, Taiwan, Roc*, 1994.
- [11] F. Ghorbel and M.W.. Spong, Integral manifolds of singularly perturbed systems with application to rigid-link flexible joint multibody systems, *International Journal of Nonlinear Mechanics* 35, pp. 133-155, 2000.
- [12] M. Innocenti, L. Greco, L. Pollini, Sliding mode control for two time scale systems : stability issues, *Automatica*, Vol. 39,pp. 273-280,2003.
- [13] P.V. Kokotovic, H.K. Khalil, O'Reilly, Singular perturbation methods in control: analysis and design, *academic Press , New york*, 1986.
- [14] P.M. Sharkey and J. O'Reilly, Exact design manifold control of a class of NLSP systems, *IEEE Trans. Automat. Contr.*, Vol.32, pp.933-937, 1987.
- [15] J.J.E. Slotine, Applied nonlinear control, *Englenwood Cliffs, NJ, Prentice Hall*, 1991.
- [16] V.A. Sobolev, Integral manifolds and decomposition of singularly perturbed systems, *Systems Control Letters*, Vol.5, pp.169-179, 1984.
- [17] M.W.Spong, K. Khorasani, P.V. Kokotovic, An Integral Manifold approach to feedback control of flexible joint robots, *IEEE J. Robot. Automat.*3 (4), pp. 291-300, 1987.

Hajer Bouzaouache, Naceur Benhadj Braiek
Laboratory of Study and Automatic Control of Processes
Address: Polytechnic School of Tunisia (EPT) BP.743, 2078 La Marsa, Tunisia.
E-mail: hajer.bouzaouache,naceur.benhadj@ept.rnu.tn

Received: November 6, 2006

Numerical Aspects and Performances of Trajectory Planning Methods of Flexible Axes

Jean-Yves Dieulot, Issam Thimoumi, Frédéric Colas, Richard Béarée

Abstract: Adequate Path Planning design is an important stage for controlling flexible axes because it may allow to cancel vibrations induced by oscillating modes. Among bang-bang profiles which are linked to optimal control, jerk assignment (acceleration derivative) and input shapers have been investigated. Theoretical results show the performance and robustness with respect to natural frequency mismatch. Practical validations on a real robot arm show the relevance of the jerk algorithm which is more robust with the same productivity performances as input shaping techniques.

Keywords: Flexible axes, Vibrations, bang-bang laws, Input shapers, Motion Planning.

1 Introduction

Vibration control of flexible Cartesian robots or axes is strongly related to productivity. Indeed, lighter structures allow material savings and higher performances in terms of speed, acceleration... which, in turn, cause undesirable oscillations. In practice, classical servo control fails to reduce vibrations, which, in many cases, restrains the operating speed [1]. The only way to damp the oscillations consists of designing proper smooth reference trajectories, which should be however as fast as possible [2]. Many methods have been introduced using the inversion motion equations or a combination of smooth trigonometric or polynomial functions, e.g. [3]. Very often, though, these methods face the robustness problem with respect to uncertainties in the dominant frequency, which is the main model parameter to be taken into account into anti-vibration algorithms design. Near-optimal bang-bang methods have been designed to solve the trade-off between productivity and vibrational behavior. These mainly consist of convolving a series of impulses with the control input, where the inter-pulse duration is adequately chosen in a way that the resulting oscillations are in phase opposition [4]. These techniques are known as input shapers, and have proven to be quite effective on linear systems e.g. [5, 6]. On another hand, the most popular damping scheme consists of a bang-bang profile in jerk (which is the derivative of acceleration), and has been proven to be related to input shapers with negative weights [7]. The goal of the paper is to compare different bang-bang laws (shapers, jerk...) in terms of productivity and sensitivity to parameter uncertainty, for a classical model of flexible axis controlled in closed-loop. In a first part, different trajectory planning methods are presented and theoretical results, in terms of vibration attenuation and robustness, are presented. The second part deals with an experimental validation on a real industrial pick-and-place robot which will draw a fair comparison in terms of productivity between these methods.

2 Preshaping laws

2.1 Architecture of CNC axes

Control of a CNC axis or a Cartesian robot arm is decomposed into three phases [1]:

- geometric motion planning which provides the desired path within the whole workspace (in 2- or 3-D)

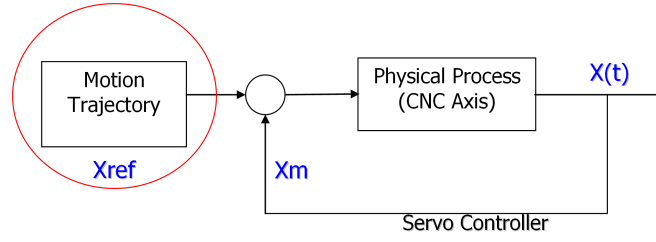


Figure 1: Control strategy of a CNC Axis

- a time-dependent path planning stage which should, of course, take into account for saturations, but, which will be shown later, should be designed to cancel undesirable vibrations
- a servo controller which should help to reject disturbances and to track the reference trajectory.

In practice, the model of a flexible axis controlled with cascaded loop will be [1]

$$\frac{x(s)}{x_{ref}(s)} = \frac{1 + \frac{k_{f_v}}{k_v} s}{1 + \frac{s}{k_v}} \frac{1 + \frac{2\zeta}{\omega} s}{1 + \frac{2\zeta}{\omega} s + \frac{1}{\omega^2} s^2} \quad (1)$$

where x is the position of the motor, x_{ref} is the reference trajectory, k_v, k_{f_v} are servo gains (position and speed gains, respectively), ζ, ω are respectively the damping ratio (assumed as very small, $\zeta \ll 1$) and the natural frequency of the axis modeled as a two-mass-spring damper unit. The main purpose of this paper will be the design of the time-dependent path-planning of the closed-loop system represented by equation (1).

2.2 Smooth continuous laws

A first way of designing the reference trajectory, would be to invert the whole path planning, such as in the so-called flatness approach [3]. In practice, though, model parameters vary since the structure consists of an assembly of flexible beams. The linear approximation of equation (1) is indeed valid for one set-point, which is the case during the short periods corresponding to the start and stop procedures, but not during the whole course. For point-to-point displacements, a stage of acceleration and deceleration is necessary. In CNC control, these stages are driven in a very sharp way, commonly a bang-bang in acceleration, which consequently excites the flexible mode of equation (1) and generates high-amplitude vibrations. Smooth trajectories based upon the natural frequency of the closed-loop system (1) can thus be designed, and an obvious method consists of introducing such laws as trigonometric trajectories (Fig. 2).

The maximal vibratory error for a "sine" profile is

$$(\epsilon_{vib})_{\max} = \bar{x}_{ref} \frac{\sin\left(\frac{\pi\tau}{2}\right)}{\pi\tau(\tau^2 - 1)} \quad (2)$$

for a square sine [2] profile ($\tau = T_f\omega/2\pi$; T_f is the motion duration, \bar{x}_{ref} is the target position). In practice, the error is significantly reduced for a movement of duration superior to 4 times the natural period. An alternative consist of building smooth polynomials which would verify smooth constraints on the dynamics such as minimizing the amplitude of the jerk during the whole displacement, the corresponding polynomial is:

$$x_{ref} = \frac{30t^3\bar{x}_{ref}}{T_f^5} \left(\frac{t^2}{5} - \frac{T_f t}{2} + \frac{T_f^2}{3} \right) \quad (3)$$

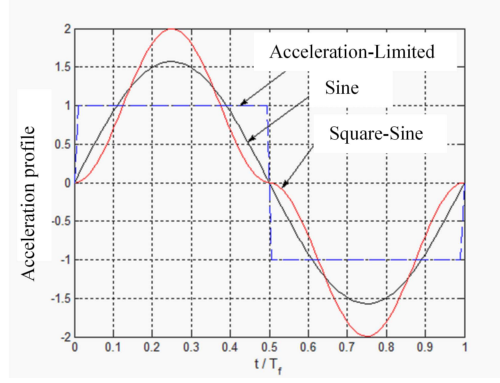


Figure 2: Smooth Control Laws

and the corresponding maximum error decreases again after a few periods [2]:

$$(\varepsilon_{vib})_{\max} = \frac{15\bar{x}_{ref}}{\pi^5 \tau^5} [3\pi\tau \cos(\pi\tau) + (-3 + \pi^2 \tau^2) \sin(\pi\tau)] \quad (4)$$

2.3 Jerk Laws

Contrary to previous laws, it is also possible to use "bang-bang" or discontinuous laws to achieve the feedforward control of CNC axes, which are related to time-optimal control as proven in [8].

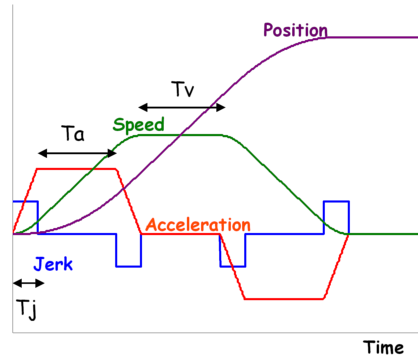


Figure 3: Bang-Bang Profile (Jerk-limited)

The maximum theoretical error for a bang-bang in acceleration is $\frac{\max_{t \geq T_f}(\varepsilon(t))}{\bar{x}_{ref}} = \left(\text{sinc}\left(\frac{\pi \cdot \tau}{2}\right)\right)^2$, $\tau = T_f \omega / 2\pi$. For a profile with a bang-bang in jerk, one obtains [2]:

$$\max_{t \geq T_f} \left| \frac{\varepsilon(t)}{\bar{x}_{ref}} \right| = \frac{4A_m}{\omega^2} \cdot \sqrt{\frac{1 + k f_v^2 \omega^2 / k_v^2}{1 + \omega^2 / k_v^2}} \cdot \left| \text{sinc}\left(\frac{T_j \omega}{2}\right) \right| \Psi(T_j, T_a, T_v) \quad (5)$$

where $T_f = 4T_j + 2T_a + T_v$ (see Fig. 3), A_m is the maximum acceleration, and:

$$\Psi(T_j, T_a, T_v) = \left| \sin((T_a + T_j) \omega / 2) \sin((T_a + 2T_j + T_v) \omega / 2) \right|$$

In theory, it is possible to find a value of Jerk for zero-vibration which will be:

$$T_j = \frac{2\pi}{\omega} \text{ and } J = \frac{2\pi}{\omega} A_m \quad (6)$$

The theoretical robustness with respect to an uncertainty in the natural period T is shown below:

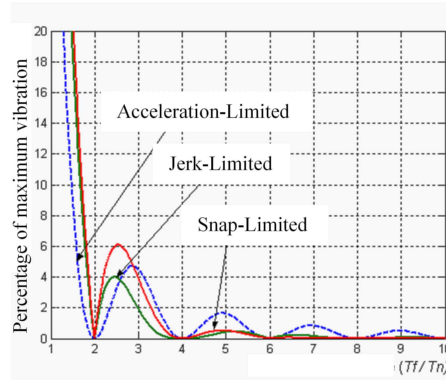


Figure 4: Residual vibrations

2.4 Input Shapers

The principle of input shapers was introduced by Singer and Seering [4] and consists of convolving the reference or the input with a series of well-chosen impulses. Jerk motion planning can be considered as input shaping with negative weights. The underlying idea is that the oscillation will be compensated

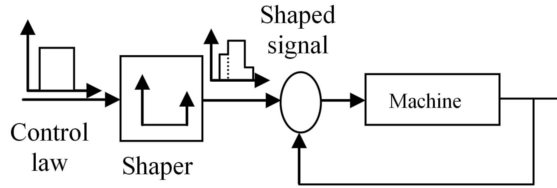


Figure 5: Input Shaper Principle

by that induced by a shifted pulse as shown Fig. 6: A shaper is thus a series of shifted pulses which can

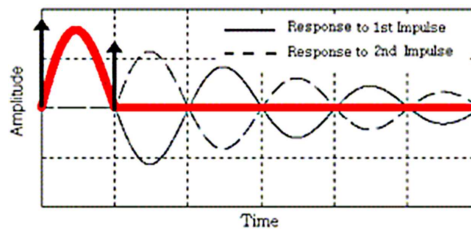


Figure 6: Superposition of oscillations

be written

$$F(s) = A_0 + \sum_{i=1}^n A_i e^{-sT_i} \quad (7)$$

where $\sum_{i=1}^n A_i = 1$. The response to a second order system will be:

$$x(t) = \sum_{i=1}^n \bar{x}_{ref} \left[\frac{A_i \omega}{\sqrt{1 - \zeta^2}} e^{-\zeta \omega (t - T_i)} \right] \sin(\omega \sqrt{1 - \zeta^2} (t - T_i))$$

- the Zero-Vibration (ZV) shaper, which is a two pulse filter for which the vibration at the stop stage should be zero; one obtains the following equations:

$$\begin{cases} A_0 + A_1 e^{\zeta \omega T_1} \cos(\omega \sqrt{1 - \zeta^2} T_1) = 0 \\ A_1 e^{\zeta \omega T_1} \sin(\omega \sqrt{1 - \zeta^2} T_1) = 0 \\ A_0 + A_1 = 1 \end{cases}$$

- the Zero-Vibration Derivative (ZVD) shaper which is a three pulse filter for which the position and its derivative at the stop stage should be zero; equations are:

$$\begin{bmatrix} A_i \\ T_i \end{bmatrix} = \begin{bmatrix} \frac{1}{D(\zeta)} & \frac{2e^{-\frac{\zeta \pi}{\sqrt{1-\zeta^2}}}}{D(\zeta)} & \frac{e^{-\frac{2\zeta \pi}{\sqrt{1-\zeta^2}}}}{D(\zeta)} \\ 0 & \frac{\pi}{\omega \sqrt{1-\zeta^2}} & \frac{2\pi}{\omega \sqrt{1-\zeta^2}} \end{bmatrix}$$

where $D(\zeta) = 1 + 2e^{-\frac{\zeta \pi}{\sqrt{1-\zeta^2}}} + e^{-\frac{2\zeta \pi}{\sqrt{1-\zeta^2}}}$

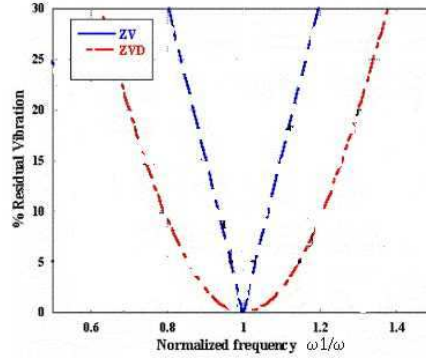


Figure 7: Shaper robustness

Figure 7 shows shaper robustness where the percentage of residual vibration is plotted versus the ratio ω_1/ω where $\omega_1 = 2\pi/T_1$ (a Specified Insensitive is a 4-pulse shaper [9]). The more pulses, the more the shaper will be robust with respect to natural frequency uncertainty. However, it can be understood that adding pulses leads to higher cycle times, as will be shown later on. One can see that the ZV shaper, which is quite performing, is not really robust with respect to natural frequency mismatch. When applied to equation (1), the ZV shaper gives a maximal error of:

$$\max_{t \geq T_f} \left| \frac{\varepsilon(t)}{\bar{x}_{ref}} \right| = \frac{A}{2 + 2T^2\omega^2} \sqrt{\left(\left(1 + \cos\left(\frac{\pi\omega}{\omega_1}\right) - T\omega \sin\left(\frac{\pi\omega}{\omega_1}\right) \right)^2 + \left(T\omega + T\omega \cos\left(\frac{\pi\omega}{\omega_1}\right) + \sin\left(\frac{\pi\omega}{\omega_1}\right) \right)^2 \right)}$$

with a theoretical cycle time of:

$$T_f = \frac{1}{2} \left(\sqrt{\frac{16\bar{x}_{ref}}{A}} - T_1 \right)$$

The ZVD shaper gives a maximal error of

$$\max_{t \geq T_f} \left| \frac{\varepsilon(t)}{\bar{x}_{ref}} \right| = \frac{A}{2 + 2T^2\omega^2} \sqrt{\left(\left(T\omega + T\omega \cos\left(\frac{\pi\omega}{\omega_1}\right) + \cos\left(\frac{\pi\omega}{\omega_1}\right) \sin\left(\frac{\pi\omega}{\omega_1}\right) + \sin\left(\frac{\pi\omega}{\omega_1}\right) \right)^2 + \left(1 + \cos\left(\frac{\pi\omega}{\omega_1}\right) + T\omega \sin\left(\frac{\pi\omega}{\omega_1}\right) + T\omega \cos\left(\frac{\pi\omega}{\omega_1}\right) \sin\left(\frac{\pi\omega}{\omega_1}\right) \right)^2 \right)}$$

and the cycle time is $T_f = \frac{1}{2} \left(\sqrt{\frac{16\bar{x}_{ref}}{A}} + T_1 \right)$, which is much longer than precedingly, and comparable to the Bang-bang of Jerk cycle time.

3 Experimental comparisons of path planning laws

3.1 Material and methods

The experimental validations are carried out on a 3-axes robot (Fig. 8). It has been equipped with a real-time "dSPACE 1103" control card. The available measurements on the motor part come from the actuator axis encoders [10]. When the horizontal axis is only moving, it will be assumed that the axis stiffness remains almost constant (with an actual variation of 30 %) and the system can be considered as linear. The validation was undertaken for a displacement on the X axis, with x_2 varying from $x_{2_0} = 0$ to $x_2 = 900\text{mm}$ and $y_2 = 0\text{mm}$ with a height $z = 315\text{mm}$. According to experimental results, the natural



Figure 8: Overview of the first test-setup prototype (stroke [mm]: X-1000 Y-400 Z-800, max. feedrate: $120 \text{ m}\cdot\text{min}^{-1}$, max. acceleration: $4 \text{ m}\cdot\text{s}^{-2}$).

frequency was calculated as $F_n = 9.8\text{Hz}$, the damping ratio was taken as $\zeta = 0.0132$. In this case, the optimal value of the jerk given by equation (6), which limits the amplitude of vibrations, is of $30 \text{ m}\cdot\text{s}^{-3}$. Parameters of the industrial control loop were $k_p = 14\text{s}^{-1}$, $k_v = 2\text{A}\cdot\text{rd}\cdot\text{s}^{-1}$.

3.2 Experimental results

One can see that, from Fig. 9, the curve follows a sinc(.) evolution. Fine jerk tuning is indeed effective. When the jerk parameter is not well-tuned, the vibrational behavior deteriorates slightly. As for the ZVD shaper (Fig. 10), one can find out what was simulated, one obtains zero vibration when $a = \omega_1/\omega$ is even, and the curve is flat around points cancelling vibrations. Results for the ZV shaper are alike and not shown here.

3.3 Comparison and discussion

One can compare experimentally the maximal error for the three laws: Figure 11 shows that the ZV shaper is not robust at all. The jerk law is quite robust with respect to input shapers, because the jerk is a continuous derivative of the acceleration during the whole motion, whereas the ZVD cancels vibrations only at the point where zero vibrations are desired. For a value of $a = 1$, the three curves have the same percentage of residual vibration (same performances). When $a = 0$, one finds again the classical bang-bang in acceleration for which by definition 100% vibrations occur (Fig. 11). The cycle time is

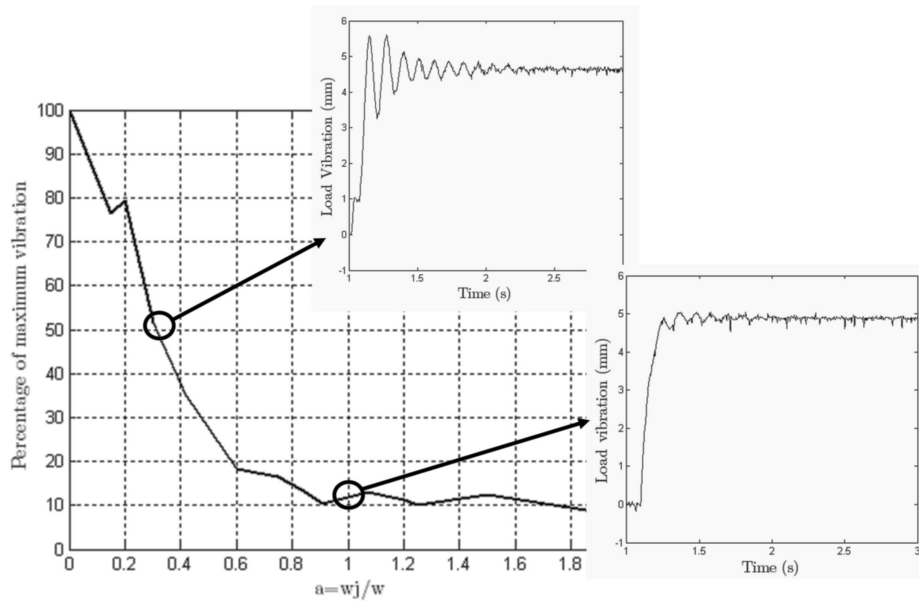


Figure 9: Jerk-limited residual vibrations (%)-(a) : variation of maximal residual vibrations as a function of $a = \omega_j/\omega, \omega_j = \frac{2\pi}{T_j}$ (b) : amplitude of vibrations at jerk $J=100$ (c) : amplitude of vibrations at jerk $J=30$

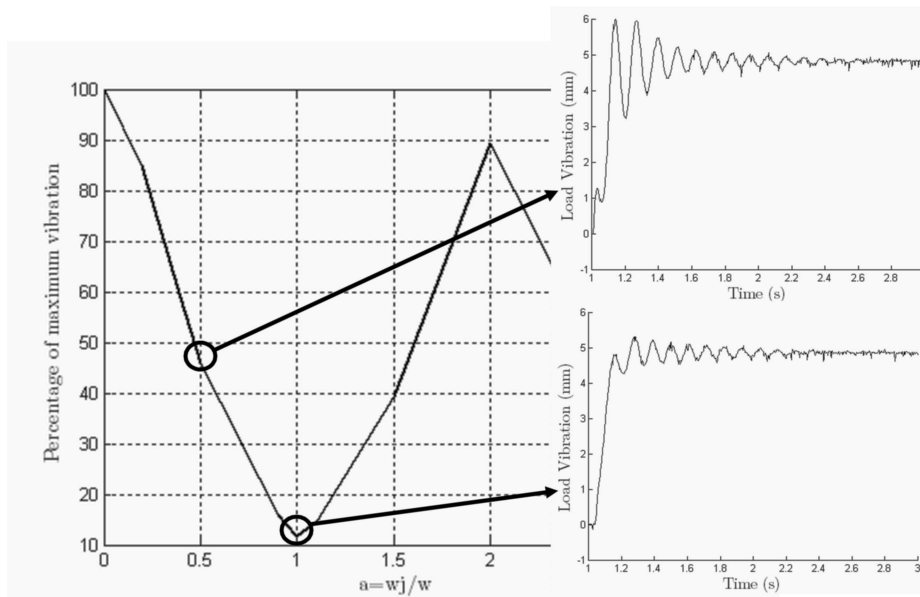


Figure 10: ZVD residual vibrations (%)-(a) : variation of maximal residual vibrations as a function of $a = \omega_1/\omega$, (b) : amplitude of vibrations at $a = 0.5$ (c) : amplitude of vibrations at $a = 1$

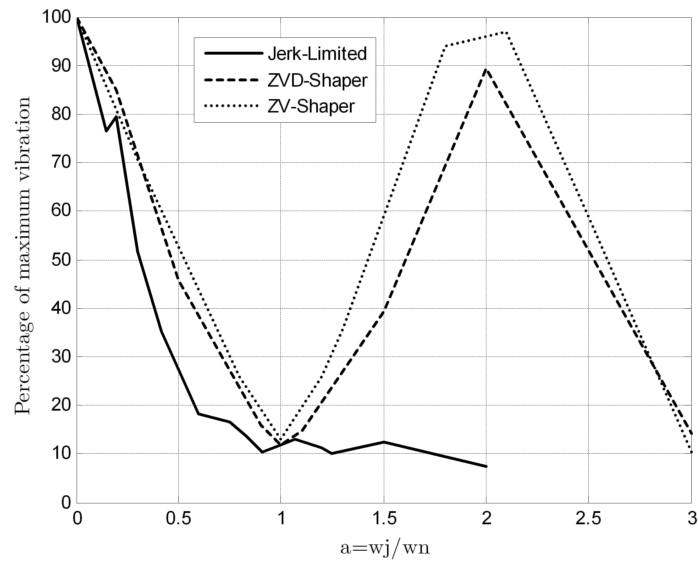


Figure 11: Comparison of planning laws: percentage of maximum vibrations

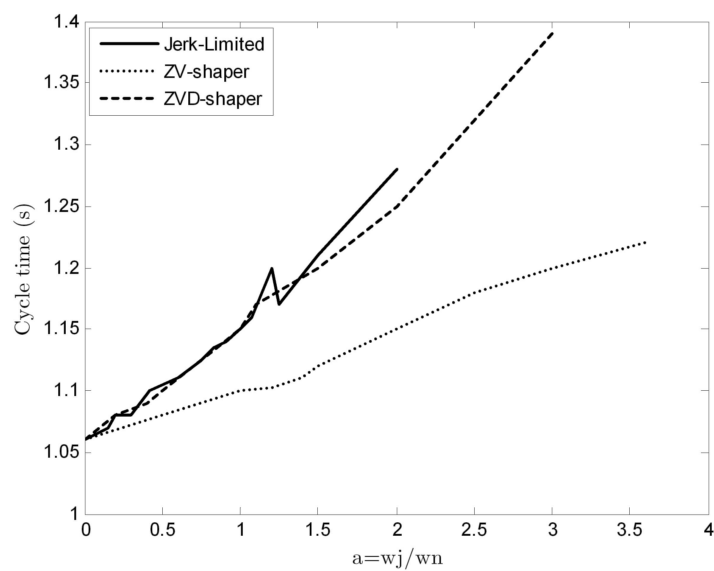


Figure 12: Comparison of planning laws: cycle time

defined as the instant for which the motor position reaches its reference by -0.2 mm. Figure 12 shows the evolution of the cycle time of the different laws. One can see that the ZV shaper is quicker by 13%.

As a conclusion, the Jerk bang-bang algorithm is more robust to parameter variations than a ZV shaper which has approximately the same cycle time. Another advantage is that this algorithm is now implemented in most industrial CNC control devices. When the frequency is always the same, fixed and well-estimated, one can expect to gain some productivity using a ZV shaper instead. A possibility to cope with non-linearities consists either of using "gain scheduling" or adaptive/iterative algorithms e.g. [11, 12].

4 Summary and Conclusions

The design and computation of near-optimal reference trajectories for CNC devices is a difficult challenge which should examine the trade-off between cancellation of undesirable vibrations and rapidity. This design can be achieved using continuous "jerk" (derivative of acceleration) laws or input shapers, which consist of convolving pulses with the control input. Theoretical and empirical results show the relevance of using jerk laws due to their productivity performances at comparable robustness properties (with respect to natural frequency uncertainties). A good calibration of the model parameters would allow to use a two-pulse shaper, which is faster but less robust. In practice, however, these algorithms have to be adapted to be implemented into CNC units, because of neglected dynamics (such as dry friction) which may cause static errors.

References

- [1] Béarée, R., Barre P.J., Bloch S., Influence of high feed rate machine tool control parameters on the contouring accuracy, *J. Intell. Robotic Systems*, Vol. 40, 2004, pp 321-342.
- [2] Barre P.-J., Bearee R., Borne P., Dumetz, E., Influence of a Jerk Controlled Movement Law on the Vibratory Behaviour of High-Dynamics Systems, *J. of Intell. Robot. Systems*, Vol. 42, 2005, 275-293.
- [3] Fliess M., Lévine J., Martin P., Rouchon, P., Flatness and defect of nonlinear systems: Introductory theory and applications, *Int. J. Control*, Vol. 61, 1995, pp 1327-1361.
- [4] Singer N., Seering W., Preshaping command inputs to reduce system vibration, *J. Dynam. Syst., Meas. Contr.*, Vol. 112, 1990, pp 76-82.
- [5] Meckl P. H., Seering W. P., Experimental evaluation of shaped inputs to reduce vibration of a cartesian robot, *J. of Dyn. Systems, Meas. Control*, Vol. 112, 1990, pp 159-165.
- [6] Peláez G., Gu. Pelaez, J.M. Perez, A. Vizán, E. Bautista, Input shaping reference commands for trajectory following Cartesian machines, *Control Eng. Practice*, Vol. 13, 2005, pp 941-958.
- [7] Singhose W., Singer N., Seering W., Time-optimal negative input shapers, *J. Dynam. Syst., Meas., Contr.*, Vol. 119, 1997, pp. 198-205.
- [8] Lau M. A., Pao, L. Y. , Input shaping and time-optimal control of flexible structures, *Automatica*, Vol. 39, 2003, pp 893-900.
- [9] Singhose W. E., Derezinski S. J., Singer N. C., Extra insensitive input shaper for controlling flexible spacecraft, *J. Guidance Control Dynamics*, Vol. 19, 1996, pp 385-391.

- [10] Dumetz E., Dieulot J.Y., Barre P.J., Colas F., Control of an Industrial Robot using Acceleration Feedback, *J. Intell Robotic Systems*, Vol. 46, 2006, pp 111-128.
- [11] Md Zain M.Z., Tokhi M.O., Mohamed Z., Hybrid learning control schemes with input shaping of a flexible manipulator system, *Mechatronics*, Vol. 16, 2006, 209-219.
- [12] Cutforth, C. F., Pao L. Y., Adaptive input shaping for maneuvering flexible structures, *Automatica*, Vol. 40, 2004, pp 685-693.

Jean-Yves Dieulot
ENSAM de Lille
Research Technological Team CEMODYNE
8 bd Louis XIV, 59000 LILLE Cedex
E-mail: jean-yves.dieulot@polytech-lille.fr

Received: November 6, 2006

The Fast Fourier and Hilbert-Huang Transforms: A Comparison

Denis Donnelly

Abstract: The conversion of time domain data via the fast Fourier (FFT) and Hilbert-Huang (HHT) transforms is compared. The FFT treats amplitude vs. time information globally as it transforms the data to an amplitude vs. frequency description. The HHT is not constrained by the assumptions of stationarity and linearity, required for the FFT, and generates both amplitude and frequency information as a function of time. The behavior and flexibility of these two transforms are examined for a number of different time domain signal types.

Keywords: fast Fourier transform, Hilbert-Huang transform, data analysis

1 Introduction

A common approach in spectrum analysis for extracting frequency information from time series data is to use the fast Fourier transform (FFT) [DON, 05]. A more recent method [HUA, 98], [HUA, 05], which generates amplitude and frequency vs. time spectra, is the Hilbert-Huang transform (HHT). These two approaches are fundamentally different. The FFT assumes stationarity and linearity of the data and relies on globally defined orthogonal basis states. The HHT does not require the same assumptions of the data. In order to represent nonlinear and nonstationary data, global basis states must be replaced with adaptive, locally determined ones, a process the first stage of the HHT does perform. The resulting basis states are, in general, not strictly orthogonal.

After a very brief review of the FFT, the HHT is described. The comparative behavior of the two transforms is then explored. Various data sets with different signal characteristics are examined. Finally, the chirp of a bat is analyzed.

2 The Fast Fourier Transform

The fast Fourier transform (FFT) provides an efficient algorithm for converting data from the time domain into the frequency domain. Typically, the data to be transformed consists of N uniformly spaced points $x_j = x(t_j)$ where $N = 2^n$ with n an integer, and $t_j = j\Delta t$ where j ranges from 0 to $N - 1$. The discrete Fourier transform can be expressed in several ways. A commonly used form is the following (with $i = \sqrt{-1}$):

$$X_k = \sum_{j=0}^{N-1} x_j \exp(-2\pi i \frac{j}{N} k) \quad (1)$$

where $k = -N/2, \dots, -1, 0, 1, \dots, N/2 - 1$ and where x_j represent the time domain data and X_k their representation in the frequency domain. The algorithm for the FFT conversion process (Cooley-Tukey or any of several other comparable algorithms) makes the FFT widely applicable as it reduces the number of computations from something on the order of n^2 to $n \log n$ which obviously provides an enormous reduction in computation time.

The frequency data are typically displayed in one of two ways: an amplitude spectrum or a power spectrum. The amplitude spectrum is typically expressed by the relation

$$A_k = \frac{2}{N} |X_k|. \quad (2)$$

Whereas the power spectrum is typically expressed by the relation

$$P_k = \frac{1}{N} |X_k^2|. \quad (3)$$

where $k = 0, 1, \dots, N/2$.

3 The Hilbert-Huang Transform

The Hilbert-Huang transform is carried out in two stages: 1) the empirical mode decomposition (EMD) process, which deconstructs the signal into a set of intrinsic mode functions (IMF) and 2) the extraction of frequency vs. time information from each of the IMF's in combination with its Hilbert transform (HT). A brief summary of the process for discretely sampled signals follows.

The EMD process deconstructs the original signal into a set of IMF's. Each IMF, extracted from the signal by a series of siftings, has two fundamental properties: 1) the number of extrema and the number of zero crossings differ, at most, by one and 2) the mean value of the envelopes defined by the local maxima and local minima is zero. Unlike the harmonic functions of a Fourier series, these oscillatory functions may vary in both amplitude and frequency over time. In this decomposition process, the first IMF contains the highest frequencies associated with the original signal; each subsequent IMF contains lower-frequency components.

Amplitudes and frequencies are extracted from these IMF's in the second stage of the HHT process. The instantaneous amplitude and angular frequency associated with each IMF depend on the amplitude and phase of a complex number that the IMF and its Hilbert transform (HT) define. The real part of the complex number is the IMF; the imaginary part of the number is the IMF's HT. The instantaneous amplitude is the amplitude of this complex number. The instantaneous angular frequency associated with that IMF is the derivative of the unwrapped phase. The entire process is repeated for each IMF to extract the complete frequency versus time information from the original data.

The computation of the HT is essentially a convolution of an IMF, $x(t)$, with $1/t$. The effect of this convolving is to emphasize the local properties of $x(t)$. This locality preserves the time structure of the signal's amplitude and frequency.

The EMD process is designed to deconstruct the complete signal into a set of IMFs, each of which is extracted from a starting data set via a sifting process. This sifting process is repeated until the criteria listed above are satisfied and the difference between successive siftings is suitably small (there is some discussion as to what the terminating difference between siftings should be; it depends to some extent on the data set being examined). The process of extracting IMF's terminates when the residual contains no significant frequency information.

This sifting process comprises several steps. Given a discretely sampled signal $y(t)$,

1. Determine the location of all maxima, $y_{max}(t)$, and minima $y_{min}(t)$ $y(t)$.
2. Fit a cubic spline through the $y_{max}(t)$ and another through the $y_{min}(t)$.
3. Calculate the mean of the spline curves at each point

$$m(t) = (y_{max}(t) + y_{min}(t))/2$$

4. Remove the trend, $m(t)$. Let $d(t) = y(t) - m(t)$.
5. Is $d(t)$ an IMF? If $d(t)$ meets the criteria defining an IMF, let $c_i(t) = d(t)$ and advance i by 1. Extract the residual $r(t) = y(t) - d(t)$. If $d(t)$ doesn't meet the criteria, further sifting is required. Repeat steps 1 through 5, substituting $d(t)$ for $y(t)$.

6. Repeat steps 1 through 5 until the residual no longer contains any useful frequency information.

The original signal is, of course, equal to the sum of its parts. If we have N IMFs and a final residual $r_N(t)$,

$$y(t) = \sum_{i=1}^N c_i(t) + r_N(t) \quad (4)$$

The second stage of the HHT process extracts the amplitude and frequency information from each IMF. The steps for amplitude and frequency extraction from a given discrete IMF are as follows:

1. Compute the IMF's discrete Fourier transform (DFT) using the series expression (1) for the transform.
2. Compute the HT. Use the real and imaginary parts of step 1's DFT as coefficients ($M = N/2$):

$$y_j = \frac{1}{N} \sum_{k=0}^M \left(\text{Re}(X_{k1}) \sin(2\pi k1 \frac{j}{N}) + \text{Im}(X_{k1}) \cos(2\pi k1 \frac{j}{N}) \right) + \left(\frac{-1}{N} \right) \sum_{k=M+1}^{N-1} \left(\text{Re}(X_{k2}) \sin(2\pi k2 \frac{j}{N}) + \text{Im}(X_{k2}) \cos(2\pi k2 \frac{j}{N}) \right) \quad (5)$$

3. Form the complex number $z_j = x_j + iy_j$, extract the phase $\phi_j = \tan^{-1}(y_j/x_j)$.
4. Unwrap the phase so that it becomes a monotonically increasing function.
5. Determine the frequency. Take the derivative of the phase

$$f_j = \frac{1}{2\pi} \frac{d\phi_j}{dt}$$

6. Determine the amplitude.

$$a_j = \sqrt{x_j^2 + y_j^2}$$

4 Examples

The first examples treat cases where the signal in the time domain has the properties of an IMF and no sifting is required. The examples are chosen to demonstrate the responses of the FFT and HHT to changes in frequency and amplitude of the time domain signal.

The first signal considered consists of two cycles of a sine wave with frequency equal to one followed after a brief pause by four cycles of a sine wave with a frequency equal to two. Fig. 1 shows both the signal and its HHT. The oscillations in the HHT are typical and vary only slightly with the amplitude of the original signal. The low frequency end of the FFT for this example is shown in Fig. 2. While it does show the major peaks at frequencies equal to one and two, it has a rather rough appearance. The complex structure of the FFT arises because, in effect, the FFT has to create a Fourier series to fit the signal comprising both the two frequencies as well as the portions where the signal is zero.

The second signal has a fixed frequency sine wave with amplitude increasing with time. The HHT, Fig. 3, is not daunted by this amplitude variation. The FFT on the other hand has an amplitude which is consistent with an average value of the peak amplitudes for the time domain data.

The third signal, a chirp, has a constant amplitude and a variable frequency which increases over time by one order of magnitude. The HHT provides an accurate representation of the frequency as long as the signal is sampled with sufficient frequency. If the number is too small the oscillations in the frequency curve grow and can have negative values. Fig. 4 shows the frequency response; here $N=2048$ and there

are more than twenty computed sample points in the last (highest frequency) cycle. The FFT (Fig. 5.) is nearly constant for the frequency spanned but drops off near the ends.

An example which clearly contrasts the behavior of the FFT and HHT and which demonstrates which process is more correct physically, is that of a sum of two sine waves with frequencies close enough to readily show a beat pattern ($f_1 = 1$, $f_2 = 1.08$). The FFT of such a pattern is shown in Fig. 6. The two original frequencies are clearly present in the amplitude spectrum. The HHT on the other hand generates a single frequency of 1.04 which is an average of the two sine wave frequencies. (When dealing with signals that show a beat pattern, for example, artifacts are likely to appear in the frequency representation near the nodal points of the signal.) The HHT amplitude function follows the beat pattern as an envelope. While the description of the beat signal as a sum of two individual frequency signals is mathematically equivalent to a single signal with a frequency equal to the average of the two frequencies used to construct the signal, times an amplitude modulating function with a frequency equal to the difference in frequency of the two signals, the two different representations are not equivalent physically. The HHT provides the physically correct frequency description; the instantaneous frequency is the average frequency. This is an important notion that is worth emphasizing. We are used to talking about the harmonic content of signals, which is a mathematically correct description, but it may not be the best representation of what is actually taking place.

It is interesting to observe what happens to the amplitude spectrum of the FFT, as a smaller and smaller number of cycles of the pattern are subjected to analysis. If the number of cycles is small enough that the signal does not go beyond the first node of the envelope, then the FFT shows only one peak at the average value of the two frequencies.

The HHT cannot treat functions such as a single cycle of a square wave as there are no maxima and minima to fit, while the FFT can readily analyze such a signal. If a small amplitude sine wave is made to ride on top of a square wave, for example, the HHT will recognize the sine wave away from the transition region. Near the step transition, the frequency response shows a large spike.

It is useful to know how differing frequencies are distributed during the EMD process. An estimate can be obtained by taking the FFT's of the first and second IMF's as the difference between two frequencies is increased. From this, we can observe the behavior of the sorting process. For example, a factor of two or greater in the frequencies is needed to shift the lower frequency signal well into the next IMF (see Table 1). For example, if the EMD process is applied to a signal comprising frequencies 1 and 0.5, the first IMF yields an average frequency value of 1 with fluctuations ranging approximately from 0.96 to 1.05; the second IMF yields an average value of 0.5 with the fluctuations ranging from 0.49 to 0.51.

Frequency 2	Peak Amplitude Frequency 1 = 1	Peak Amplitude Frequency 2 IMF1	Peak Amplitude Frequency 2 IMF2
0.95	526	489	
0.9	521	482	
0.8	516	444	14
0.7	513	362	55
0.6	510	188	178
0.5	507	34	327
0.4	508		409

For a final application, we look at the chirp of a bat: 400 data points sampled at 7 intervals. The bat's chirp does consist of frequencies decreasing over time, consequently, an FFT of the entire signal would not yield useful information. Instead, to use the FFT, a sliding window approach is used [DON, 06]. For example, look at 64 point subsets of the entire data set. In this time range, the inherent frequency structure is revealed. As this short window slides along, the changing frequencies can be tracked. The HHT of the chirp, shows information of interest in the first and second IMF's. Results are shown in Fig. 7. The

second harmonic had too small an amplitude for the HHT process to recognize it. Both analysis forms would benefit from a shorter sampling interval. In the figure, the fit to the fundamental is proportional to $\exp(-const \sqrt{t})$. The fit to the first harmonic is simply two times that of the fundamental. Because of the complexity of the signals in the figure, the FFT results for the sliding window technique are not shown. But they approximate the fitted lines shown in the figure. There is a weak second harmonic which can be extracted from the data when using the FFT process. However, that signal is too weak for the HHT to recognize.

5 Final Comments

The combination of sifting associated with the EMD process, and then taking the HT, unwrapping the phase, and taking the derivative of each IMF is computationally much more demanding than taking the FFT. However, the HHT not only provides instantaneous frequency and amplitude descriptions, it results in representations that are more meaningful physically.

Acknowledgments: I thank Curtis Condon, Ken White and Al Feng of the Beckman Institute of the University of Illinois for the bat chirp data and for permission to use it in this article. I thank Edwin Rogers for helpful comments.

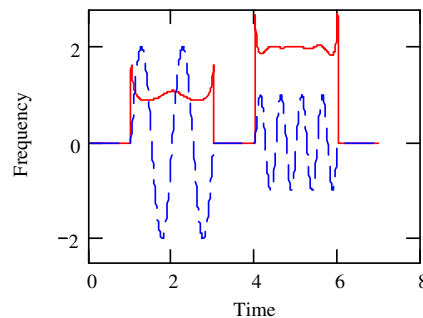


Figure 1: HHT frequency representation (solid line) of the time domain signal (dashed).

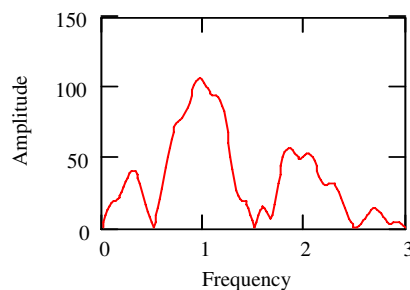


Figure 2: FFT amplitude spectrum (solid line) of the (dotted) signal shown in Fig. 1. Only the lower frequencies are displayed for emphasis.

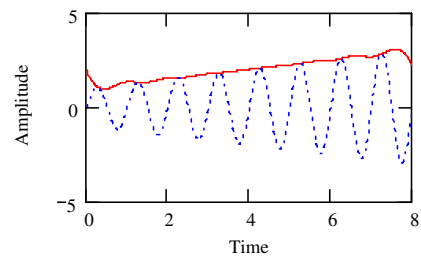


Figure 3: HHT amplitude spectrum (solid line) of the (dotted) signal.

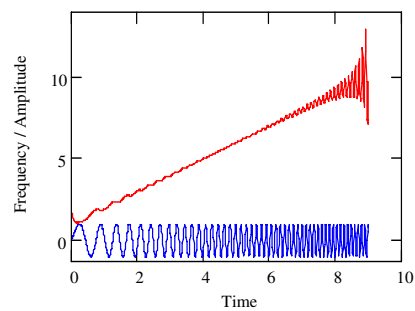


Figure 4: HHT frequency representation of a chirp signal. The HHT follows the increase in chirp frequency as it scales from one to ten. The amplitude one chirp signal is also shown.

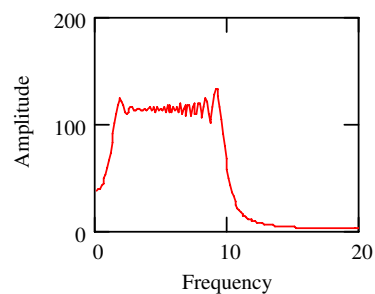


Figure 5: FFT of a chirp signal with a frequency ranging from one to ten. Only the lower frequencies are displayed for emphasis.

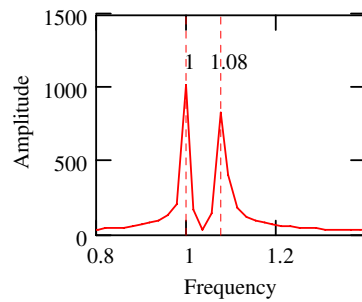


Figure 6: The FFT of a signal consisting of the sum of two sine waves with frequencies 1 and 1.08. Only a portion of the FFT is shown for emphasis.

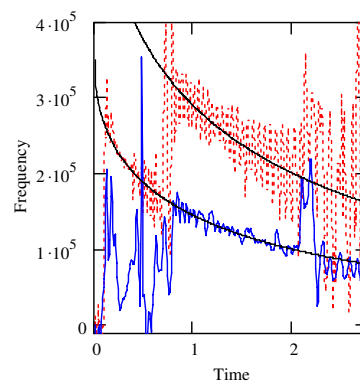


Figure 7: Frequency vs. time of a bat chirp as determined via HHT. The fluctuating curves represent the HHT results. The solid curve corresponds to the fundamental. The dotted curve is the first harmonic. The two smooth curves are fits to the data.

References

- [1] Denis Donnelly and Bert Rust, "The Fast Fourier Transform for Experimentalists: Part I Concepts," *Computing in Science & Eng.*, vol. 7, no. 2, pp. 80-88, 2005.
- [2] Denis Donnelly, "The Fast Fourier Transform for Experimentalists: Part VI Chirp of a Bat," *Computing in Science & Eng.*, vol. 8, no. 2, pp. 72-78, 2006.
- [3] Norden E. Huang et. al., "The empirical mode decomposition and the Hilbert spectrum for nonlinear and non-stationary time series analysis," *Proc. R. Soc. Lond. A.*, vol. 454, pp. 903-995, 1998.
- [4] Norden E. Huang and Samuel Shen, Eds. New Jersey: World Scientific, 2005.

Denis Donnelly
Siena College
Department of Physics
Loudonville, NY 12211
E-mail: donnelly@siena.edu

Received: November 8, 2006

An Iterative Method for the Design Process of Mode Handling Model

Nadia Hamani, Nathalie Dangoumau, Etienne Craye

Abstract: This paper focuses on formal verification and validation of a model dedicated to *mode handling* of flexible manufacturing systems. The model is specified using the synchronous formalism Safe State Machines. A structured framework for the design process is presented. The obtained model is characterized by a strong hierarchy and concurrency that is why within the design process an iterative approach for specification, verification and validation is proposed in order to improve this process. The main properties being verified are presented and the approach is illustrated through an example of a manufacturing production cell.

Keywords: Flexible Manufacturing Systems, supervision, mode handling, functional and behavioral modeling, verification, validation.

1 Introduction

According to our design approach of fault tolerant control systems, *mode handling* is a function of supervision. In view of a disturbance (failures, breakdowns) *mode handling* allows implementing the decisions about mode and configuration changing. The design of *mode handling* function needs to provide a model representing the operating modes of the production system and its subsystems. To this aim, it is important to use an adequate modeling method and powerful specification formalisms. Those characterizing the most significant approaches are compared in [9]. We proposed in our early work a modeling approach for reactive *mode handling* of Flexible Manufacturing Systems (FMS) [10]. This approach is based on a functional modeling [11] and a synchronous reactive approach using Safe State Machines (SSM) [1] [2].

Due to increasing complexity and flexibility of FMS, some problems characterize mode changing if coherence and safety constraints are not taken into account in the specification / modeling stages. So it is necessary to verify and validate the proposed models at the early stages of the design process. A greater interest has been allocated for few years to formal verification methods, which guarantee that for all possible evolutions of a model, several properties are satisfied. For our modeling approach, one of the interests of using SSM formalism relies on its strong semantics leading to the possibility of using analysis tools in order to formally prove that the behavior of the system respects some properties.

The purpose of this paper is to present the iterative approach used in the design process of the model dedicated to *mode handling*. The paper is organized as follows. In section 2 the basic concepts of V&V are reminded and the design process based on formal methods is introduced. The stages of this design process including V&V are detailed in section 3 and section 4. The iterative approach is introduced and the main properties being verified within the design process are presented. Finally the approach is illustrated using an example of a flexible manufacturing cell.

2 The design process

A design process should involve many intermediary stages of V&V. This enables to detect and eliminate as soon as possible the specification or modeling errors. The modifications are thus carried out with a lower cost in particular in the final step. Indeed, V&V characterize any correct development process. According to [14] verification is the proof that the internal semantics of a model is correct independently of the modeled system whereas validation determines if the model corresponds to the

attempts of the designer formulated in the functional requirements. The required properties are either **generic**, they depend on the formalism we use, or **specific** to the modeled system.

V&V consists of analyzing the properties that should be satisfied by the final model using some analysis tools. Two complementary **methods** exist, simulation and formal verification. We are interested in our study only in **formal methods** for V&V. For formal verification, we have to build a formal model representing the behavior of the system and formal specifications of the properties. Fig. 1 shows the design process including V&V:

- The formal specification as well as the structured modeling process that we remind in the next section, allow ensuring a correct development process.
- V&V of the obtained model is an iterative approach characterized by some corrections, which require reconsidering the specification/modeling stages as needed.
- Based on the verified and validated model the implementation is ensured through automatic code generation.

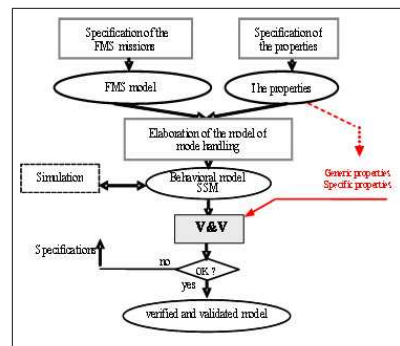


Figure 1: The design process

3 Specification/Modeling

The functional requirements provide the informal specifications about *mode handling* function: the intended behavior of the FMS and the properties that should be satisfied. Other properties such as determinism are also mandatory. The designer formalizes those informal requirements to provide **formal specifications** of the model, of the required properties and, if necessary, some assumptions about the environment. The **formalization** task provides the following models.

3.1 The formal model representing the behavior of the system

The specifications of the model dedicated to FMS *mode handling* are detailed in our earlier work [10][11]. We remind in the following the main characteristics of the modeling process.

The FMS subsystems. In our approach, an operating sequence characterizes each part. The specification method of FMS subsystems was described in [11]. The idea is to decompose and identify the functional subsystems, which take part in the realization of its missions. A mission corresponds to a set of operating sequences that the system should produce simultaneously. The FMS functional model is obtained by a hierarchical decomposition leading to the elementary machining and transfer operations that the FMS performs. The structural aspect completes this specification by associating the resources to the elementary operations they perform. The obtained subsystems are organized in six layers as shown in Fig. 2.

The functional representation is a graph composed of functional subsystems (called entities) linked by logical relationships (AND, OR). OR nodes correspond either to an inclusive or an exclusive logical operator according to the constraints given in the functional requirements.

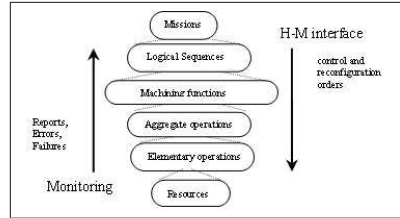


Figure 2: The FMS functional model

Behavior specification. Given the FMS functional model, one should provide behavioral specifications. It is necessary to represent the activation and deactivation mechanisms at all the hierarchy levels of the specification as well as the availability of the resources and the functions of the FMS. The activation/deactivation of an entity is represented by the working mode. The functioning mode represents the availability/unavailability of an entity. The aim is to handle concurrently the information flows downwards to transmit high-level control and reconfiguration orders and upwards to follow up the reports and failures detected by the monitoring function. The reactivity needed for this bi-directional exchange of information, in addition with the characteristics of concurrency and preemption, require a synchronous approach. The behavior of the identified FMS subsystems and the logical relationships between them are specified using the synchronous formalism SSM [1][2]. SSM inherits many features from Statecharts [12] but offers several forms of preemption and benefits of more strict semantics fully compatible with that of Esterel synchronous language [4]. SSM supports also, with a very rigorous semantics, hierarchy, communication, concurrency, and various forms of preemption, which characterize our modeling approach. In addition, SSM takes advantage of an industrial development environment [7], which provides necessary tools for a design process.

The behavior of each entity of the model, whatever its level, is represented by a SSM model. This model allows knowing, at any time, if an entity belonging to the current mode of the FMS is in normal state e_N , degraded state e_D or out of order state e_OUT according to the functioning mode point of view; and if it is activated x_Active or inactive (in stopping state) e_OFF according to the working mode point of view.

The change-of-state of the entities of the model belonging to successive levels is carried out according to precise rules which depend on the kind of the logical relation and the number of child entities. Several cases are studied in [10].

For the representation of the model, we proposed some reference models specified using SSM [10]. These are generic models depending on the number of the child entities and the logical relationships that connect them. The reference models are instantiated for each entity of the model. The proposed method is iterative, it is necessary to specify the models of level i , then we encapsulate the SSM of level i in the SSM of level $i+1$ until completing the specification of the model (see Fig. 3). The encapsulation of the models enables representing the hierarchical levels which characterize the model. The aim is to improve the legibility in the specification/modeling stage. The hierarchy is represented using the encapsulation of successive levels whereas the entities belonging to the same level are separated by dashed lines; these are used to represent concurrency in SSM syntax (see [2]).

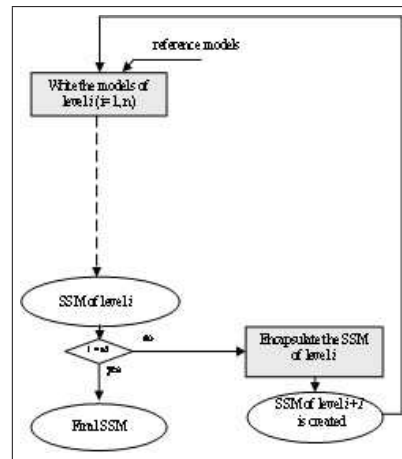


Figure 3: The modular specification

3.2 The formal specification of properties

Predictability and dependability are the main characteristics of reactive systems. In our work, we consider only properties of logical behavior such as *determinism* and *safety properties*. As we adopt a reactive synchronous approach based on SSM formalism, **generic properties** of reactivity and determinism should be verified. The rigorous semantics of SSM enable to provide formal verification mechanisms ensuring such properties. Several **properties specific** to *mode handling* function can be verified. The main properties are presented in section 4.

4 Verification and validation

In the verification stage (Fig. 1), one checks if the model satisfies **generic properties**. SSM specifications are automatically translated into Esterel program which is compiled in a system of Boolean equations (logical circuits) an implicit form of Finite State Machines (FSMs). The properties of logical correctness of Esterel programs can then be verified on this system. The **analysis technique** used to this aim is the constructive causality analysis carried out by Esterel compiler v5_x. Causality analysis is a semantic analysis which allows accepting or rejecting Esterel programs according to whether they are constructive or not [5]. The processor which implements the algorithms of constructive analysis builds the reachable state space using symbolic techniques based on Binary Decision Diagrams (BDD).

One checks in the validation stage if the model satisfies the **specific properties** formalized in the specification stage. The **analysis techniques** used are *model-checking* and/or *theorem proving*. Several *model-checking* tools were developed for Esterel language. For instance *Built-in verifier* tool an evolution of XEVE (*XEsterel VErifier*) [6] is currently integrated into Esterel Studio. XEVE takes as input the system of Boolean equations and built the reachable state space using BDD (symbolic *model-checking* [13]) in order to check the statutes of output signals of the model or the observers [8] representing the properties.

Failing of V&V stage implies that there is a specification or a modeling error. It is then necessary to go back over this model as needed. The formal specifications are may be incorrect. The errors are either in the specifications of: the model, the property, the correspondence between the model and the property or the assumptions related to the environment.

If the specification/modeling stages are considered to be correct then we should reconsider informal requirements. Indeed, within the formal specification of the model or the properties, errors are may be caused by the ambiguity or the incompleteness of the informal requirements provided in the functional

requirements. In this case, these requirements must be improved and formalized again.

We propose to complete the modular and hierarchical specification shown in Fig. 3 by introducing an iterative method of V&V. This method is presented in the following. The aim is to reduce the specification/modeling errors and to enable their early correction by introducing intermediate stages of V&V into the multi level specification stage.

4.1 An iterative method for V&V

We propose at first to check each single reference model used for the specification of the model. The aim is to prove reactivity and determinism. The verification of these reference models is performed using the analysis tools integrated into Esterel Studio environment.

The single verification of the reference models:

For each reference model

Write the model

Verify the model

If the verification fails, correct the specification and repeat the verification as needed.

The single reference models checked in this way are instantiated in order to obtain the behavioral models of the FMS subsystems. Then the integration of these models allows editing progressively the whole model. Using the SSM graphical editor, the best way is to follow a bottom up approach based on the encapsulation of SSM of level i in the SSM of level $i+1$. At each level we should be sure that the intermediary SSM satisfies some properties and the accumulation of errors will be avoided. That is why we propose to associate with this specification an iterative method of V&V. If the V&V does not converge then it is necessary to correct the specification and to repeat the V&V process as needed. Indeed, V&V is carried out in an iterative way until the whole model (the final SSM) will be verified and validated. The method described in the following is represented in Fig. 4.

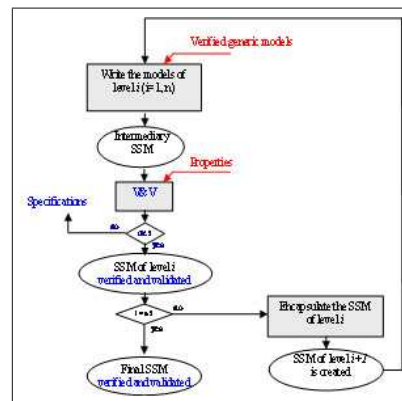


Figure 4: The iterative V&V

Repeat for all the models of level i ($i = 0, n$)

(1) Write the models of level i

The specification is carried out by instantiation of the predefined and verified models

(2) Verify then validate the SSM of level i

If the V&V fails, correct the specification and repeat the previous step as needed

If $i = n$ go to (4) if not

(3) Encapsulate the models of level i 'SSM of level $i+1$ is then created'

$i = i + 1$

End of the procedure

(4) *The SSM represents the FMS model (the top level corresponds to the whole model)*
If the previous steps converge, we conclude that the final SSM is verified and validated. When the final SSM is verified and validated, the code could be generated.

The properties being verified within this process are presented in the following.

4.2 The properties

The model dedicated to *mode handling* is translated automatically into Esterel language. Esterel compiler is composed of several processors for type checking, syntactical and lexical analysis. Semantic analysis also called causality analysis allows checking **generic properties** (deadlock freeness, reactivity, determinism).

Deadlock freeness. Causality analysis makes it possible to prove that the program is causal according to the constructive causality defined by Berry [5]. Constructive causality of Esterel programs ensures deadlock freeness, which characterizes synchronous languages. Deadlocks are due to the synchronism assumption (see causality problems in [3]).

Reactivity and determinism. If an Esterel program is constructive then it is reactive and deterministic. A program is said to be reactive if it provides a well-defined solution for each input. It is deterministic if this solution is unique [5].

The aim of **specific properties** is to ensure coherence and safety constraints of *mode handling*. We have proposed three kinds of safety properties: mode reachability, the mission uniqueness of a FMS and mutual exclusion of incompatible modes.

States reachability. We can check the reachability of the states specified by the model (according to the specifications, an output signal is associated with each control state of the model). To this aim, the statutes of output signals that correspond to control states of the model are tested.

The mission uniqueness of a FMS. This property ensures operation safety of the FMS according to the selected mission. Indeed, selecting a mission implies performing some operations and activating the resources, which take part in this mission. Thus, the operations and the resources, which do not take part in the current mission, should not be activated for safety and coherence reasons. The property is guaranteed by construction of the model.

Incompatibility of the modes. In order to ensure mode coherence, the proposed specifications guarantee mutual exclusion of incompatible states (each state is belonging to a distinct mode) of the entities of the model. It is about mutual exclusion of working states of the entities related with the logical relation XOR (for example redundant resources).

The previous properties are verified within the iterative approach of V&V. The intermediate verifications are important because if causality cycles are detected early their correction will be easier. Contrary to verification, intermediate validations are may be expensive and some properties are checked only on the final model, in particular the properties related to the uniqueness of the FMS mission.

In addition to the main properties, other properties of *mode handling* model can be checked. They deal with the conditions of mode changing and the respect of modes sequence [10].

5 Illustration

We have applied our approach to the example of the cell represented in Fig. 5. This cell consists of two machines M1, M2 and input/output buffers (I/O). The transport system is composed of two robots R1, R2. We suppose that M1 is loaded by R1 and M2 is loaded by R2, this later will be used to load the

two machines when R1 is failing. The machining functions performed by this system are turning and milling. Turning (t) is carried out by M1, milling (f) by M1 or M2. The cell has three missions, *M1*, *M2* and *M3*. The corresponding operating sequences are respectively OS1 (t), OS2 (f) and then OS1 and OS2 simultaneously.

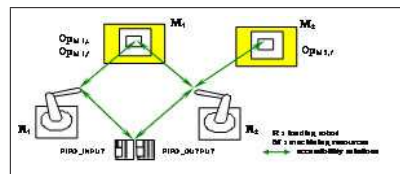


Figure 5: Illustration example

The obtained model using our modeling method is specified using 4 reference models and 29 instances for 809 lines of Esterel code generated from the SSM models. This model needs 34 input signals and 145 output signals.

We simulated at first some scenarios of behavior in order to correct the specification errors so that the intended behavior will be in conformity with the functional requirements. The interactive simulator XES [7] is used.

The studied cell can be extended with addition of machining resources (simple or polyvalent) and redundancies of the transport system (robots, conveyor). This allows studying the problem with increasing complexity. For the specification, adding or removing reference or instantiated models enable integrating easily the changes on the model thanks to the modularity and the hierarchy of the specification approach. However, due to increasing complexity of the cell some tests performed by the model-checker could not be concluded (out of memory problem). We try to solve this problem in a future work.

6 Summary and Conclusions

This paper deals with V&V within the design process of a model dedicated to *mode handling* of FMS. The first contribution of this study is a structured process for carrying out V&V. It is an extension of our control system design approach in order to take into account V&V stage. An iterative method is used for specification and V&V stages of the design process. The aim is to refine the model construction by introducing intermediate steps of V&V for an early correction of errors. Within the proposed framework the required properties (determinism, reachability, mutual exclusion of incompatible modes,..) are given. The analysis tools integrated into Esterel Studio are used in this process.

The proposed approach can be extended to deal with environment constraints in the specification stage. In addition, further work aims at studying some examples of increasing complexity.

References

- [1] C. André, Representation and Analysis of Reactive Behaviors: A Synchronous Approach, in Proc. of the IEEE-SMC Computational Engineering in Systems Applications (CESA 96), Lille, France, July, 1996, pp. 19-29.
- [2] C. André, Semantics of SSM (Safe State Machines), Guyancourt, France, April 2003, Available at: <http://www.esterel-technologies.com>
- [3] A. Benveniste, P. Caspi, S. Edwards, N. Halbwachs, P. Le Guernic, and R. de Simone, The Synchronous Languages Twelve Years Later, in Proc. of the IEEE, 91(1), special issue on Embedded Systems, pp. 64-83, 2003.

- [4] G. Berry, G. Gonthier, The Esterel synchronous programming language: design, semantics, implementation, *Science of Computer Programming*, Vol. 19(2), pp. 87-152, 1992.
- [5] G. Berry, *The constructive semantics of pure Esterel* Draft version 3, 1999, Available at: <http://www.esterel-technologies.com>
- [6] A. Bouali, XEVE an Esterel Verification Environment, in Proc. 14th Int. Conf. on Computer Aided Verification CAV'98, LNCS, UBC, Vancouver, Canada, June 1998.
- [7] Esterel Studio™, Available at: <http://www.esterel-technologies.com>.
- [8] N. Halbwachs, F. Lagnier and P. Raymond, Synchronous observers and the verification of reactive systems, in Proc. of AMAST'93, 1993.
- [9] Hamani N, Dangoumau N, Craye E, A comparative study of mode handling approaches, in Proc. of the 35th International Conference on Computers & Industrial Engineering (CIE 05), Istanbul Turkey, June 19-22, 2005.
- [10] N. Hamani, A contribution to modeling and verification for mode handling of manufacturing systems, PhD dissertation, Ecole Centrale de Lille, France, 2005 [in french].
- [11] N. Hamani, N. Dangoumau, E. Craye, Functional modeling for mode handling of Flexible Manufacturing Systems, in Proc. 12th IFAC Symposium on Information Control Problems in Manufacturing, Saint Etienne, France, 2006.
- [12] D. Harel, StateCharts: a visual approach for complex systems, *Science of Computer Programming*, Vol. 8, n°3, pp. 231-275, 1987.
- [13] K.L. McMillan, *Symbolic Model Checking*, Kluwer Academic Publishers, 1993.
- [14] J.M. Roussel, and J.J. Lesage, Validation and Verification of Grafcet using finite state machines, in Proc. of IMACS-IEEE Multiconference on Computational Engineering in Systems Applications, Lille, France, 1996, pp. 758-764.

Nadia Hamani, Nathalie Dangoumau, Etienne Craye
Laboratoire d'Automatique, Génie Informatique et Signal (LAGIS), CNRS UMR 8146
Ecole Centrale de Lille, BP. 48, Villeneuve d'Ascq, F-59650 France
E-mail: nadia.hamani@ec-lille.fr

Received: November 6, 2006

Time Disturbances and Filtering of Sensors Signals in Tolerant Multi-product Job-shops with Time Constraints

Nabil Jerbi, Simon Collart Dutilleul, Etienne Craye, Mohamed Benrejeb

Abstract: This paper deals with supervision in critical time manufacturing job-shops without assembling tasks. Such systems have a robustness property to deal with time disturbances. A filtering mechanism of sensors signals integrating the robustness values is proposed. It provides the avoidance of control freezing if the time disturbance is in the robustness intervals. This constitutes an enhancement of the filtering mechanism since it makes it possible to continue the production in a degraded mode providing the guarantees of quality and safety. When a symptom of abnormal functioning is claimed by the filtering mechanism, it is imperative to localize the time disturbance occurrence. Based upon controlled P-time Petri nets as a modeling tool, a series of lemmas are quoted in order to build a theory dealing with the localization problem.

Keywords: P-time Petri net, sensor signal, filtering, time disturbance, localization

1 Introduction

This paper concerns critical time manufacturing job-shops. For each operation is associated a time interval. Its lower bound indicates the minimum time needed to execute the operation. The non respect of this value means that the operation was not achieved. The upper bound fixes the maximum time to not exceed otherwise the quality of the product is deteriorated. Such systems have a robustness property in order to maintain product quality when there are time disturbances [1], [2]. The robustness is defined as the ability of the system to preserve the specifications facing some expected or unexpected variations. So the robustness characterizes the capacity to deal with disturbances. The robustness is interpreted into different specializations. The passive robustness is based upon variations included in validity time intervals. There is no control loop modification to preserve the required specifications. On the other hand, active robustness uses observed time disturbances to modify the control loop in order to satisfy these specifications. Therefore, the robustness intervals must be integrated in the filtering mechanism of sensors signals. Furthermore, the observability of time disturbances occurrence is a fundamental data necessary for the control loop modification. It is also an important aspect of the maintaining task [3], [4]. When an abnormal functioning is claimed, it is important to know the initial occurrence of the disturbance. The localization problem is really difficult in robust systems since the rejection of disturbances may hide them [5].

The first part of this paper presents a filtering mechanism of sensors signals taking into account the robustness values. The second part considers the localization of time disturbances. It is necessary to perform this task when the disturbance value passes through the filter. Controlled P-time Petri nets are used for modeling the considered workshops. Afterward, the localization problem of time disturbances in critical time manufacturing systems is tackled. Some definitions and lemmas are quoted in order to build a theory dealing with such problems.

2 Robustness integration in the filtering of sensors signals

At the occurrence of a dysfunction in a manufacturing workshop, it is crucial to react as soon as possible to maintain the productivity and to ensure the safety of the system. It has been recognized that

the real time piloting, without human intervention, has a significant contribution regarding this type of problem [6], [7].

In the category of the workshops concerned by this article, the operations have temporal constraints which must be imperatively respected. The violation of these constraints can blame the health of the consumers. Thus, the detection of a constraint violation must automatically cause the stop of the production. On the other hand, when taking into account the system robustness, it is proven that this type of violation did not take place. In this case, we plan to maintain the production while describing it as degraded production [8]. Of course, the product is not degraded, but the production is degraded because the deliveries moments of the products are not those envisaged initially. It is this context which we propose to integrate in the generation of symptoms as it was presented in [9].

The finality of this section is not to contribute to the state of the art of the monitoring-diagnosis, but to show how the knowledge of the robustness could make the supervision more efficient. By considering this criterion, the filtering of sensors signals of [9] appears pedagogically interesting.

2.1 Symptoms generation

The idea consists in modeling any operation from a temporal approach. At each operation A_i is associated a sensor signal CR_i . At each sensor signal CR_i is associated a temporal window $[\Delta t_{m/CR_i}, \Delta t_{M/CR_i}]$ (Figure 1). CR_i is valid only inside this window. $\Delta t_{m/CR_i}$ and $\Delta t_{M/CR_i}$ are defined relatively to the beginning of the operation A_i (Start-Event). The filtering principle is to position the temporal window of each sensor signal CR_i when his Start-Event was received. Two types of symptoms are distinguished [9].

Symptoms type I noted S_i^1 : this class of symptoms corresponds to awaited sensor signal which is not received at $\Delta t_{M/CR_i}$. The detection mechanism of this symptom type corresponds to the traditional mechanism of watchdog, but implemented in a separate way of the control. Symptoms type II noted S_i^2 : it is generated by the occurrence of a sensor signal which is not expected. Two cases are considered. The first one corresponds to an action but its sensor signal occurs before the validation interval. The second case corresponds to the occurrence of a sensor signal in absence of any order which can create it.

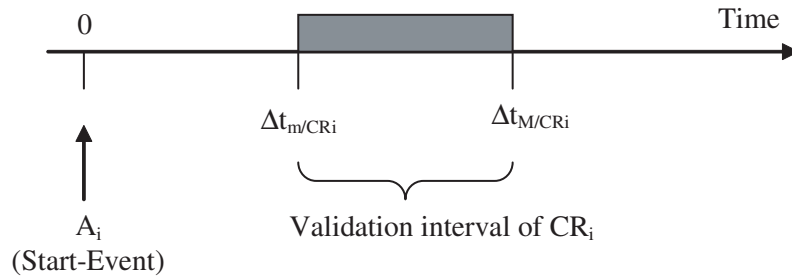


Figure 1: Operation associated model [9]

2.2 Robustness integration

The tool used to represent the filtering mechanism is the interpreted T-time Petri net. Initially, we point out the definition of the interpreted T-time Petri net. After, we give the filtering mechanism of sensors signals integrating the two properties of passive and active robustness.

Definition 1. A T-time Petri net is given by a pair $\langle R; IS' \rangle$, where R is a Petri net and $IS' : T \rightarrow (Q^+) \times (Q^+ \cup +\infty)$ [10].

Definition 2. Interpreted T-time Petri net is a T-time Petri net including an operative part whose state is defined by a set of variables. This state is modified by the operations associated to the places. It determines the value of the conditions (predicates) which are associated to the transitions.

The mechanism of watchdog is easily represented by an interpreted T-time Petri net. For example, figure 2 shows the detection of a normal state and an abnormal one. If the sensor signal arrives in $[t_m, t_M[$, the system is in a normal state. If the sensor signal arrives at the instant t_M , the system is in an abnormal one.

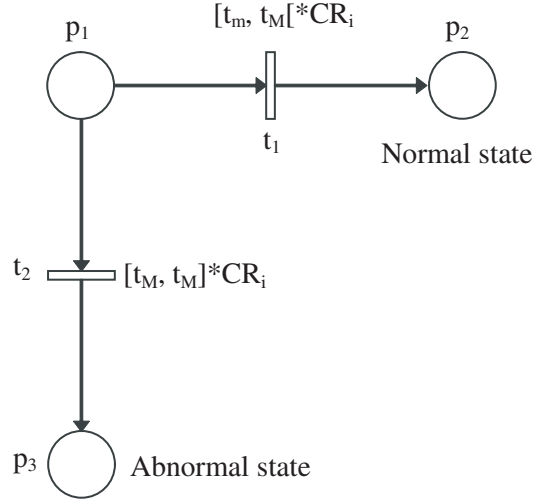


Figure 2: Watchdog mechanism with interpreted T-time Petri net

Within the framework of the robustness integration in the supervision of manufacturing systems with time constraints, we define, figure 3, five time intervals namely:

$$I_{1i} = [\Delta t_{m''}/CR_i, \Delta t_{m'}/CR_i[, I_{2i} = [\Delta t_{m'}/CR_i, \Delta t_m/CR_i[, I_{3i} = [\Delta t_m/CR_i, \Delta t_M/CR_i[, I_{4i} = [\Delta t_M/CR_i, \Delta t_{M'}/CR_i[\text{ and } I_{5i} = [\Delta t_{M'}/CR_i, \Delta t_{M''}/CR_i[.$$

The margin of passive robustness is available in $(I_{2i} \cup I_{4i})$ whereas the margin of active robustness is in $(I_{1i} \cup I_{5i})$. From a functional point of view, there are three intervals of use in which it is possible to prove the validity: interval of normal functioning, interval of passive robustness and interval of active robustness. In the case of an abnormal functioning, there is always duality of advance and delay scenarios.

The adopted filtering mechanism is described by the interpreted T-time Petri net of the figure 4. Several cases can arise [11].

- If there are absence of order (not A_i) and presence of CR_i , there are freezing of the control and generation of a symptom S_i^2 (place p_3).
- If the sensor signal CR_i arrives in the time interval $[0, \Delta t_{m''}/CR_i[$, there are freezing of the control and generation of a symptom S_i^2 (place p_3).
- If the sensor signal CR_i arrives in the time interval $I_{1i} = [\Delta t_{m''}/CR_i, \Delta t_{m'}/CR_i[$, there are change of the control (active robustness to an advance) and memorizing a symptom S_i^2 (place p_4).
- If the sensor signal CR_i arrives in the time interval $I_{2i} = [\Delta t_{m'}/CR_i, \Delta t_m/CR_i[$, there is no change of the control (passive robustness to an advance) but only a memorizing of a symptom S_i^2 (place p_5).
- If the sensor signal CR_i arrives in the time interval $I_{3i} = [\Delta t_m/CR_i, \Delta t_M/CR_i[$, the behavior of the system is normal (place p_6).

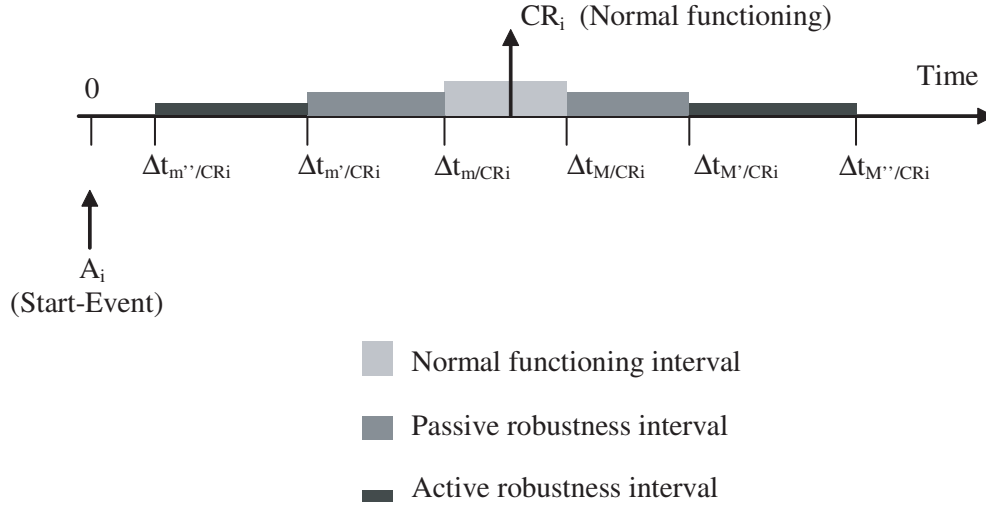


Figure 3: Robustness integration in the operation associated model

- At the instant $\Delta t_{M/CR_i}$ (transition t_7), there is automatically memorizing of a symptom S_i^1 (place p_7).
- If the sensor signal CR_i arrives in the time interval $I_{4i} = [\Delta t_{M/CR_i}, \Delta t_{M'/CR_i}[$, it is a case of passive robustness to a delay (place p_8). The symptom S_i^1 is already memorized (place p_7).
- If the sensor signal CR_i arrives in the time interval $I_{5i} = [\Delta t_{M'/CR_i}, \Delta t_{M''/CR_i}[$, a change of the control is necessary (active robustness to a delay, place p_9).
- At the instant $\Delta t_{M''/CR_i}$ (transition t_{10}), there is freezing of the control (place p_{10}).

3 Localization of time disturbances in a given topology

When, for example, the filtering mechanism executes a control freezing, it is necessary to know where the initial disturbance was occurred. This task is performed on a model of the workshop which uses P-time Petri net in order to integrate the staying time constraints in its structure. This aspect is presented in the following section.

3.1 Controlled P-time Petri net

The formal definition of a P-time Petri net is given by a pair $\langle R; IS \rangle$, where [12]:

- R is a marked Petri net,
- $IS: P \rightarrow (Q^+ \cup 0) \times (Q^+ \cup +\infty)$
 $p_i \rightarrow IS_i = [a_i, b_i]$ with $0 \leq a_i \leq b_i$.

IS_i defines the static interval of staying time of a mark in the place p_i belonging to the set of places P (Q^+ is the set of positive rational numbers). A mark in the place p_i is taken into account in transition validation when it has stayed in p_i at least a duration a_i and no longer than b_i . After the duration b_i the token will be dead.

Using [15], controlled P-time Petri net is defined as a quadruplet $Rpc = (Rp, \varphi, U, U_0)$ such that:

- Rp is a P-time Petri net which describes the opened loop system,

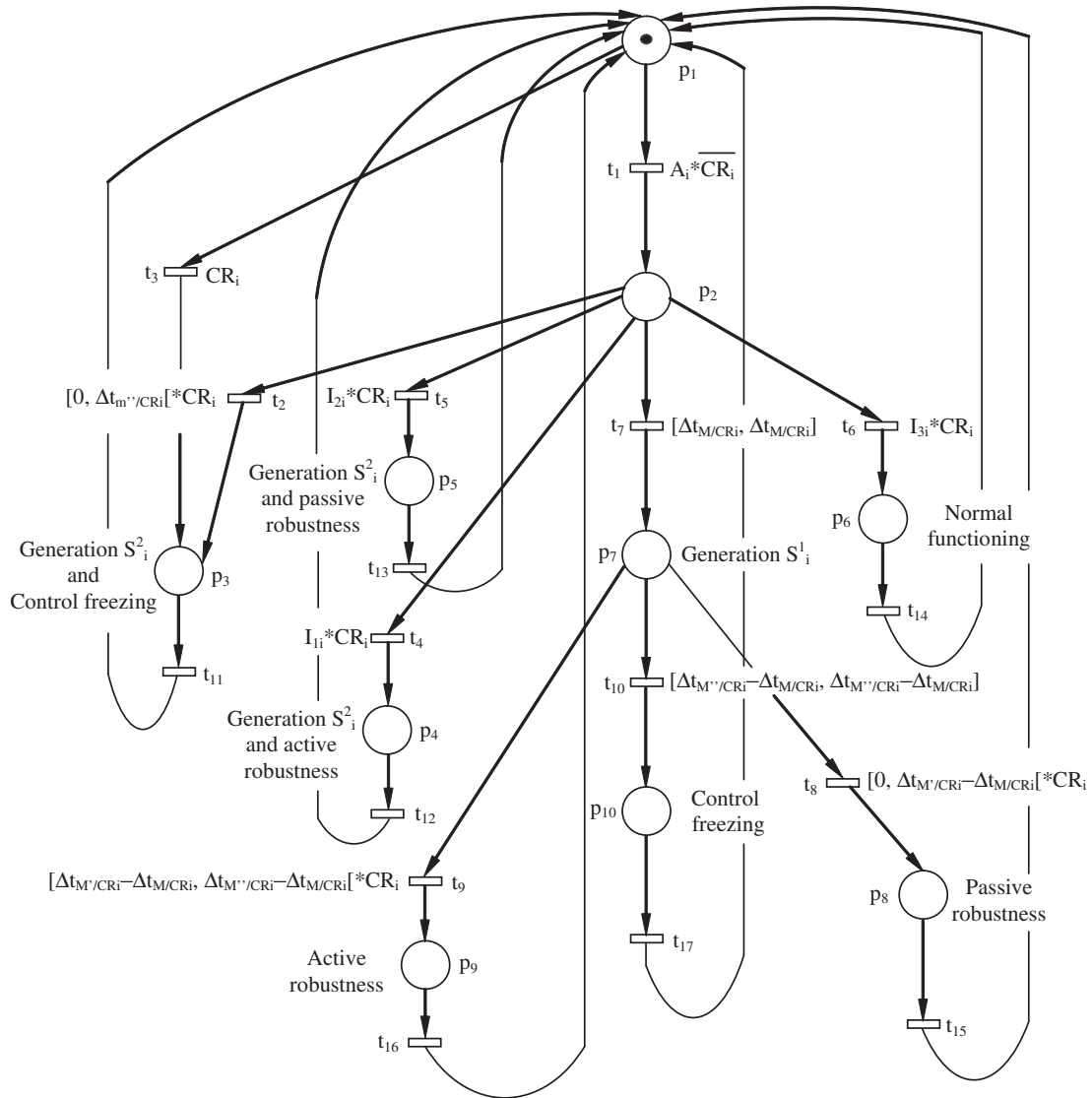


Figure 4: Robustness integration in the filtering mechanism of sensors signals

- φ is an application from the set of places (P) toward the set of operations (Γ): $\varphi : P \rightarrow \Gamma$,
- U is the external control of the set of transitions (T) built on the predicates using the occurrence of internal or external observable events of the system: $U : T \rightarrow \{0, 1\}$,
- U_0 is the initial value of the predicate vector.

Let us denote by:

- T_O : the set of observable transitions,
- T_{UO} : the set of non observable transitions,
- T_S : the set of synchronization transitions,
- T_{NS} : the set of non synchronization transitions,
- T_P : the set of parallelism transitions,
- t_i° (*resp.* ${}^\circ t_i$) : the output (*resp.* the input) places of the transition t_i ,
- p_i° (*resp.* ${}^\circ p_i$) : the output (*resp.* the input) transitions of the place p_i ,
- q_{ie} : the expected sojourn time of the token in the place p_i ,
- $St_e(n)$: the n^{nd} expected firing instant of the transition t ,
- $St(n)$: the n^{nd} effective firing instant of the transition t .

3.2 Functional decomposition

A workshop in repetitive functioning mode is modeled by a Strongly Connected Event Graph (SCEG) [13]. Performances of a SCEG running in mono-periodic functioning mode are proved to be the same as when using the K-periodic functioning [13]. Consequently, a mono-periodic functioning is used in order to decrease the complexity of the supervisory problem [14]. In this case, for each transition t , $St_e(n+1) = St_e(n) + \pi_0$ where π_0 is the period of the periodic functioning of the given discrete event system. In this paper, the scheduling task is supposed to be done. Therefore, the SCEG corresponding to the system is provided. Moreover, the setting of transitions firing instants is fixed too.

As the sojourn times in places have not the same functional signification when they are included in the sequential process of a product or when they are associated to a free resource, a decomposition of the P-time Petri net model into four sets is made using [15]. The assumption of multi-product job-shops without assembling tasks as it was established in [16] is used:

- R_U is the set of places representing the used machines,
- R_N corresponds to the set of places representing the free machines which are shared between manufacturing circuits,
- $Trans_C$ is the set of places representing the loaded transport resources,
- $Trans_{NC}$ is the set of places representing the unloaded transport resources (or the interconnected buffers).

Figure 5, shows a P-time Petri net (G) modeling a system composed by two sequential processes GO_1 and GO_2 with two shared machines (M_1, M_2), where:

$R_U = \{p_2, p_4, p_{11}, p_{13}, p_{15}\}$, $R_N = \{p_6, p_7, p_8, p_9\}$, $Trans_C = \{p_1, p_3, p_{10}, p_{12}, p_{14}\}$, $Trans_{NC} = \{p_5, p_{16}\}$, $GO_1 = (t_{12}, p_{10}, t_6, p_{11}, t_7, p_{12}, t_8, p_{13}, t_9, p_{14}, t_{10}, p_{15}, t_{11})$ and $GO_2 = (t_5, p_1, t_1, p_2, t_2, p_3, t_3, p_4, t_4)$.

The intervals (IS_i) and the expected staying times (q_{ie}) associated to the places (p_i) are:

$IS_1 = [30, 50]$, $q_{1e} = 38$, $IS_2 = [5, 12]$, $q_{2e} = 7$, $IS_3 = [10, 20]$, $q_{3e} = 15$, $IS_4 = [5, 20]$, $q_{4e} = 10$, $IS_5 = [1, +\infty]$, $q_{5e} = 10$, $IS_6 = [0, +\infty]$, $q_{6e} = 5$, $IS_7 = [0, +\infty]$, $q_{7e} = 8$, $IS_8 = [8, +\infty]$, $q_{8e} = 13$, $IS_9 = [8, +\infty]$, $q_{9e} = 15$, $IS_{10} = [5, 15]$, $q_{10e} = 12$, $IS_{11} = [15, 20]$, $q_{11e} = 17$, $IS_{12} = [3, 7]$, $q_{12e} = 6$, $IS_{13} = [2, 20]$, $q_{13e} = 5$, $IS_{14} = [2, 7]$, $q_{14e} = 5$, $IS_{15} = [15, 20]$, $q_{15e} = 16$, $IS_{16} = [1, +\infty]$ and $q_{16e} = 19$.

The initial expected firing instants of each transition are:

$St_{1e}(1) = 15$, $St_{2e}(1) = 22$, $St_{3e}(1) = 37$, $St_{4e}(1) = 7$, $St_{5e}(1) = 17$, $St_{6e}(1) = 12$, $St_{7e}(1) = 29$, $St_{8e}(1) = 35$, $St_{9e}(1) = 0$, $St_{10e}(1) = 5$, $St_{11e}(1) = 21$ and $St_{12e}(1) = 0$.

The repetitive functioning mode is characterized by the period $\pi_0 = 40$.

Definition 3. A mono-synchronized subpath is a path containing one and only one synchronization transition which is its last node.

Definition 4. An elementary mono-synchronized subpath is a mono-synchronized subpath beginning with a place p such as $\circ p$ is a synchronization transition.

In figure 5, there are eight elementary mono-synchronized subpaths constituting a partition of G : $Lp_1 = (p_{13}, t_9, p_{14}, t_{10}, p_{15}, t_{11}, p_{16}, t_{12}, p_{10}, t_6)$, $Lp_2 = (p_{13}, t_9, p_9, t_1)$, $Lp_3 = (p_2, t_2, p_3, t_3)$, $Lp_4 = (p_2, t_2, p_8, t_8)$, $Lp_5 = (p_4, t_4, p_5, t_5, p_1, t_1)$, $Lp_6 = (p_4, t_4, p_6, t_6)$, $Lp_7 = (p_{11}, t_7, p_7, t_3)$ and $Lp_8 = (p_{11}, t_7, p_{12}, t_8)$.

Property 1. A place p_{mp} belonging to a sequential process represents a shared machine if and only if $p_{mp}^\circ \in T_P$ or $\circ p_{mp} \in T_S$.

Property 2. The first node of an elementary mono-synchronized subpath is a place belonging to R_U and representing a shared machine.

3.3 Time disturbances localization

Let us remember some definitions.

Definition 5. A time disturbance is detectable if, when it occurs, there exists at least one transition $t \in T_O$ such as $St(n) \neq St_e(n)$.

Definition 6. A time disturbance is quantifiable if its value can be analytically known.

Definition 7. A time disturbance is localizable when its occurrence node can be identified.

Definition 8. A time disturbance is partially localizable when its occurrence node location can be proved to belong to a given subset of P .

Definition 9. A time disturbance is observable when it is detectable, quantifiable and localizable.

Definition 10. The time passive rejection capacity interval of a path Lp is $RC(Lp) = [Ca(Lp), Cr(Lp)]$ where:

$$Ca(Lp) = \sum_{p_i \in (Lp \cap (R_N \cup Trans_{NC}))} (q_{ie} - b_i), \quad (1)$$

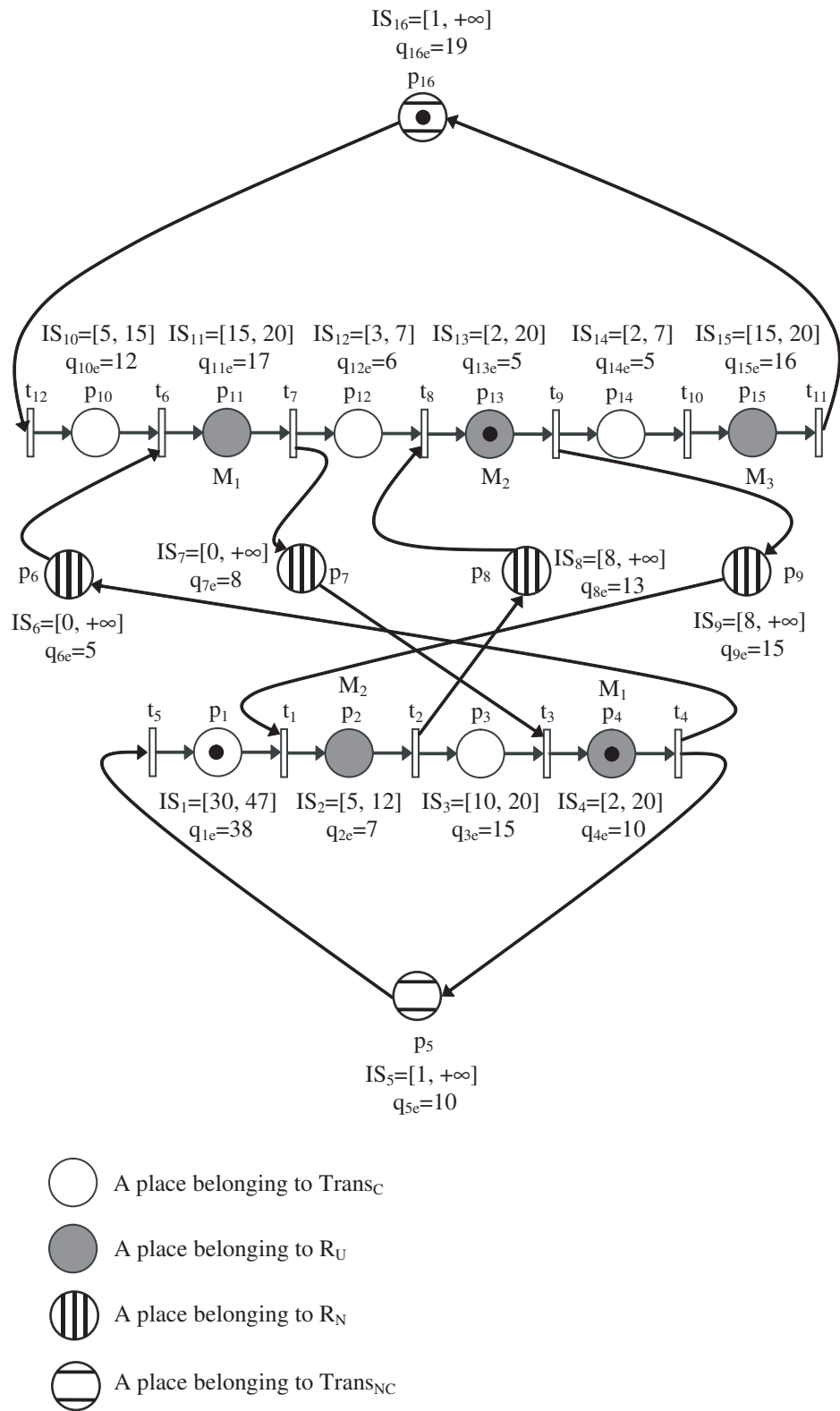


Figure 5: An Hillion like model with functional decomposition

$$Cr(Lp) = \sum_{p_i \in (Lp \cap (R_N \cup Trans_{NC}))} (q_{ie} - a_i). \quad (2)$$

Ca(Lp) (resp. Cr(Lp)) is called the time passive rejection capacity for an advance (resp. a delay) time disturbance occurrence.

Definition 11. Let δ a time disturbance and SN a set of nodes belonging to a P-time Petri net. $\delta \in SN$ (resp. $\delta \notin SN$) means that the occurrence of δ is (resp. is not) in a node of SN.

Used notations:

- C_{se} is the set of elementary mono-synchronized subpaths.
- $IN(Lp)$ is the first node of the path Lp .
- $OUT(Lp)$ is the last node of the path Lp .
- $Lp(t^*, t)$ is the oriented subpath of Lp beginning with t^* and ending with t .
- $M_{n-1}(Lp(t^*, t))$ is the number of tokens in $Lp(t^*, t)$ after the completion of the cycle $(n-1)$.
- Given a time disturbance δ , $\delta r_t(n)$ is the resulting residue quantified at the transition t which is fired at $St(n)$.
- $EC(IN^\circ(Lp), t)$ is the set of oriented paths connecting the node $IN^\circ(Lp)$ of the path Lp to the transition t .
- $H(IN^\circ(Lp), t) = \min_{L_i \in [EC(IN^\circ(Lp), t) \setminus Lp(IN^\circ(Lp), t)]} (Cr(L_i)) + \delta r_t(n)$.
- $H'(IN^\circ(Lp), t) = \min_{L_i \in EC(IN^\circ(Lp), t)} (Cr(L_i)) + \delta r_t(n)$.

Lemma 12. Let $Lp \in C_{se}$, $t \in (Lp \cap T_O \cap T_{NS})$, $t^* \in (Lp \cap T_O)$ and δ a time disturbance having a residue $\delta r_t(n) \neq 0$ quantified at the transition t . The following results are established [17]:

$$\delta r_{t^*}(n - M_{n-1}(Lp(t^*, t))) = 0 \implies \delta \in [Lp(t^*, t) \setminus \{t^*\}], \quad (3)$$

$$\delta r_{t^*}(n - M_{n-1}(Lp(t^*, t))) \neq 0 \implies \delta \notin [Lp(t^*, t) \setminus \{t^*\}]. \quad (4)$$

This lemma discusses the case of two observable transitions, t and t^* , such that t is not a synchronization one. When a disturbance is detected at a downstream transition t and is not detected at t^* , it is generated between these two transitions. Otherwise, the disturbance occurrence is outside the restriction of the considered path that connects t^* to t .

Lemma 13. Let $Lp \in C_{se}$, $t \in (Lp \cap T_O)$, $tp \in (Lp \cap T_P)$, $I_{Lp} = \{L_i \in C_{se} / OUT(L_i) = \circ IN(Lp)\}$ and δ a time disturbance having a residue $\delta r_t(n) > 0$ quantified at the transition t . The following assertion is true [17]:

$$\delta r_{tp}(n - M_{n-1}(Lp(tp, t))) < H'(tp, t) \implies \delta \notin \left\{ \bigcup_{L_i \in I_{Lp}} \{L_i \setminus \{IN(L_i), IN^\circ(L_i)\}\} \cup \{\circ tp, tp\} \right\}. \quad (5)$$

In other words, when the residue of the disturbance at the parallelism transition tp does not justify the residue at the transition t , forcibly the disturbance has not crossed tp .

Lemma 14. *Let $Lp \in C_{se}$, $t \in (Lp \cap T_O \cap T_S)$, $t^* \in (Lp \cap T_O)$ and δ a time disturbance having a residue $\delta r_t(n) > 0$ quantified at the transition t . The following results are established [17]:*

$$\delta r_{t^*}(n - M_{n-1}(Lp(t^*, t))) = 0 \implies \delta \notin [Lp(IN^\circ(Lp), t^*) \setminus \{IN^\circ(Lp)\}], \quad (6)$$

$$\begin{cases} 0 \leq Cr(Lp(IN^\circ(Lp), t^*)) < H(IN^\circ(Lp), t) \\ \delta r_{t^*}(n - M_{n-1}(Lp(t^*, t))) = 0 \end{cases} \implies$$

$$\begin{cases} \delta \notin [(Lp \setminus Lp(t^*, t)) \cup \{t^*\}] \\ \delta r_{IN^\circ(Lp)}(n - M_{n-1}(Lp(IN^\circ(Lp), t))) < H(IN^\circ(Lp), t) \end{cases}, \quad (7)$$

$$\begin{cases} \delta r_{t^*}(n - M_{n-1}(Lp(t^*, t))) \neq 0 \\ \delta r_t(n) + Cr(Lp(t^*, t)) \neq \delta r_{t^*}(n - M_{n-1}(Lp(t^*, t))) \end{cases} \implies \delta \notin [Lp(IN^\circ(Lp), t) \setminus \{IN^\circ(Lp)\}]. \quad (8)$$

The above lemma discusses the case of two observable transitions, t and t^* , such that t is a synchronization one. Several results are given.

If the residue at the transition t^* is equal to zero, the disturbance does not belong to the restriction of Lp between its only parallelism transition $IN^\circ(Lp)$ and t^* .

If the disturbance has crossed the parallelism transition of Lp ($IN^\circ(Lp)$) and if its residue at $IN^\circ(Lp)$ is greater than the passive rejection capacity of the restriction of Lp between $IN^\circ(Lp)$ and t^* , the residue at t^* must be different of zero. Otherwise, the disturbance has not crossed $IN^\circ(Lp)$.

If the residue at t^* is different of zero and if it does not justify the residue at the transition t , the occurrence of the disturbance is not in the restriction of Lp between $IN^\circ(Lp)$ and t .

Lemma 15. *Let $Lp \in C_{se}$, $tp \in (Lp \cap T_P \cap T_{UO})$, $t \in (Lp \cap T_O)$ and $Cr(Lp(tp, t))$ the time passive rejection capacity of Lp between tp and t for delay occurrence. Let us call $DIF(tp)$ the set of paths beginning with tp . Let us denote $DIF_n(tp)$ the restriction of $DIF(tp)$ such that: $\forall Lp' \in DIF_n(tp)$, $\forall t' \in Lp'$, we have $St'(n + m_{t'}) < St(n)$ where $m_{t'} = M_{n-1}(Lp'(tp, t')) - M_{n-1}(Lp(tp, t))$. Now, let $Lp' \in DIF_n(tp)$, $t^* \in (Lp' \cap T_O)$ and $Cr(Lp'(tp, t^*))$ the passive rejection capacity of Lp' between tp and t^* . Given a delay time disturbance δ , the following results are true [17]:*

$$\begin{cases} (t \notin T_S) \wedge (\delta r_t(n) > 0) \\ \delta r_t(n) + Cr(Lp(tp, t)) - Cr(Lp'(tp, t^*)) > 0 \\ \delta r_{t^*}(n + m_{t^*}) = 0 \end{cases} \implies \delta \in [Lp(tp, t) \setminus \{tp\}], \quad (9)$$

$$\begin{cases} (t \notin T_S) \wedge (\delta r_t(n) > 0) \\ \delta r_{t^*}(n + m_{t^*}) \neq 0 \end{cases} \implies \delta \notin [(Lp(tp, t) \cup Lp'(tp, t^*)) \setminus \{tp\}], \quad (10)$$

$$\begin{cases} (t \in T_S) \wedge (\delta r_t(n) > 0) \\ Cr(Lp'(tp, t)) < H'(tp, t) \\ \delta r_{t^*}(n + m_{t^*}) = 0 \end{cases} \implies \begin{cases} \delta \notin \{^\circ tp, tp\} \\ \delta r_{tp}(n - M_{n-1}(Lp(tp, t))) < H'(tp, t) \end{cases}, \quad (11)$$

$$\begin{cases} (t \in T_S) \wedge (\delta r_t(n) > 0) \\ \delta r_{t^*}(n + m_{t^*}) \neq 0 \end{cases} \implies \delta \notin [Lp(tp, t) \setminus \{tp\}]. \quad (12)$$

When tp is a non observable parallelism transition, the following assertion may be used: if a disturbance modifies the tp firing instant, it must be seen downstream of tp . Consequently, when the value of the residual effect of the disturbance is greater than the rejection capacity of a given path, a residual variation has to be observed.

The different lemmas formulated constitute a tool aiming to define the set of nodes where the disturbance may occur and the subset where it is proved that it did not occur. Then the question of using the above lemmas in order to make them collaborate has to be tackled. In other words, it remains to establish an algorithm using these lemmas while testing all mono-synchronized subpaths of the given P-time Petri net model.

4 Conclusions

This paper deals with supervision in critical time manufacturing job-shops. In such systems operation times are included between a minimum and a maximum value. A filtering mechanism of sensors signals integrating the robustness values is described. It provides the avoidance of control freezing if the time disturbance is in the robustness intervals. Therefore, it makes it possible to continue the production in a degraded mode providing the guarantees of quality and safety. It should be noted that the knowledge of robustness intervals is a significant parameter in the proposed mechanism. The assumptions formulated in these lines are very restrictive. It is natural to consider different scenarios where the temporal specifications of the process are not fulfilled, nevertheless the production can continue. It is necessary to introduce a finer classification of abnormal functioning and their impact on the considered systems. In this context, fuzzy logic can be used.

When a symptom of an abnormal functioning is claimed by the filtering mechanism, it is imperative to localize the time disturbance occurrence. Based upon controlled P-time Petri nets as a modeling tool, a series of lemmas are quoted in order to build a theory dealing with localization problem. This is quite useful for the maintenance task.

In the near future, it is essential to develop an algorithm using the lemmas results and providing localization of time disturbances.

References

- [1] S. Calvez, P. Aygalinc, and P. Bonhomme, Proactive/Reactive Approach for Maintenance Tasks in Time Critical Systems, *IEEE International Conference on Emerging Technologies and Factory Automation (ETFA'2005)*, Catane, Vol. 1, pp. 947-953, September 2005.
- [2] S. Collart Dutilleul, and E. Craye, Performance and tolerance evaluation, *SAFEPROCESS'03, IFAC Symp. on Fault Detection, Supervision and Safety for Technical Processes*, Washington, June 2003.
- [3] A. Boufaied, A. Subias, and M. Combacau, Chronicle modeling by Petri nets for distributed detection of process failures, *IEEE Conference on Systems, Man, and Cybernetics (SMC'02)*, Hammamet, October 2002.
- [4] P. Declerck, and M. K. Didi Alaoui, Modelling and analysis of P-time event graphs in the (min, max, +) algebra, *IEEE Conference on Systems, Man, and Cybernetics (SMC'04)*, The Hague, Vol. 2, pp. 1807-1812, October 2004.
- [5] N. Jerbi, S. Collart Dutilleul, E. Craye, and M. Benrejeb, Observability of Tolerant Multi-product Job-shops in Repetitive Functioning Mode, *IMACS'05*, Paris, July 2005.

- [6] A. E. K. Sahraoui, Contribution à la surveillance et à la commande d'ateliers, Ph.D. Thesis, *Université Paul Sabatier*, Toulouse, 1987.
- [7] A. Toguyeni, E. Craye, and J. C. Gentina, A method of temporal analysis to perform on-line diagnosis in the context of Flexible Manufacturing System, *IECON'90*, Vol. 1, pp. 445-450, Pacific Grove-California, November 1990.
- [8] M. Nourelfath, Extension de la théorie de la supervision à la commande des systèmes à événements discrets: application à la sécurité opérationnelle des systèmes de production, Ph.D. Thesis, *INSA de Lyon*, France, July 1997.
- [9] A. Toguyeni, Surveillance et diagnostic en ligne dans les ateliers flexibles de l'industrie manufacturière, Ph.D. Thesis, *Université des Sciences et Technologies de Lille*, November 1992.
- [10] M. Diaz, *Les réseaux de Petri - Modèles fondamentaux*, Ed. Hermès, Paris, 2001.
- [11] N. Jerbi, S. Collart Dutilleul, E. Craye, and M. Benrejeb, Intégration de la robustesse dans la supervision de systèmes manufacturiers à contraintes de temps, *Conférence Internationale Francophone d'Automatique (CIFA'06)*, Bordeaux, May 2006.
- [12] W. Khansa, P. Aygalinc, and J. P. Denat, Structural analysis of P-Time Petri Nets, *Computational Engineering in Systems Applications (CESA'96)*, Lille, pp. 127-136, July 1996.
- [13] S. Laftit, J. M. Proth, and X. Xie, Optimisation of invariant Criteria for Event Graph, *IEEE Trans. on Automatic Control*, Vol. 37, no. 5, pp. 547-555, May 1992.
- [14] S. Collart Dutilleul, J. P. Denat, and W. Khansa, Use of Periodic Controlled Petri Net for Discrete Event Dynamical System Control Synthesis, *ECC'95*, Rome, pp. 2060-2065, September 1995.
- [15] J. Long, and B. Descotes-Genon, Flow Optimization Method for Control Synthesis of Flexible Manufacturing Systems Modeled by Controlled Timed Petri Nets, *IEEE International Conference on Robotics and Automation*, Atlanta, Georgia, Vol. 1, pp. 598-603, May 1993.
- [16] H. P. Hillion, and J. M. Proth, Performance evaluation of job-shop systems using timed event graphs, *IEEE Trans. on Automatic Control*, Vol. 34, no. 1, pp. 3-9, 1989.
- [17] N. Jerbi, S. Collart Dutilleul, E. Craye, and M. Benrejeb, Localization of Time Disturbances in Tolerant Multiproduct Job-shops Without Assembling Tasks, *Computational Engineering in Systems Applications (CESA'06)*, Beijing, pp. 45-50, October 2006.

Nabil Jerbi^{1,2}, Simon Collart Dutilleul¹, Etienne Craye¹, Mohamed Benrejeb²

¹Ecole Centrale de Lille
Laboratoire d'Automatique, Génie Informatique et Signal
Cité Scientifique, BP 48, 59651 Villeneuve d'Ascq, France

²Ecole Nationale d'Ingénieurs de Tunis
Unité de recherche LARA-Automatique
BP 37, Le Belvédère, 1002 Tunis, Tunisie

E-mail: nabil.jerbi@isetso.rnu.tn, simon.collart_dutilleul@ec-lille.fr,
etienne.craye@ec-lille.fr, mohamed.benrejeb@enit.rnu.tn

Received: November 11, 2006

Switching LPV Controllers for a Variable Speed Pitch Regulated Wind Turbine

Fabien Lescher, Jing-Yun Zhao, Pierre Borne

Abstract: This paper deals with the control of a variable speed, pitch regulated wind turbine in the whole plant operating area. The wind turbine operating area can be divided into several zones, depending on the wind speed, and the control objectives are different for each operating zone. An hybrid control system composed by several LPV controllers which switches during transitions from one operating area to another is designed in order to ensure asymptotic stability and a good level of performances in the whole operating area. The LPV controllers are calculated from a convex LMI formulation of the problem in order to minimize an H_2/H_∞ criteria that optimizes the energy conversion of the system and that reduces the mechanical fatigue of the plant mechanical structure. The proposed controller is finally compared with two more conventional ones.

Keywords: wind energy, LPV modeling, $\mathcal{H}_2/\mathcal{H}_\infty$ control, switching systems, mechanical fatigue.

1 Introduction

Wind energy has widely grown during the last decades and is nowadays the most competitive form of renewable energy. Nevertheless wind energy is not yet cost effective, and consequently, development of new technologies will be crucial for successful penetration of wind energy into electricity market. Implementation of advanced control systems is considered as a promising way to improve wind energy conversion and to decrease wind energy cost. The wind turbine control objectives are mainly to optimize wind energy conversion, and to reduce dynamic loads experienced by the plant mechanical structure. Indeed, dynamic loads hardly affect wind turbine lifetime and mainly determine mechanic components design, and consequently their cost [1].

Designing a control system for a variable speed, pitch regulated wind turbine presents several issues: the system behavior is both highly non linear and quite uncertain, especially because of blades aerodynamic properties which are sensitive to climatic conditions. Moreover, the control purpose is a multiobjective task, because the control system has to optimize a trade off between energy conversion maximization and alleviation of mechanical dynamic loads which result from very lightly damped resonant modes of the structure. The wind turbine operation is also decomposed into several operating zones, depending on the wind speed passing through the rotor: for low wind speeds, the wind energy system has to maximize produced power, whereas for high wind speed, the electric power has to be maintained to the generator nominal power. Another difficulty of this wind turbine control problem is the uncontrollable and stochastic nature of the main component acting on the plant: the wind speed. Moreover, the effective wind speed acting on the whole turbine rotor is a fictitious quantity and is hence not measurable and not available for control operation.

In response to this multivariable and multiobjective control problem, the usual implemented controllers are calculated from a linearization of the model around an operating point by designing several separate and decoupled loops, each loop being tuned for one objective [2][3]. These controllers are therefore non optimal for the multiobjective problem and moreover, this design task has to be repeated for several linearization points on the reference trajectory that the system must follow.

In this paper, a gain-scheduled wind turbine control system is designed for the whole operating region using Linear Matrix Inequalities (LMIs) optimization and the Linear Parameter Varying (LPV) systems

framework [4]. The system non-linearities inherent to the aerodynamics subsystem are taken into account by an affine quasi-LPV model, obtained from a Jacobian linearization of the system along the reference trajectory. An optimal time-varying controller, calculated through a LMI problem formulation, is calculated in order to minimize an H_2/H_∞ criterion composed by the different control objectives. This frequency domain criteria optimization is notably known to be efficient to reduce the fatigue of flexible mechanical structure, and is coupled with the output power regulation objective. This controller synthesis procedure has already demonstrated its efficiency for a simpler wind turbine model, especially for mechanical fatigue reduction [5].

Besides, the proposed synthesis methodology also allows to handle the problem of transition between the operating zones of the system, for which the control objectives and the available actuators are not the same. The transitions between the operating zones is a serious problem, which can generate transient phenomena and losses of performance, and moreover this transition occurs frequently during the system operating life. The proposed approach generates a hybrid controller composed by switched LPV controllers which guarantees stability and control performances even during the transition between the controllers, from the construction of a piecewise-affine parameter dependent Lyapunov function [6][7]. The wind turbine system is described in the first part of the paper. The control objectives over the whole operation area are then presented. The LPV modeling of the wind turbine is described, before the hybrid controller synthesis part. The performances of the proposed controller are finally compared with the ones of two other more conventional controllers.

Notations: For two symmetric matrices, A and B , $A > B$ means that $A - B$ is definite positive. A^T denotes the transpose of A . \star stands for symmetric blocks; \bullet stands for an element that has no influence on the development.

2 System Description

The structure of a variable speed, pitch regulated wind energy conversion system is presented in Fig.1. The system is formed by the rotor, the mechanical structure, and by a generator unit, composed by the generator and the static converter connected to the electrical grid. The control system acts on generator in order to apply the reference electromagnetic torque $T_{G,ref}$ and on the pitch actuator in order to control the pitch angle of the blades β , calculated from the measurements of the rotational speed of the shaft at the generator side, and of the flexion speed of the tower by an accelerometer located at the tower top.

The effective wind speed $v(t)$ passing through the rotor is considered as a first order dynamic process disturbed by an exogenous signal $m_v(t)$

$$\dot{v} = -\frac{1}{T_v}v + m_v(t) \quad (1)$$

with the time constant T_v calculated from the stochastic properties of the wind speed [8].

The mechanical model describing the structure of the plant has three degrees of freedom: the flexions of the blades (blades flap motion) and of the tower (tower fore-aft motion) in the direction of the wind, and the torsion of the drive train shaft (Fig.2). A spring-damper representation is used to describe the flexibility of each component. Moreover, the three blades are supposed to move conjointly and to be affected by the same forces at the same time. A linear model of the dynamic behavior of this structure is established using Lagrange's equations.

The electrical subsystem, corresponding to the generation unit, composed by the generator and the power electronic components, has very fast dynamics compared with dynamics of the other subsystems. Consequently, and considering the study objectives, the electrical dynamics are neglected. Hence, electromagnetic torque T_G is supposed equal to its reference $T_{G,ref}$.

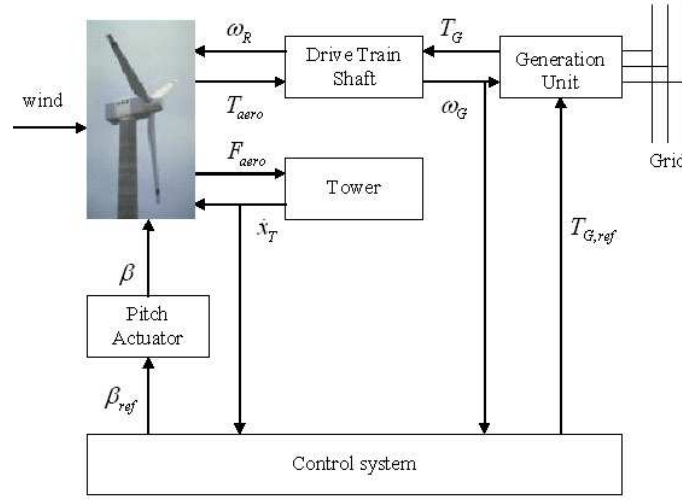


Figure 1: Wind energy conversion system structure.

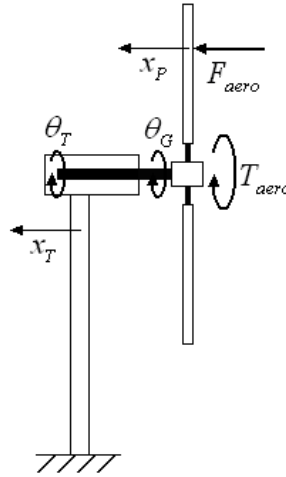


Figure 2: Wind Turbine Mechanical Structure

The pitch actuator subsystem represents the hydraulic or electric system which makes the blades revolve around their lengthwise axis. This system is described by a first order transfer function with a time constant T_β .

The aerodynamic conversion process of the turbine rotor is characterized by the extracted torque T_{aero} and by the out-of-plane thrust force F_{aero} , which are functions of the air mass density ρ , the wind velocity v , the rotational speed of the turbine ω_T , the horizontal blades speed \dot{x}_P and the power and thrust coefficients C_p and C_t :

$$\begin{aligned} T_{aero} &= \frac{1}{2} \rho \pi R^2 \frac{(v + \dot{x}_P)^3}{\omega_T} C_p(\lambda, \beta), \\ F_{aero} &= \frac{1}{2} \rho \pi R^2 (v + \dot{x}_P)^2 C_t(\lambda, \beta), \end{aligned} \quad (2)$$

with R the length of the rotor blades. The aerodynamic coefficients C_p and C_t are non-linear functions depending on blades pitch angle β and tip speed ratio $\lambda = \frac{\omega_T R}{v}$.

3 Control Task

The controller objectives are to ensure:

- stability along the reference trajectory for the whole operation,
- good performances of the selected outputs, i.e. energy conversion and alleviation of mechanical loads affecting the plant structure.

The wind turbine operation area can be divided into three zones, depending on the wind speed acting on blades. The energy conversion objectives, and thus the control objectives, are different for each zone.

For low wind speed, i.e. for $v < v_1$, the main objective is to maximize system energy conversion yield. In this Partial Load 1 zone, system has to operate at $C_p(\lambda, \beta) = C_{p,max}$. Pitch angle β is then maintained constant at β_{opt} and rotational speed ω_T is controlled to minimize the criteria $\delta\lambda = \lambda - \lambda_{opt}$, by acting only on generator electromagnetic torque T_G .

For higher wind speed, corresponding to $v_1 < v < v_2$, turbine rotational speed ω_T is maintained at the nominal generator speed by acting on electromagnetic torque T_G . Pitch angle β is also maintained at β_{opt} to maximize energy conversion efficiency (Partial Load 2).

For high wind speed, i.e. $v > v_2$, wind turbine operates in Full Load and electric produced power P_{elec} has to be regulated at nominal generator power. Turbine rotational speed is maintained around nominal generator speed and pitch angle β is controlled in order to reduce power coefficient $C_p(\lambda, \beta)$. Control system is then multivariable in this zone, because it acts on both generator torque and pitch angle.

Evolution of the main variables in function of wind speed are presented in Fig.3. The control system has

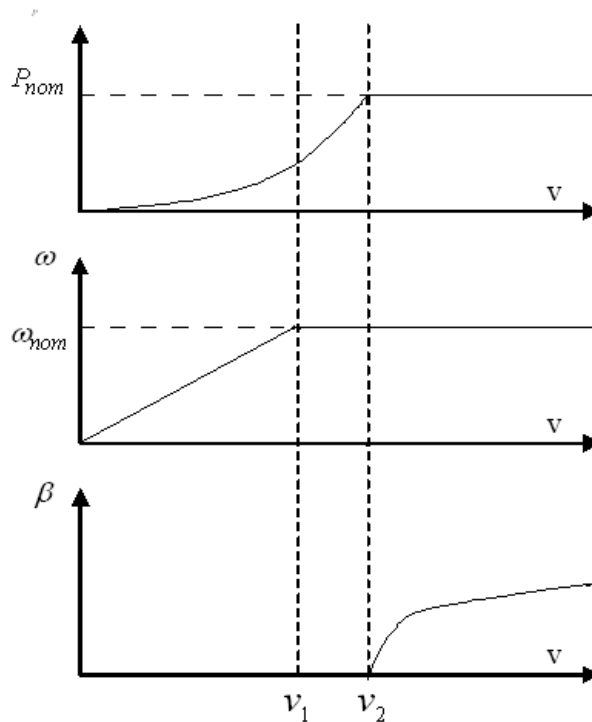


Figure 3: Evolution of the main variables in function of wind speed.

to operate over the full envelope of wind speeds. Hence, transitions between these different operating zones have to be handled by the control system in a smooth manner, which avoids the generation of large transients.

The other main control objective is to reduce mechanical fatigue of most expensive plant components, especially blades, drive train and tower. Hence, the control system will be designed in order to reduce the variations of the drive train torsion torque T_D and the blades and tower flexion forces F_B and F_T , expressed by:

$$\begin{aligned} T_D &= d_D(\omega_T - \omega_G) + k_D(\theta_T - \theta_G) \\ F_B &= d_B \dot{x}_B + k_B x_B \\ F_T &= d_T \dot{x}_T + k_B x_T \end{aligned}$$

with d and k the damper and spring coefficients of the corresponding components.

The control system will be designed in order to optimize a trade-off between these objectives by minimizing a criterion expressed in the frequency range. H_2 norm optimization permits to reduce the average variations of the energy conversion parameter, i.e. $\delta\lambda$, $\delta\omega_T$ or δP_{elec} , in the whole frequency range. H_∞ cost minimization is able to alleviate, in the frequency range, the maximum response of the mechanical loads to a variation of wind speed, which is generally the response corresponding to the resonance frequency of the component, and which is the most damaging.

4 LPV Modeling

The LPV model can be considered as a group of linear local descriptions of nonlinear descriptions. Given the nonlinear system describing the wind turbine behavior

$$\begin{aligned} \dot{x} &= f(x, u, w) \\ y &= g(x, u, w) \\ z_2 &= h_2(x, u, w) \\ z_\infty &= h_\infty(x, u, w) \end{aligned} \quad (3)$$

with x the state of the system, u the control input, w the external disturbance, y the measured output and z_2 and z_∞ the performance outputs, the Jacobian linearization approach can be used to create an LPV system based on the first-order Taylor series expansion of the nonlinear model. A family of linear plants is obtained by linearizing the nonlinear system with respect to a set of equilibrium points located on the reference trajectory, which are parametrized by the scheduling parameter ρ and satisfy $f(x_e(\rho), u_e(\rho), 0) = 0$. Corresponding to a specified family of equilibrium points, the family of the linearized plants can be written in the following form:

$$\begin{bmatrix} \delta \dot{x} \\ \delta y \\ \delta z_2 \\ \delta z_\infty \end{bmatrix} = \begin{bmatrix} \left. \frac{\partial f}{\partial x} \right|_e & \left. \frac{\partial f}{\partial u} \right|_e & \left. \frac{\partial f}{\partial w} \right|_e \\ \left. \frac{\partial g}{\partial x} \right|_e & \left. \frac{\partial g}{\partial u} \right|_e & \left. \frac{\partial g}{\partial w} \right|_e \\ \left. \frac{\partial h_2}{\partial x} \right|_e & \left. \frac{\partial h_2}{\partial u} \right|_e & \left. \frac{\partial h_2}{\partial w} \right|_e \\ \left. \frac{\partial h_\infty}{\partial x} \right|_e & \left. \frac{\partial h_\infty}{\partial u} \right|_e & \left. \frac{\partial h_\infty}{\partial w} \right|_e \end{bmatrix} \begin{bmatrix} \delta x \\ \delta u \\ \delta w \end{bmatrix} \quad (4)$$

where the deviation variables are defined by

$$\begin{aligned} \delta x &= x - x_e(\rho) \\ \delta u &= u - u_e(\rho) \\ \delta y &= y - y_e(\rho) \\ \delta w &= w - w_e(\rho) \end{aligned}$$

and where $J|_e$ represents the value of the Jacobian coefficient J at the equilibrium point $(x_e(\rho), u_e(\rho))$. Before deriving the LPV model of the wind turbine, the scheduling parameters must be selected so

that the appropriate equilibrium point can be located on the reference trajectory. Because the reference trajectory is decomposed into three parts, corresponding to the three operating areas, the parameter set $\mathcal{P} = [\rho_{min}, \rho_{max}]$ is partitioned into three subsets

$$\begin{aligned}\mathcal{P}_1 &= [\rho_{1,min}, \rho_{1,max}] \\ \mathcal{P}_2 &= [\rho_{2,min}, \rho_{2,max}] \\ \mathcal{P}_3 &= [\rho_{3,min}, \rho_{3,max}]\end{aligned}$$

with $\rho_{1,max} = \rho_{2,min}$ and $\rho_{2,max} = \rho_{3,min}$ corresponding to v_1 and v_2 , i.e. the transitions between the different operating regions.

Hence, by calculating the Jacobian coefficients as functions of the scheduling parameter ρ along the reference trajectory for each parameter subset \mathcal{P}_i , and considering the wind turbine system configuration, the dynamic behavior of the model (4) for the wind turbine system is governed by the equation:

$$\begin{bmatrix} \delta \dot{x} \\ \delta y \\ \delta z_2 \\ \delta z_\infty \end{bmatrix} = \begin{bmatrix} A_i(\rho) & B_i & G_i \\ C_{y,i}(\rho) & 0 & 0 \\ C_{z_2,i}(\rho) & D_{z_2,i}(\rho) & 0 \\ C_{z_\infty,i}(\rho) & D_{z_\infty,i}(\rho) & 0 \end{bmatrix} \begin{bmatrix} \delta x \\ \delta u \\ \delta w \end{bmatrix} \quad (5)$$

$i = \{1, 2, 3\}$.

The Jacobian coefficients of the expression of the aerodynamic torque and of the thrust force (2) are calculated along the reference trajectory and are approximated by affine functions of the scheduling parameter ρ . Hence matrices $A_i(\rho)$ have the following form:

$$A_i(\rho) = A_{i,0} + \rho A_{i,1} \quad (6)$$

and are continuous in the whole parameter set \mathcal{P} .

5 LPV Control Design

From the developed family of LPV models of the wind turbine, we aim at designing a family of LPV dynamic output-feedback controllers in the form:

$$\begin{bmatrix} \dot{x}_K \\ u \end{bmatrix} = \begin{bmatrix} A_{K,i}(\rho) & B_{K,i}(\rho) \\ C_{K,i}(\rho) & D_{K,i}(\rho) \end{bmatrix} \begin{bmatrix} x_K \\ y \end{bmatrix}, i = \{1, 2, 3\}. \quad (7)$$

The order of each controller is the same than the plant order, and the controllers dynamics are allowed to be discontinuous at the boundaries of the subsets \mathcal{P}_i .

Hence one LPV controller is designed in each subset \mathcal{P}_i in order to optimize a set of performances, expressed as a multichannel H_2/H_∞ criteria, corresponding to the control objectives of the operating area. The control synthesis is based on the LMI optimization and on the construction of a continuous piecewise-affine Lyapunov function depending on the scheduling parameter ρ , which mimics the parameter dependence of the plant model (6). Hence, the parameter dependent Lyapunov function is defined as:

$$V(x_{cl}, \rho) = x_{cl}^T P(\rho) x_{cl} \quad (8)$$

where $x_{cl}^T = (x^T \ x_K^T)$ and $P(\rho) = \phi_i(\rho) P_i(\rho)$, with $\phi_i(\rho) = 1$ if $\rho \in \mathcal{P}_i$, and $\phi_i(\rho) = 0$ otherwise. In order to apply the linearizing changing of variables described in [9], matrices $P_i(\rho)$ and $P_i^{-1}(\rho)$ are partitioned as:

$$P_i(\rho) = \begin{pmatrix} Y_i(\rho) & S_i(\rho) \\ S_i^T(\rho) & \bullet \end{pmatrix} \quad P_i^{-1}(\rho) = \begin{pmatrix} X & R \\ R^T & \bullet \end{pmatrix} \quad (9)$$

with $I - Y_i(\rho)X = S_i(\rho)R^T$. As explained in [4], matrices X and R are constrained to be constant over the whole parameter set \mathcal{P} in order to obtain a family of controllers independent of the gain-scheduling parameter rate $\dot{\rho}$, which is not available in real-time. Moreover, matrices $Y_i(\rho)$ are affine in the parameter ρ in each subset \mathcal{P}_i :

$$Y_i(\rho) = Y_{i,0} + (\rho - \rho_{i,\min})Y_{i,1} \quad (10)$$

and the function $Y(\rho) = \phi_i(\rho)Y_i(\rho)$ is constrained to be continuous over the whole parameter set \mathcal{P} :

$$Y_i(\rho) = Y_j(\rho) \forall \rho \in \mathcal{P}_i \cap \mathcal{P}_j \quad (11)$$

By verifying that for the wind turbine model the triple $(A_i(\rho), B_i(\rho), C_{y,i}(\rho))$ is stabilizable and detectable for all $\rho \in \mathcal{P}$, and by assuming that the scheduling parameter rate $\dot{\rho}$ is bounded in a set $[-\dot{\rho}_{\max}, \dot{\rho}_{\max}]$, the family of controllers can be calculated by applying the following theorem¹:

Theorem:[9][6] *Suppose there exist symmetric definite positive matrices X and Y such as (10) and (11), matrices*

$$\begin{aligned} \hat{A}_i(\rho) &= \hat{A}_{i,0} + (\rho - \rho_{i,\min})\hat{A}_{i,1} + (\rho - \rho_{i,\min})^2\hat{A}_{i,2} \\ \hat{B}_i(\rho) &= \hat{B}_{i,0} + (\rho - \rho_{i,\min})\hat{B}_{i,1} + (\rho - \rho_{i,\min})^2\hat{B}_{i,2} \\ \hat{C}_i(\rho) &= \hat{C}_{i,0} + (\rho - \rho_{i,\min})\hat{C}_{i,1} \\ \hat{D}_i(\rho) &= \hat{D}_{i,0} + (\rho - \rho_{i,\min})\hat{D}_{i,1} \end{aligned}$$

symmetric semi-definite positive matrices

$$M_i = \begin{pmatrix} M_{1,i} & \star \\ M_{2,i} & M_{3,i} \end{pmatrix}$$

and a symmetric matrix Q satisfying the following matrix inequalities

$$\begin{aligned} &\begin{pmatrix} U + U^T & \star \\ \hat{A}_i + (A_i + B_i\hat{D}_iC_{y,i})^T & \dot{\rho}Y_{i,1} + V + V^T \\ G^T & G^TY_i \\ C_{z_\infty}X + D_{z_\infty}\hat{C}_i & C_{z_\infty} + D_{z_\infty}\hat{D}_iC_{y,i} \end{pmatrix} \\ &\begin{pmatrix} \star & \star \\ \star & \star \\ -\gamma I & \star \\ 0 & -\gamma I \end{pmatrix} + (\rho - \rho_{i,\min})^2 \begin{pmatrix} M_i & 0 \\ 0 & 0 \end{pmatrix} < 0 \\ &\begin{pmatrix} X & \star & \star \\ I & Y_i & \star \\ D_{z_2}\hat{C}_i + C_{z_2}X & C_{z_2} + D_{z_2}\hat{D}_iC_{y,i} & Q \end{pmatrix} > 0 \\ &Tr(Q) < \nu \\ &\begin{pmatrix} M_{1,i} & \star \\ M_{2,i} + \hat{A}_{i,2} & M_{3,i} + Y_iA_i + \hat{B}_{i,2}C_{y,i} \end{pmatrix} > 0 \end{aligned} \quad (12)$$

for all pairs $(\rho, \dot{\rho}) \in \{\rho_{i,\min}, \rho_{i,\max}\} \times \{\dot{\rho}_{i,\min}, \dot{\rho}_{i,\max}\}$, with

$$\begin{aligned} U &= A_iX + B_i\hat{C}_i \\ V &= Y_iA_i + \hat{B}_iC_{y,i} \end{aligned}$$

¹the dependance on ρ is dropped for the notation convenience

Then the family of dynamic controllers (7) with, $\forall \rho \in \mathcal{P}$:

$$\begin{aligned} D_{K,i} &= \hat{D}_i \\ C_{K,i} &= (\hat{C}_i - D_{K,i} C_{y,i} X) R^{-T} \\ B_{K,i} &= S_i^{-1} (\hat{B}_i - Y_i B_i D_{K,i}) \\ A_{K,i} &= S_i^{-1} (\hat{A}_i - S_i B_{K,i} C_{y,i} X - Y_i B_i C_{K,i} R^T \\ &\quad - Y (A_i + B_i D_{K,i} C_{y,i}) X) R^{-T} \end{aligned}$$

where matrices R and S_i verify for all $\rho \in \mathcal{P}$ the relation $RS_i^T = I - XY_i$, guarantees that:

- the elements of the family of closed-loop systems composed by (5) and (7) are asymptotically stable;
- the H_∞ -norm of the transfer $w \rightarrow z_\infty$ is less than $\sqrt{\gamma}$;
- the H_2 -norm of the transfer $w \rightarrow z_2$ is less than \sqrt{v} .

Note that the LMI problem formulated in this theorem has a finite number of inequalities, thanks to the introduction of matrices M_i , and permits to do without the gridding phase which is commonly used for LPV synthesis and which is very computationally intensive.

Moreover, in order to facilitate the control system implementation, and to prevent the system from having too fast dynamics, additional LMIs constraints are formulated to place the poles of the closed loop systems in a determined region of the state-space domain. Placing the poles in a circle centered at the origin of the state-space permits to prevent for obtaining too fast poles and too few damped fast poles. Hence if the following LMIs are satisfied for $\forall \rho \in \{\rho_{i,min}, \rho_{i,max}\}$ and for semi-definite positive matrices

$$N_i = \begin{pmatrix} N_{1,i} & \star \\ N_{2,i} & N_{3,i} \end{pmatrix}:$$

$$\begin{aligned} &\begin{pmatrix} -rX & \star & \star & \star \\ -rI & -rY_i & \star & \star \\ A_i X + B_i \hat{C}_i & \hat{A}_i & -rX & \star \\ A_i + B_i \hat{D}_i C_{y,i} & Y_i A_i + \hat{B}_i C_{y,i} & -rI & -rY_i \end{pmatrix} \\ &\quad + (\rho - \rho_{i,min})^2 \begin{pmatrix} N_i & 0 \\ 0 & N_i \end{pmatrix} < 0 \\ &\begin{pmatrix} N_{1,i} & \star & \star & \star \\ N_{2,i} & N_{3,i} & \star & \star \\ 0 & \hat{A}_{i,2} & N_{1,i} & \star \\ 0 & \hat{B}_{i,2} C_{y,i} + Y_{i,1} A_{i,1} & N_{2,i} & N_{3,i} \end{pmatrix} > 0 \end{aligned}$$

(13)

then the poles of the closed-loop systems composed by (5) and (7) are located in a circle of rayon r and of center the origin of the state-space.

Hence, an optimal family of dynamic controllers that minimize the H_2 -norm of the transfer $w \rightarrow z_2$ for a given H_∞ -norm $\sqrt{(\gamma)}$ of the transfer $w \rightarrow z_\infty$ can be designed by solving the following convex LMIs problem:

$$\min v \text{ subject to the LMIs (12) and (13)} \quad (14)$$

6 Wind Turbine Control System Design and Simulation

The wind turbine control system is designed from the family of developed LPV systems by calculating LPV controllers which optimize a trade-off between the energy conversion, i.e. the energy yield

maximization in Partial Load and the output energy regulation in Full Load, and the reduction of mechanical loads. Hence the performance output z_2 represents the energy optimization variables $\delta\lambda$, $\delta\omega_T$ or δP_{elec} , depending on the operating area, and then the subset of the scheduling parameter, augmented by the corresponding weighting functions. In the Full Load operation, and in order to reduce the pitch actuator fatigue, the pitch angle deviation $\delta\beta$ is added to this vector. The performance output vector z_∞ is composed by the mechanical forces affecting the plant structure, F_T , F_P and T_D , augmented by the corresponding weighting functions. In order to reduce the vibrations of the mechanical components for frequencies above their resonance frequencies, the outputs F_T , F_P and T_D are multiplied by a high-pass filter, in order to penalize the high-frequency variations of these outputs during the controller synthesis. Inversely, the energy optimization variables are multiplied by a low-pass filter in order to ensure to the energy conversion output a good tracking at low frequency. Indeed, at high frequency, a good tracking of these components is not reached because it would induce an increase of dynamical loads on the actuators and on the mechanical structure.

The scheduling parameter ρ is chosen to be $\rho = P_{elec} + k\beta^2$, $k > 0$, because it permits to locate the operating point on the reference trajectory and is directly measured, contrary to the wind speed crossing over the turbine rotor. Moreover, the bounds of the scheduling parameter rate $\dot{\rho}$ are derived from the actuators rate limitations.

By solving numerically the problem (14), three LPV controllers are designed, one for each operating area. Therefore, the control applied to the plant actuators can be discontinuous during controllers switching. Because the switchings between Partial Load 2 and Full Load occur for $\beta = 0$, the pitch control is ensured to be continuous, whereas no continuity guarantees are provided concerning the generator torque. To ensure this, a structural constraint on the controllers matrices is added during the synthesis of the LPV controllers: the lines of the controllers matrices $C_{K,i}$ and $D_{K,i}$ corresponding to the generator torque are constrained to be equal at the boundaries of the subsets \mathcal{P}_j :

$$\begin{aligned} C_{K,i(1)}(\rho) &= C_{K,j(1)}(\rho) \\ D_{K,i(1)}(\rho) &= D_{K,j(1)}(\rho) \end{aligned}$$

for all $\rho \in \mathcal{P}_i \cap \mathcal{P}_j$.

The efficiency of the proposed controller is compared, at the sight of simulation results, with the ones of the two other existing controllers, a gain scheduling PI-based controller, and a multivariable gain scheduling LQG one, for the Full Load operation. Indeed, this operating area is the most challenging in the viewpoint of control design because the controller is multivariable, because the mechanical loads affecting the plant are the highest, and because the pitch action is really efficient to alleviate these loads with a carefully designed controller [2].

As mentioned in [2] and [3], the PI-based controller is designed by calculating controllers for two separate loops: firstly, a PI controller is tuned to guarantee power regulation from generator speed measurement. Then a tower speed feedback is designed to increase tower fore-aft damping, by calculating a controller which appropriately filters blades flap excitation and which does not interact with the bandwidth of the first loop. Unlike the proposed controller, this controller acts only on pitch angle.

The gain scheduling LQG controller is designed from the same augmented model and with the same performances outputs as the proposed controller. The LQG methodology permits to design a multivariable controller which optimizes a time domain quadratic criteria representing a trade off between the different control objectives. Unlike the proposed LPV design methodology, the LQG design does not provide guarantees of stability and performances along the reference trajectory, but only in several operating points on this trajectory. Actually, one LQG controller has to be designed at each linearization point of the trajectory, and a gain scheduling process has to be used to interpolate the different LQG controllers. Moreover, and contrary to the proposed method, the LQG design does not provide any specification of performance in the frequency range such as H_∞ or H_2 norms.

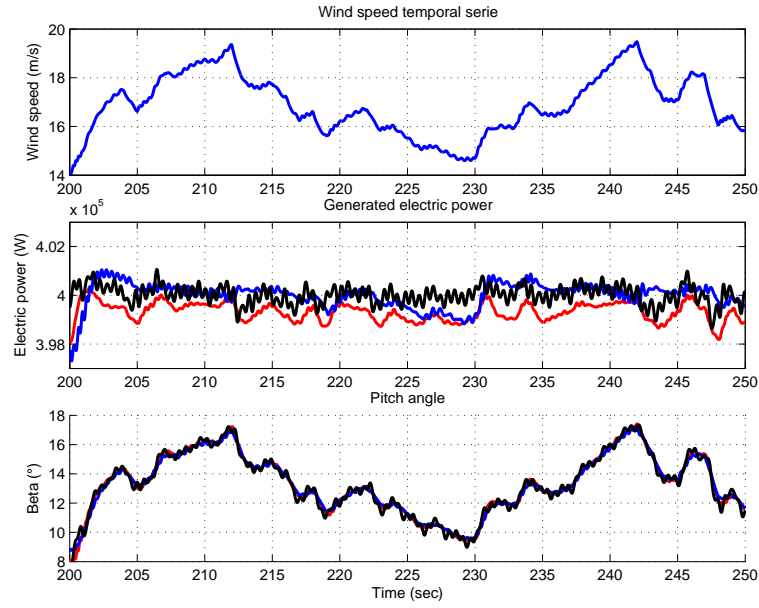


Figure 4: Temporal series. - LPV controller; - PI-controller; - LQG controller.

Table 1: Equivalent Load: Ratio between the different controllers and PI controller.

Controller	Shaft	Tower	Blades
LPV controller	57.3%	63.8%	82.9%
LQG controller	59.0%	73.4%	87.8%
PI controller	100%	100%	100%

The simulations are based on a dynamic model implemented in Matlab-Simulink of a three blades 400 kW wind turbine containing:

- non linear and stationary aerodynamics, with rotational effects disturbances due to wind shear and tower shadow.
- flexible drive train model, flexible tower model including first fore-aft mode, flexible blades in flapwise direction,
- pitch actuator limitations on pitch rate ($\pm 10^\circ/s$) and pitch amplitude ($0^\circ - 30^\circ$).

The simulated wind speed respects stochastic properties of Van der Hoven spectra with high fluctuations. The controllers performances are compared for both power regulation and alleviation of mechanical fatigue. These controllers have equivalent bandwidths and are tuned in order to guarantee a similar level of performance for power regulation. Evaluation of mechanical fatigue is provided by using the Rainflow Counting Algorithm, which calculates the number of load cycles from time domain simulations results, and the fatigue equivalent load for each component [10].

Temporal series of wind speed, produced power P_{elec} and pitch angle β are presented in Fig.4. Fatigue equivalent loads for the shaft, blades and tower are calculated from the simulations, and Table 1 presents the ratio between the equivalent loads obtained with the different controllers and with the PI-controller.

The proposed LPV controller is seen to be more effective for the two selected control objectives, especially for mechanical fatigue reduction for each component, and despite a pitch activity inferior to the pitch activity caused by the LQG controller. A sensitive gain of lifetime of the mechanical components of the plant, or a sensitive reduction of the mass, and consequently of the cost of these components can

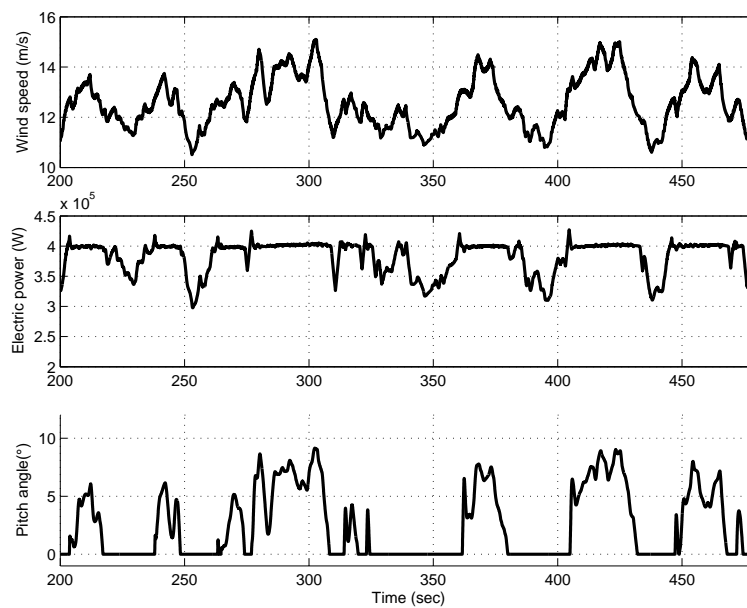


Figure 5: Transitions between Partial Load 2 and Full Load.

then be expected.

The behavior of the plant with the proposed control system is also shown during the transition between Partial Load 2 and Full Load in Fig.5, i.e. for wind speeds around the rated wind speed, which is about 12.2m/s . The control system is then seen to handle efficiently this transition.

7 Conclusion

In this paper, an hybrid controller composed by several LPV controllers has been proposed for the whole operating area of a variable speed, pitch regulated wind turbine. This control system achieves the optimization of a trade-off between the energy conversion and the reduction of the mechanical loads for the whole envelope of wind speeds acting on the plant, taking into account the different objectives of the energy conversion for the different operating areas.

Moreover, the employed LPV modeling, as well as the LMI formulation of the problem, provides a good framework for additional possible constraints of the control problem during the synthesis, like actuator saturation, or for ensuring the robustness to the system parameters uncertainties.

References

- [1] T. Burton, D. Sharpe, N. Jenkins, and E. Bossanyi, *Wind Energy Handbook*. John Wiley and Sons, 2001.
- [2] E.A. Bossanyi, The design of Closed Loop Controllers for Wind Turbines, *Wind Energy*, vol.3, 2001, pp.149-163.
- [3] W.E. Leithead, S. Dominguez and C.J. Spruce, Analysis of Tower/Blade interaction in the cancellation of the tower fore-aft mode via control, *Proc. European Wind Energy Conference*, London, UK, 2004.

- [4] P. Apkarian and R. J. Adams, §Advanced gain-scheduling techniques for uncertain systems, Ĥ *IEEE Transactions on Control System Technology*, vol. 6, pp. 21–32, 1997.
- [5] F. Lescher, J. Zhao, and P. Borne, §Robust gain scheduling controller for pitch regulated variable speed wind turbine, Ĥ *Studies in Informatics and Control*, vol. 14, pp. 299–315, 2005.
- [6] S. Lim, Analysis and Control of Linear Parameter-Varying Systems, Ph.D. Dissertation, Stanford University, 1999.
- [7] B. Lu and F. Wu, Switching LPV control designs using multiple parameter-dependent Lyapunov functions, *Automatica*, vol.40, 2004, pp. 1973-1980.
- [8] C. Nichita, D. Luca, B. Dakyo, and E. Ceanga, §Large band simulation of the wind speed for real time wind turbine simulators, Ĥ *IEEE Transactions on Energy Conversion*, vol. 17, pp. 523–529, 2002.
- [9] C. Scherer, P. Gahinet, and M. Chilali, §Multiobjective outputfeedback control via lmi optimization, Ĥ *IEEE Transactions on Automatic Control*, vol. 42, pp. 896–910, 1997.
- [10] M. Matsuiski and T.Endo, Fatigue of metals subjected to varying stress, *Japan Soc. Mech. Engrg*, 1969.

F. Lescher and P. Borne
Ecole Centrale de Lille
LAGIS Laboratory
BP 48, Cité Scientifique, 59651 Villeneuve d’Ascq Cedex, France
E-mail: fabien.lescher@eigsi.fr

J.Y. Zhao
EIGSI La Rochelle
ERPA Laboratory
26 rue Vaux Le Foletier, 17000 La Rochelle, France
E-mail: jing-yun.zhao@eigsi.fr

Received: November 2, 2006

Realization of Embedded Multimedia System Based On Dual-Core Processor OMAP5910

Peng Li, Yu Lu, Shen Li, Hongxing Wei

Abstract: This paper focuses on the realization of a complete embedded system using the dual-core processor OMAP5910. Detailed description of how to compose the hardware system is presented with a description of the software system on our platform. Tasks communication between the two cores is realized using the DSP driver. The system bootloader and the DSP bootloader are described in detail. The implementation of the MPEG-4 video decoder has been realized on the presented system. Higher speed can be achieved and less power is needed for MPEG-4 video processing on the dual-core platform. This dual-core system can be applied to 3G wireless communication, robot control and vision systems.

Keywords: Embedded System, MPEG-4 decoder, ARM, Omap5910, Multimedia Platform, Multimedia application, Operating system.

1 Introduction

With the growth of the 2.5/3G wireless markets, full-featured multimedia services are required by the wireless applications. More and more powerful processors are used to achieve the requirement. Dual-core architecture processors meet the rapid processing needs of next-generation embedded devices. Owing to the urgent need of the dual-core processor application, this paper presents a platform using the dual-core processor OMAP5910 and applications on this platform.

The OMAP5910 chip is a highly integrated hardware and software platform. It integrates a TMS320 C55xDSP core with a TI-enhanced ARM925 core on a single chip for the optimal combination of high performance with low power consumption. This unique architecture makes it ideal for audio and video processing in multimedia applications [1], [2].

The remaining part of this paper will be compiled as follows. In section 2, the composing of the hardware system is described and in section 3, the software system architecture is presented. In section 4, a detailed description of the system bootloader and DSP bootloader is given. Since video processing is one of the most important applications in multimedia systems, the implementation of the video decoding is described at the end of the paper.

2 Hardware System

OMAP5910 contains numerous interfaces for connecting to peripherals or external devices [3]. The complete Embedded Multimedia System we designed is illustrated as Figure 1.

As illustrated by Figure 1, 32M SDRAM and 16M NOR FLASH are used to compose the minimum system. The NOR FLASH is used to store the bootloader and the operating system. Another 256K SRAM is applied. A jumper is used to control the boot overlay mode, in which the SRAM is mapped to bank 0 and the NOR FLASH is mapped to bank 3.

Besides the minimum system, other devices of the platform are as follows: a camera for video capturing, a TFT color LCD for displaying, an audio codec for audio input and output, an Ethernet controller for operating system downloading and data transmitting, a PS/2 mouse and a keyboard as human device interfaces. The USB host/function interfaces and SD/MMC card interface are included in OMAP5910. They are used for the data storage in our system.

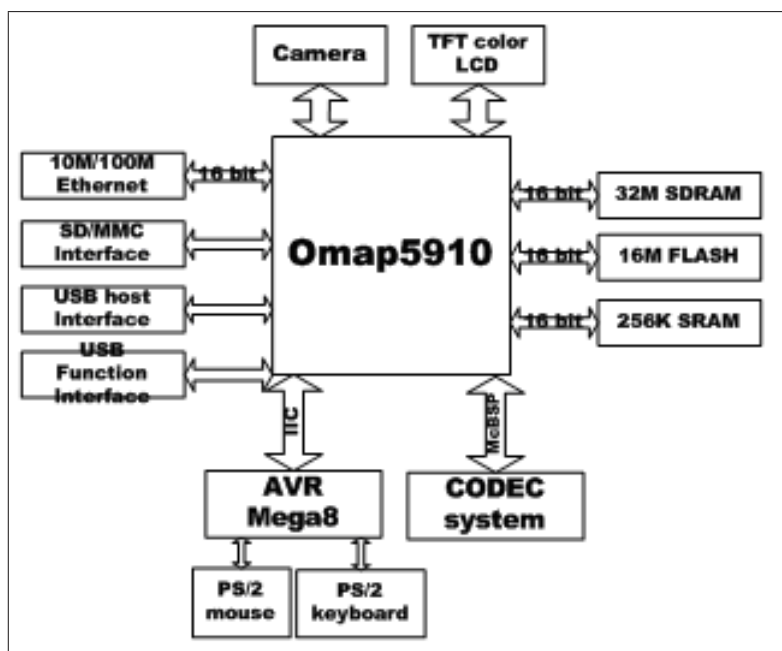


Figure 1: Hardware System

Due to the integration of the camera interface for CMOS sensors on OMAP5910, we choose the OV7648 for video capturing. The OV7648 is a sensor-on-board camera and lens module designed for mobile applications. The control interface of the sensor is the SCCB (OmniVision Serial Camera Control Bus), a 3-wire serial bus. Three MPU I/Os are used to realize the SCCB protocol. OV7648 output format is YCrCb 4:2:2 or RGB, and the YCrCb format is chosen in the system.

The color LCD controller on OMAP5910 supports a direct connection to the LCD panel and an 18bit TFT LCD is chosen for displaying. A high priority, dedicated DMA channel has been implemented in the system specifically for the LCD Controller. This dedicated DMA-LCD channel ensures minimum latency in real-time LCD operations.

Ethernet makes high-speed data exchanging, a very important function in multimedia systems, available between PC and the platform. It also provides an efficient way for system debugging. Here we adopt a fast Ethernet controller AX88796. The AX88796 is a high performance and highly integrated local CPU bus Ethernet Controller with embedded 10/100Mbps PHY/Transceiver and 8K*16 bit SRAM. It supports both 8 bit and 16 bit local CPU interfaces including MCS-51 series, 80186 series, MC68K series CPU and ISA bus. The 80186 16bit mode is chosen to meet the 16bits data bus of OMAP5910.

Because OMAP5910 does not have sufficient general I/Os, an AVR microcontroller is used to interface the PS/2 mouse and the keyboard. IIC bus is used to realize communicate between the AVR microcontroller and the OMAP5910. It is a good solution for the shortage of the GPIO in the system.

Since three McBSPs (Multi-channel Buffered Serial Ports) are integrated on the OMAP5910, an audio codec is connected to one of them directly. TLV320AIC23B, a high-performance stereo audio codec with highly integrated analog functionality, is selected to compose our codec system. The TLV320AIC23B supports glueless interface to the TI McBSP. We use the IIC bus to implement its control interface.

Various multimedia applications can be realized using this hardware platform on which we have implemented a MPEG4 video decoder.

3 Software System

We choose the DAS U-BOOT as the bootloader for the system, and the Linux 2.4.21 as the kernel. The software tools we used to develop programs are Code Composer Studio (CCS) and the GNU Tool Chain. CCS is used to develop DSP programs, while the GNU Tool Chain is used to compile the bootloader and the kernel. Programs on the MPU and the DSP are developed separately. In our system, the ARM RISC is used for handing control code, such as user interface, OS and OS application, while the DSP is used for the real-time signal-processing. Both the system bootloader and the kernel run on the MPU, and the DSP is registered as a character device in the kernel.

Applications that run on the MPU can not access or make use of the DSP directly, so they must use the DSP driver to control or communicate with DSP core. The DSP driver in the kernel provides user applications with the capability of controlling and the interfaces to communicate with DSP. To communicate or make use of DSP, applications have to send read, write or I/O control request to kernel, then kernel would deliver such request to DSP driver. Subsequently, DSP driver set the corresponding control registers and send the control code or application data to the DSP.

There are three ways we used to communicate between the MPU and the DSP. The first one is to use the MPUI port. It allows access to the full memory space (16M bytes) of the DSP, and it is the only way for the MPU and the system DMA to access the I/O spaces of the DSP. Since configuration and data registers for all the peripherals of the DSP reside in the DSP subsystem I/O space, we use this way to set the corresponding peripherals registers in the DSP. The second way is to use the MPU MMU and the DSP MMU, through which shared access to system memory can be realized between the two cores. The MPU MMU performs virtual-to-physical address translations and accesses permission checks for access to the system memory. The DSP MMU is controlled by the MPU. When the DSP MMU is on, the DSP MMU translates addresses from the DSP (virtual address) to addresses mapped by the traffic controller. The DSP MMU is used when the DSP software accesses external memory and we adopt the DSP MMU to map the external memory space of the DSP on the external SDRAM. We also utilize the MPU MMU to map an appropriate system addressing space on the external SDRAM. Then both the MPU and the DSP can access this shared memory regions. The third way is to use the mailbox-interrupt mechanism. This mechanism provides a very flexible software protocol between the two cores. We use it to create handshaking interrupts which will properly synchronize the MPU and DSP operations. The software architecture is shown in Figure 2.

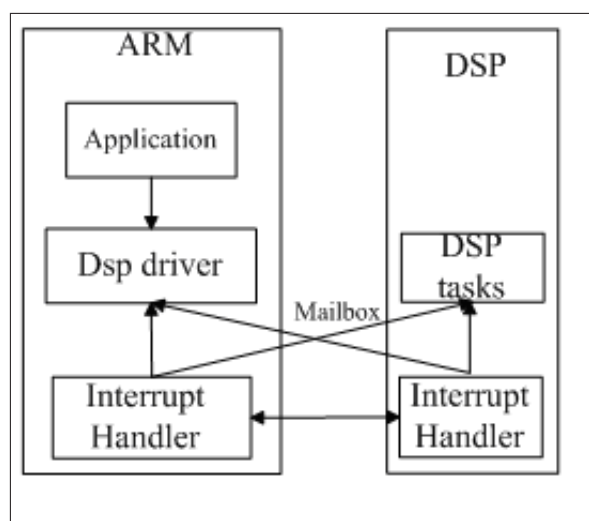


Figure 2: Software Architecture

When certain user application wants to utilize DSP to accomplish a specific calculating task, it must

send a request to the DSP driver. The DSP driver would write this request code and application data to the Mailbox. So the DSP core can get to know what the user application wants and where is the storage of the raw data. Then DSP would be interrupted, and both the control code and the application data address could be obtained during this Mailbox interrupt. With these data, DSP starts to do the corresponding calculation as the application asks. After finishing the application task, DSP returns a response to the MPU by writing to the Mailbox. DSP driver would process this Mailbox interrupt on the MPU side, and fetch the result of the application task.

4 System bootloader and DSP bootloader

Boot process is very important to both the MPU and the DSP. Each of the two cores needs their own bootloader. The system (MPU) bootloader is adopted to perform a simple initialization and to load the kernel to the system memory. U-BOOT is a bootloader for embedded system based on PowerPC and ARM processors. It is a full featured bootloader that is small and also easy to build and use. One of the most useful features of U-BOOT is the supporting of the TFTP downloading. The U-BOOT 1.1.1 supports the ARM925t architecture and the OMAP5910 processor. We need to set appropriate configurations and write drivers for various peripherals used during the booting process. The Ethernet controller driver enables the TFTP boot feature of U-BOOT and such TFTP boot function greatly facilitates the debugging process of the kernel. Much higher speed could be achieved when loading kernel to the system RAM, compared with the using of serial or parallel port. The loading process can be fully automatic by the U-BOOT when power on. The MPU is the master in the system and is responsible for setting up and bringing the DSP out of reset. Appropriate boot mode of the DSP must be set by MPU before releasing the DSP from reset.

When the DSP core is taken out of reset, DSP bootloader will be executed. The bootloader of the DSP resides in the DSP subsystem PDRAM. It performs some initialization of the DSP resources before loading code. After the initialization, the bootloader branches to the starting point address specified by the selected boot mode. There are four boot modes: direct boot, external memory boot, DSP idle boot, internal memory boot. The internal memory boot mode is selected in our system, because it is more convenient compared with other modes.

To adopt the internal boot mode, we have to load code and data sections into DSP subsystem internal memory. The MPU core or system DMA can be used to accomplish this task. We utilize MPU core with the MPU interface (MPUI) to perform the loading. MPUI allows the MPU to communicate with the DSP and its peripherals. The endian mode should be noticed during the data loading process. The MPU (TI925T) operates in little endian mode while the DSP operates in big endian mode. Therefore, data have to be converted into big endian format when loaded into the DSP's memory. There are swapping buffers between the DSP and the MPUI, and the word or byte swapping can be programmed. After loading data into DSP internal memory, the MPU core can call the DSP subsystem out of reset, then the DSP bootloader begins to execute. The DSP bootloader transfers execution to the appropriate byte address, and the loaded application starts running. It should be noticed that the output format of CCS is DSP COFF format, and it cannot be used directly in ARM side. So we utilize the HEX55 utility to convert the COFF format file into HEX format file. The hex file could be parsed to get the DSP code and its running address.

5 System application

MPEG video processing is a very important application for multimedia systems. Due to the high-speed requirement of the computation, powerful processors are needed to process these data. Our dual-core system provides a better solution for video processing compared with normal RISC [6] or DSP

systems.

Handling of the control code and the real-time signal processing are implemented by the MPU and the DSP separately. The ARM RISC is well suited for handling control code, such as user interface, OS and OS applications. On the other hand, the DSP side is better suited for real-time data processing. Appropriate division of the work makes the dual-core system get a better performance.

The C55x DSP is especially suited for multimedia signal processing. Three hardware accelerators are included along with the C55x DSP core to enhance the multimedia processing capability [4]. They are discrete cosine transform (DCT) and its inverse IDCT accelerator, motion estimation accelerator and pixel interpolation accelerator. DCT/IDCT, motion estimation, and pixel interpolation are common tasks to all industry video-imaging standards. They are also the most time-consuming tasks in video processing. These C55x hardware accelerator modules assist the DSP core in implementing algorithms that are commonly used in video compression applications such as MPEG4 encoders/decoders. These accelerators enable implementation of such algorithms using fewer DSP instruction cycles and dissipating less power than the DSP core is operating alone.

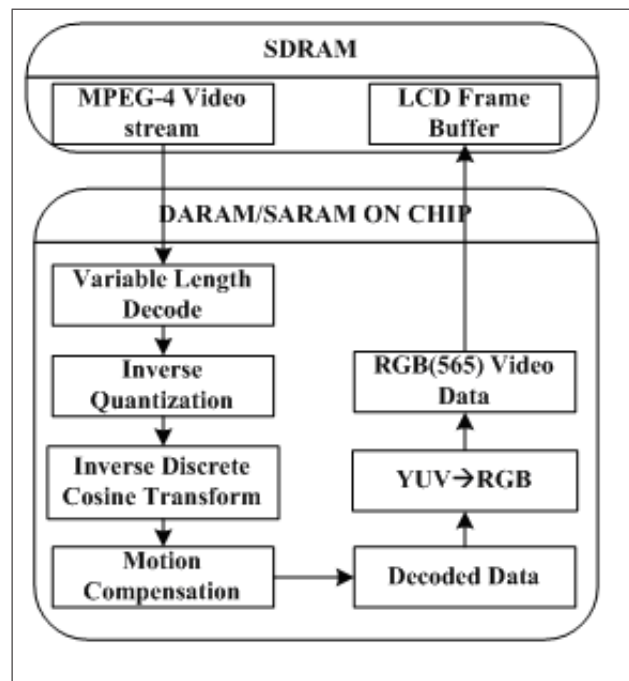


Figure 3: The decoding procedure on the DSP

The hardware accelerators are utilized via functions from the TMS320C55x Image/Video Processing Library available from Texas Instruments [5]. IMGLIB is an optimized image/video processing functions library for C programmers using TMS320C55x devices. It includes many C-callable, assembly-optimized, general-purpose image/video processing routines. These routines are typically used in computationally intensive real-time applications where optimal execution speed is critical. By using these routines, we achieve execution speeds considerably faster than equivalent code written in standard ANSI C language.

The hardware accelerator and the IMGLIB are utilized to implement a MPGE-4 video decoder on our multimedia system. The decoding procedure on the DSP core is illustrated as Figure 3.

The MPEG-4 bit-streams are stored in shared system memory. Because the DSP accesses the internal DARAM and SARAM at much higher speed, the decoding process is completed in its own local memory. By the help of the TMS320C55x Image/Video Processing Library, we get the decoded data in the local memory. Because the decoded data are in YUV 4:2:0 formats, post-processing is needed to convert the

	ARM9E	C5510	Units
MPEG-4/H.263 decoding QCIF at 15 fps	16	9.6	Mcycles/s
MPEG-4/H.263 encoding QCIF at 15 fps	90	33	Mcycles/s

Figure 4: Results of comparative benchmarking

decoded data into RGB format. Having converted the data into 16 bits RGB (565) format, we send it to the LCD Frame buffer for displaying [7].

Compared with a RISC processor ARM9, the performance of the decoding process is greatly improved. Results of comparative benchmarking by Pace Soft Silicon are shown in Figure 4.

These benchmarks demonstrate that multimedia tasks require three times as many cycles and two times as much power to execute on a latest-generation RISC processor as they do on a C55x DSP [4].

6 Summary and Conclusions

This embedded multimedia system is successfully designed and implemented. Various multimedia applications can be realized on such platform. The software system presented herein provides a solution for communication between the dual-core. The successful implementation of the MPEG4 decoding procedure on this system proves that the higher speed can be achieved and the less power is needed.

With the growth of the 3G wireless markets, dual-core architecture systems will be widely used. The authors believe that the presented platform is suitable for many 3G wireless multimedia applications in the near future.

References

- [1] James Song, Thomas Shepherd, Minh Chau, A low power open multimedia application platform for 3G wireless, *Proceedings of SOC Conference, 2003, IEEE International*, pp. 377-380, Sept.2003.
- [2] JCheng-Nan Chiu, Chien-Tang Tseng, and Chun-Jen Tsai, Tightly-coupled MPEG-4 video encoder framework on asymmetric dual-core platforms, *ISCAS 2005, IEEE International*, pp. 2132-2135, May 2005.
- [3] Texas Instruments, OMAP5910 Dual-Core Processor Technical Reference Manual, *TI Technical Document SPRU602B*, Jan.2003.
- [4] Texas Instruments, TMS320C55x Hardware Extensions for Image/Video Applications Programmer's Reference, *TI Technical Document SPRU098*, Feb.2002.
- [5] Texas Instruments, TMS320C55x Image/Video Processing Library Programmer's Reference Preliminary, *TI Technical Document SPRU037C*, Jan.2004.

- [6] Hae-Yong Kang, Kyung-Ah Jeong, Jung-Yang Bae, Young-Su Lee, Seung-Ho Lee, MPEG4 AVC/H.264 DECODER WITH SCALABLE BUS ARCHITECTURE AND DUAL MEMORY CONTROLLER, *Circuits and Systems, 2004. ISCAS '04. Proceedings of the 2004 International Symposium on*, Vol. 2, pp.II - 145-8, May. 2004
- [7] Thanh Tran, OMAP 5910 Video Encoding and Decoding, *TI Application Report SPRA985*, Dec. 2003.

Peng Li, Yu Lu

Beijing University of Aeronautics and Astronautics
School of Automation Science and Electrical Engineering

Shen Li

Beijing University of Aeronautics and Astronautics
School of Software

Hongxing Wei

Beijing University of Aeronautics and Astronautics
School of Mechanical Engineering and Automation
No. 37 Xue Yuan Road, Haidian district 100083 Beijing P.R. China
lastmars@gmail.com

Received: November 5, 2006

Obstacle Detection in Cluttered Traffic Environment Based on Candidate Generation and Classification

Qing Li, F.C. Sun

Abstract: A novel method to detect vehicles is presented in the paper. Assumption of the vehicle is made using the geometrical features of the vehicle rear by the statistical histogram. Then hypothesis is verified using the property of the shadow cast by the car according to a prior acknowledgement of traffic scene. Finally, the vehicle detection is realized by hypothesis and verification of objects. The experimental results show the efficiency and feasibility of the method.

Keywords: objects hypothesis, objects verification, statistical histogram, vehicles detection

1 Introduction

The statistics of traffic accidents show that drivers have to face threats mainly from other vehicles. It is very significant to detect preceding vehicles in real time for keeping safe distance and avoiding collision. At the same time, vehicles detection is the precondition of safe driving and primary requirement of driver assist systems, active safety systems and automatic vehicles[1]. Many methods based on vision are used to detect vehicles, such as according to symmetry, shadow, texture, horizontal/vertical edge, color, stereo vision, depth, movement, template, view point, information fusion and parallax. We mainly detect preceding vehicles, including all vehicles running along same direction, even in other lanes, by vision sensors. Furthermore, head-on vehicles shall not be considered because we emphasize on systems for structural road where contrary lanes are separated by rail fence. A method based on objects assumption and verification for vehicle detection is suggested in the paper. Firstly, vehicles assumption is made by statistical histogram according to geometrical features. Secondly, the assumption is verified according to prior acknowledge. Lastly, the vehicles detection is realized. The experimental results show the method is valid and feasible.

2 Object assumption

The colorful video is gathered and conversed into frames of images. The images are preprocessed in the procedure of objects assumption. Then the potential vehicles are located in the whole image by several standards according to features of vehicles.

A. Finding Edge Features in the Image

Firstly, the object area is found approximately by camera calibration. Secondly, the color space is transformed in order to utilize color information effectively. Firstly, the horizontal gradient, the vertical gradient and the characteristic gradient are calculated in different color channel. In order to detect vehicles on the road, some features of vehicles are analyzed, including symmetry and edges. Vehicles mainly consist of horizontal structure, especially when they are observed from the rear. Though other horizontal structures exist in the road scene, the areas can usually be marked and their physical feasibility can be judged. Some experiments show horizontal edges are useful cue to confirm area of interest where vehicles appear possibly. In order to obtain horizontal edge response I_h and vertical edge response I_v , a direct edge filter is used. The input image is masked by two $n \times n$ template. The values of I_h and I_v is compared to obtain an edge response map I_r [2]. In fact, man-made objects have more obvious edge response than natural objects. The value I_r is relatively distinct for vehicles, so it is regarded as a basic

feature to detect vehicles(Fig.1)(Top: horizontal addition of the vertical histogram; bottom: horizontal lines representing vehicle (overlapped on the original image)).

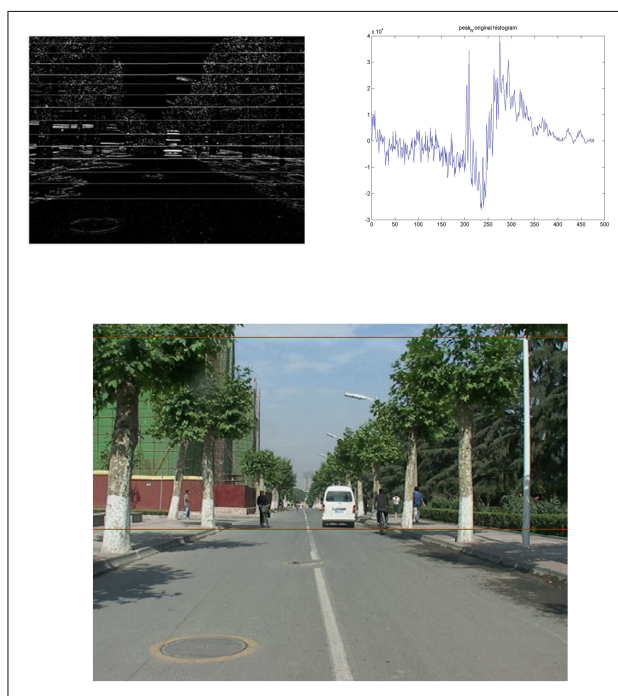


Figure 1: Object location in the vertical direction

B. Statistical Histogram Process

Firstly, we shall determine the possible location of vehicles in the vertical direction. The statistical histogram is formed by adding values of the edge responding map in a line and smoothed. The shift mean is used to smooth the curve in the paper. The potential vehicle is located by the local maximum of the smoothed curve. It is the most important to find and detect peak for segmenting the maximum of the histogram. Some methods are suggested to choose obvious mode. By examining the steepness or area of the peak value[3], the peak value will be detected. If it is not enough steep or big, the peak will be deleted[4]. The road surface is supposed as flat. The vehicles on road show symmetrical shape and certain ratio of high to width.(0.8-1.2).The ratio is set to 1.0 in the paper. The other feature is the size of vehicles in the image. The object will be far from the driver if the size is very little and will not be considered. The width of object responds the distance between the object and the driver. The smallest car far from 100 meter responds the width of 30 pixels. If the imaging width of the object is over 30 pixels, the distance will exceed 100 meters. Usually, the distance of 100 meters is enough to respond for drivers of the speech of vehicles is below 120 km/h.

Though the approximate position of vehicles can be determined by the above work, the imaging size of vehicles can't be solved and more work will be finished. The possible position locates the middle bottom of vehicles in Fig.2(top: vertical addition of the horizontal histogram; bottom: vertical lines located(overlapped on the original image) and possible position of vehicles). The area of interest of position (u_0, v_0) is as $A(u, v), u \in (u_0 - h_1, u_0 + h_2), v \in (v_0 - v_1, v_0 + v_2)$ (Fig. 3). The vertical edges of vehicles is searched in the area of interest $A(u, v)$. The statistical histogram of the area of interest is formed by the edge gradient in the vertical direction. The peak value of the left edge and the right edge of the vehicle can be found by the method. The peak value just near the candidate point is chosen if many peak values exist. No vehicles exist in the area of interest if only one peak value exist. The symmetry distance is introduced and obtained by calculating the mean square error of gray value g_{left} and g_{right} [5].

$$SD = E[(g_{left} - g_{right})^2] \quad (1)$$

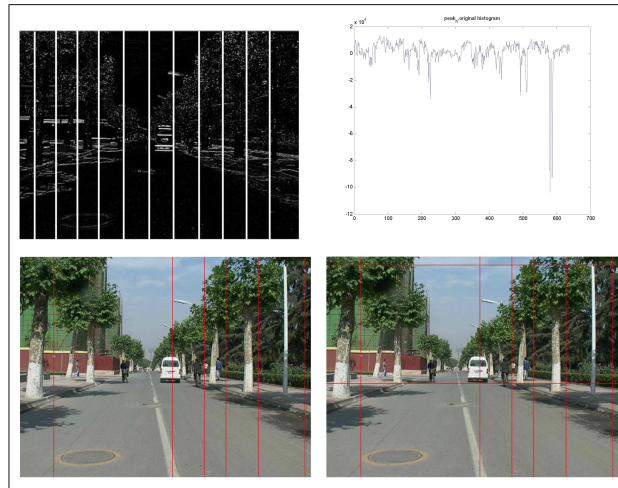


Figure 2: Object location in the horizontal direction

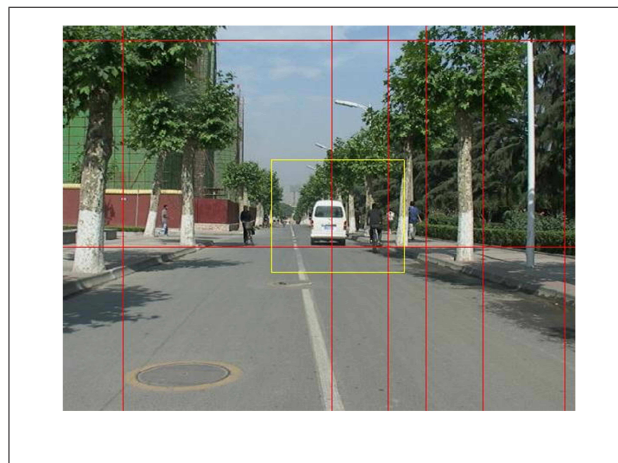


Figure 3: The area of interest determined.

If the SD is below a certain value, the obstacle more possibly exist(Fig.4). The area with maximum is defined as candidate area of vehicles(Fig.5).

3 Assumption verification

Even a potential object meets three standards, the assumption would be further verified because of weak grouping condition to seek potential vehicles. The object is verified based on shadow. Many methods are used to detect vehicles by utilizing the shadow below vehicles[6][7][8].

4 Experiment

Different types of vehicles are detected in the different road and weather condition. The variational P_r/P_R , P_g/P_G and P_b/P_G are illustrated in Fig.6 when the bar box moves. The different areas detected

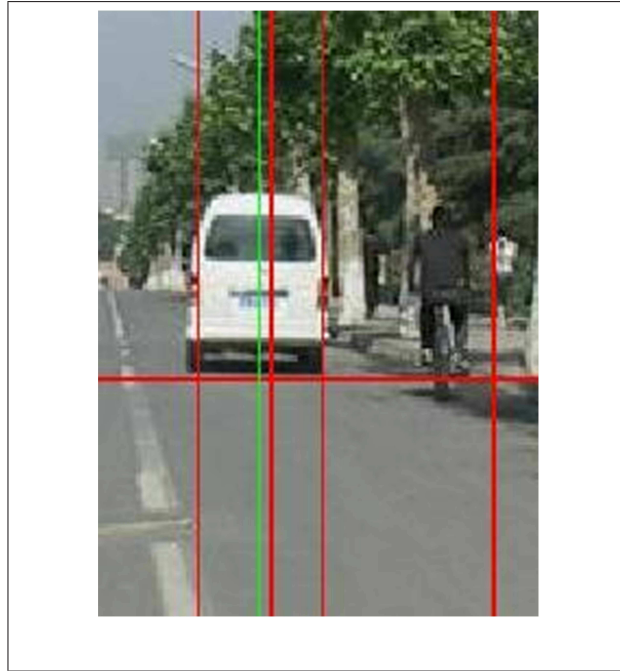


Figure 4: The vertical edges of the vehicle being located in the area of interest

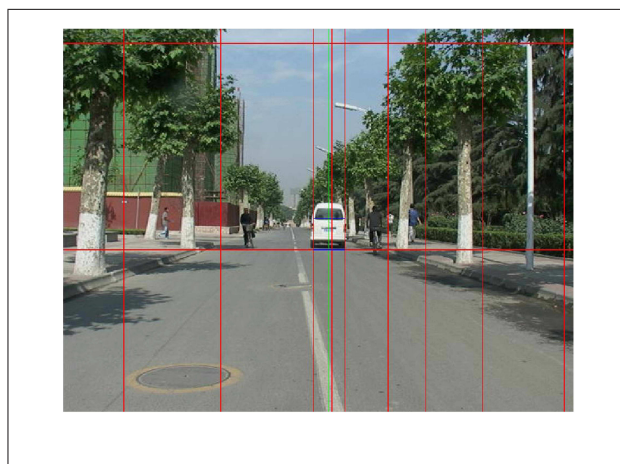


Figure 5: The candidate object

by object assumption and verification are showed in Fig.7. The position of preceding vehicles can be determined by combining with lane detection in Fig.8.

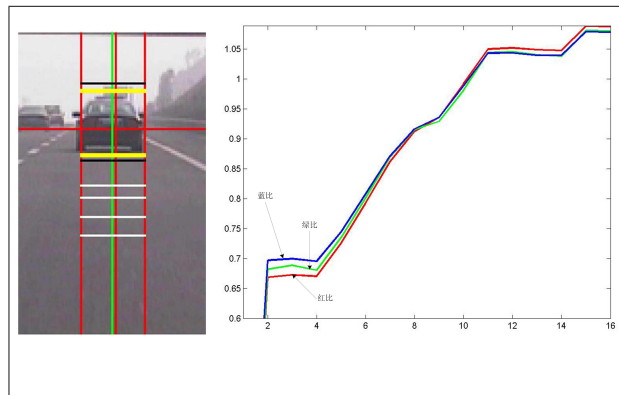


Figure 6: Blue ratio, green ratio and red ratio in the vertical candidate area

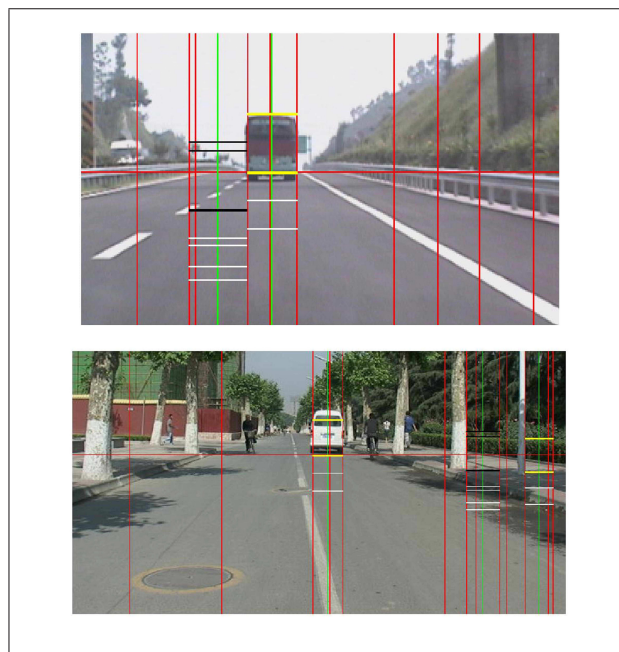


Figure 7: The different areas detected by object assumption and assumption verification

5 Summary and Conclusions

Because size, shape and color of vehicles are different, it is very challenging to detect vehicles by optical sensors. Additionally, surface of vehicles relies on their pose and is affected by ambient objects. It is difficult to control complicated outdoor environment. The method is composed of object assumption and assumption verification. Horizontal edge and symmetry of vehicle rear is used to seek candidate vehicles in assumption. Shadow is used to verify vehicles in verification. Experimental results show feasibility of the method.

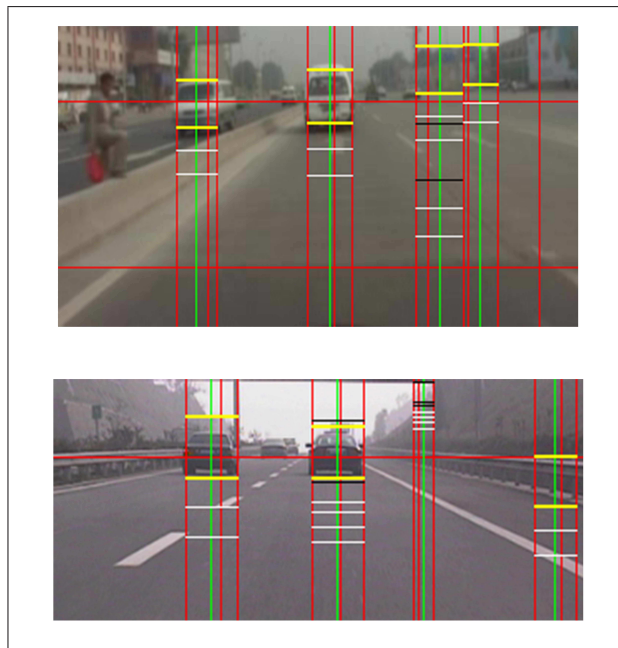


Figure 8: Some results of vehicle detection

6 Acknowledge

This work was jointly supported by the National Natural Science Foundation of China (Grant No: 60334020, 60321002, 60474025, 60504003 and 90405017), the National Excellent Doctoral Dissertation Foundation (Grant No: 200041), the National Key Project for Basic Research of China (Grant No: G2002cb312205) and the Specialized Research Fund for the Doctoral Program of Higher Education(Grant No: 20050003049).

References

- [1] M. Bertozzi, A. Broggi, A. Broggi, A. Fascioli, Vision-based intelligent vehicles: state of the art and perspectives, *Robotics and Autonomous Systems*, Vol. 32, pp. 1-16, 2000.
- [2] N. Matthews, P. D. Charnley, C. Harris, Vehicle detection and recognition in greyscale imagery, *Control Engineering Practice*, Vol. 4, pp. 473-479, 1996.
- [3] D. C. Tseng, C. H. Chang, Color segmentation using perceptual attributes, *Proceedings of IEEE International Conference on Image Processing*, pp. 228-231, 1992.
- [4] H. D. Cheng, Y. Sun, A hierarchical approach to color image segmentation using homogeneity, *IEEE Transactions on Image Processing*, Vol. 9, No. 12, pp. 2071-2082, 2000.
- [5] H. Mori, N. M. Charkari, Y. T. Matsushita, On-line vehicle and pedestrian detections based on sign pattern, *IEEE Transactions on industrial electronics*, Vol. 41, No. 4, pp. 384-391, 1994.
- [6] M. Y. Chern, B. Y. Shyr, Locating nearby vehicles on highway at daytime based on the front vision of a moving car, *Proceedings of Robotics and Automation*, Vol. 2, pp. 2085-2090, 2003.
- [7] S. Kyo, T. Koga, K. Sakurai, S. Okazaki, M. A robust vehicle detecting and tracking system for wet weather conditions using the LMAP-VISION Image Processing Board, *Proceedings of IEEE International Conference on Intelligent Transportation Systems*, pp. 423-428, 1999.

- [8] S. Nadimi, B. Bhanu, Physical models for moving shadow and object detection in video, *IEEE Transactions on Pattern Analysis and Machine Intelligence*, Vol. 26, No. 8, pp. 1079-1087, 2004.

Q. Li, F.C. Sun
Tsinghua University
Department of Computer Science and Technology
Beijing, China
E-mail: qli@mail.tsinghua.edu.cn

Received: November 10, 2006

Computation on the Optimal Control of Networked Control Systems with Multiple Switching Modes Over High Speed Local Area Networks

Gang Zheng, Wenli Zeng, Fanjiang Xu

Abstract: The optimal control problem for the networked control system with multiple switching modes over high speed local area networks is addressed, where an initial state is a parametric vector. Because in the general case, the time delay is much less than the sampling period and the possibility of the packets collision is much lower, it can be assumed that the influence of the time delay and the packets loss on the optimal controller design can be ignored. On the basis of the assumption, the networked control systems with multiple switching modes are modeled as a hybrid system. Moreover, based on the Bellman type inequality for the hybrid systems, a dynamic program to solve the optimal control with a parameter vector is proposed, in every step of the technique, the feasible region is divided into evenly distributed grid points, and then, the optimal control law is transformed into maximizing the lower bound of the cost to go function in grid points. Finally, an experiment setup of the networked control system with multiple switching modes is constructed and a simulation example is given to illustrate the optimal control computation results.

Keywords: networked control systems, hybrid systems, optimal control, dynamic program, multiparametric program

1 Introduction

Networked control systems (NCS) are feedback control systems wherein the control loops are closed through a real-time network[1]. The defining feature of an NCS is that information (reference input, plant output, control input, etc.) is exchanged using a network among control system components (sensors, controller, actuators, etc.). The use of a communication network offers advantages in terms of reliability, enhanced resource utilization, reduced wiring, and reconfigurability. Networked control systems typically involve switching between several different modes, depending on the range of operation. In order to improve the performance of the system and save the operation cost, it is important to design an optimal control law for the systems with different switching modes. At present the methodologies of designing the optimal controllers for such networked control systems are few. [2] assumes that the controller-plant communication in NCS is periodic, the optimal controller design problem is formulated as one for sampled-data feedback systems with periodic discrete-time components, and give a necessary and sufficient condition for existence of discrete time periodic controller in terms of LMIs, and derive a controller construction algorithm. [3]discusses the optimal H_∞ control problem for networked systems with limited communication constraint, which is formulated as a periodic control problem, and proposes a heuristic search approach in conjunction with the convex optimization of controller to solve the optimization problem. The switching process in [2] and [3] is time-controlled. However, in practice, the switching may be completely determined by the system state, for such networked control systems, the whole state space is divided into cells which each correspond to a particular control mode, so that each cell has its own continuous dynamics associated to it. This type of the system is state-controlled and can be regarded as a hybrid system. Hybrid systems have attracted considerable attention in recent years [4]. Also, in practice, the initial state of networked control systems may be not determined, and for those with multiple switching modes, the unpredicted initial states may make the optimization process more complex. This paper model the class of networked control systems with multiple switching modes as a hybrid system, based on the model, a general cost function is defined and the optimal control problem

for a general cost function is addressed, where a initial state is a parametric vector and is not predicted. Furthermore, a solution to the optimal feedback control law is proposed, which combine the dynamic program and multiparametric program. Finally, an example is given to illustrate the optimal computation results.

2 Problem Formulation

2.1 Modeling networked control systems with multiple switching modes

Consider a class of networked control systems shown in figure 1. The plant, the sensors, the controller and the actuators are spatially distributed and connected together through a control network. In general, there are multiple control modes in the controller of the class of systems, and every mode corresponds to the range of the continuous state of the physical plant. We assume that the control network is a high speed local area network, e.g. Ethernet, and the transmitting data policy is scheduled releasing policy, the time delay is much less than the sampling period in practice and the possibility of message collision is much lower, therefore, in this paper, it is reasonable to ignore the influence of the time delay and packets loss on the optimal controller design in the networked control systems with multiple switching modes.

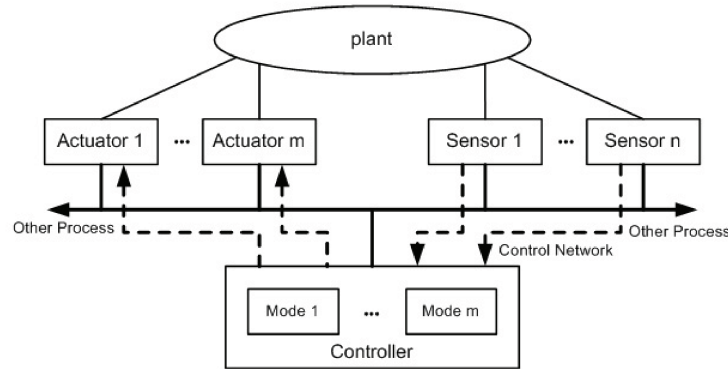


Figure 1: The networked control system with multiple control modes

On the basis of the assumption, the class of networked control systems with multiple modes can be modeled as a hybrid system. Hybrid systems contain continuous dynamics and discrete events [4]. The controller in networked control systems can calculate the state of the plant and determine the control modes, and the switching between different modes corresponds to the occurrence of the discrete event in hybrid systems. We assume that clock-driven sensors sample the plant outputs periodically at sampling instants, then the networked control system can be modeled as a hybrid system as following:

$$\begin{cases} x(k+1) = f_{q(k)}(x(k), u(k)) \\ q(k+1) = v(x(k), q(k)) \end{cases} \quad (1)$$

where continuous state variable $x \in X \triangleq \mathbb{R}^n$, continuous input variable $u \in U \triangleq \mathbb{R}^m$, k denotes k -th sampling period, $k = 0, 1, 2, \dots$, $q \in Q$, Q is a finite countable set, whose elements correspond to the modes in the networked control system, $f_q : X \times U \rightarrow X$ denotes the continuous dynamics in discrete mode q , $v : X \times Q \rightarrow Q$ denotes the discrete dynamics, which is a transition process between operation modes. Without the loss of the generality, we think the transition between two modes occurs in the sampling time instant.

The hybrid system model (1) of the networked control system with multiple modes can also be denoted a hybrid automaton[5]. In addition, if the continuous dynamics can be denoted by the linear time invariant system, the model can transformed into the piecewise affine system[6], where different modes correspond to different ranges of state variable x .

2.2 Optimal Control Formulation

Based on the model (1), the optimal control formulation in finite time horizon is discussed as follows. Firstly, define the cost function of the networked control system

$$J(U_N, x(0)) = F_{q(N)}(x_N) + \sum_{k=0}^{N-1} [F_{q(k)}(x_k, u_k) + G(x_k, q(k), q(k+1))] \quad (2)$$

where N is the time horizon, starting from the state $x_0 = x(0)$, x_k denotes the continuous state vector at time k and $q(k)$ denotes the discrete state vector corresponding operation mode at time k , the column vector $U_N \triangleq [u_0^T, \dots, u_{N-1}^T]^T \in \mathbb{R}^m$, $F_{q(N)}(x_N) > 0$ is a cost at end time, $F_{q(k)}(x_k, u_k) > 0$ is a cost for continuous evolution in an operation mode and $G(x_k, q(k), q(k+1)) \geq 0$ is a cost for switching from one mode to another mode, if there is no switching, i.e. $q(k) = q(k+1)$, $G(x_k, q(k), q(k+1)) = 0$. Note that, we don't consider the problem of infinitely many jumps in transition time instants. Also, it should be noted that $q(0)$ is not written in the left of cost function (2), because the operation modes correspond to the range of the state variable, if the initial condition $x(0)$ is given, and the discrete mode $q(0)$ is fixed, too.

The optimal control problem of the networked control system is

$$J^*(x(0)) \triangleq \min_{\{U_N\}} J(U_N, x(0)) \quad (3)$$

$$\text{s.t.} \begin{cases} x_{k+1} = f_{q(k)}(x_k, u_k) \\ q(k+1) = v(x_k, q(k)) \\ x_N \in \mathcal{X}_f \\ x_0 = x(0) \end{cases} \quad (4)$$

where \mathcal{X}_f is the terminal region, in addition, \mathcal{X}_j denotes the set of states x_j at time j for which (3) is feasible.

In general, the optimal control problem (3)-(4) may not have a minimum for some feasible $x(0)$. This is caused by discontinuity of the hybrid system in the input space. We will consider problem (3)-(4) assuming that a minimizer $U_N^*(x(0))$ exists for all feasible $x(0)$.

Note that in this paper we will distinguish between the current state $x(k)$ of the system (1) at time k and the variable x_k in the optimization problem (3)-(4), that is the predicted state of the system (1) at time k obtained by starting from the state $x_0 = x(0)$ and applying the input sequence u_0, \dots, u_{k-1} to system (1). Analogously, $u(k)$ is the input applied to system (1) at time k while u_k is the k -th optimization variable of the optimal control problem (3)-(4).

In the optimal control problem (3)-(4), the initial state $x(0)$ is a vector of parameters, the goal in this paper is to solve (3)-(4) for all values of $x(0)$ of interest, and to make this dependence explicit. Therefore, the optimal control problem of the networked control system with multiple modes is a multiparameter program problem.

3 Solution to the Optimal Control of the Networked Control Systems

For the networked control systems with multiple modes, the optimal control problem can be viewed as a parametric programming one. The parametric program is one of the important optimization techniques in mathematical program, where the optimality is affected by the uncertainty of the parameters

in the cost function or the constrained conditions. Because the parameters are either unknown or that will be decided later, parametric programming need to subdivide the space of parameters into characteristic regions, which depict the feasibility and corresponding performance as a function of the uncertain parameters, and hence provide the decision maker with a complete map of various outcomes [6].

In the networked control system, different operation modes correspond to different range of the state variable, the switching sequence between different modes is related with the initial condition of the system, which is not fixed. If the switching sequence is fixed, the optimal control problem is equivalent to a finite time optimal control problem for a hybrid system, which can be solved by multiparametric program, in this case, the optimal solution is a optimal control candidate for the networked control system. If all of the switching sequences in the networked control system are given, the solution to the optimal control problem (5) can be obtained by comparing the values of cost function corresponding to the optimal control candidate in different switching sequences.

However, with the increase of the control modes, the computing process gets more complex and the computing efficiency gets much lower because we must enumerate all the possible switching sequences of the networked control system, which is a little same as the famous traveling salesman problem (TSP) in the optimization theory. In order to decrease the computation complexity and improve the computation efficiency, the dynamic program technique is proposed to solve the optimal control problem of the networked control system with multiple control modes.

The dynamic programming solution of the optimal control problem is denoted as follows:

$$J_n^*(x_n) \triangleq \min_{\{u_n\}} \{ [F_{q(n)}(x(n), u(n)) + G(x(n), q(n), q(n+1))] + J_{n+1}^*(x(n+1)) \} \quad (5)$$

$$\text{s.t. } x(n+1) \in \mathcal{X}_{n+1}, n = N-1, \dots, 0 \quad (6)$$

with terminal conditions:

$$\mathcal{X}_n = \mathcal{X}_f \quad (7)$$

$$J_N^*(x(N)) = F_{q(N)}(x_N) \quad (8)$$

where \mathcal{X}_j is the set of all initial states for which dynamic program problem (5)-(8) is feasible, $\mathcal{X}_j = \{x \in \mathbb{R}^n | \exists u, f_{q(j)}(x, u) \in \mathcal{X}_{j+1}\}$.

The first step of dynamic program is as follows:

$$J_{N-1}^*(x(N-1)) \triangleq \min_{\{u_{N-1}\}} \{ [F_{q(N-1)}(x(N-1), u(N-1)) + G(x(N-1), q(N-1), q(N))] + J_N^*(x(N)) \} \quad (9)$$

$$\text{s.t. } \begin{cases} f_{q(N-1)}(x(N-1), u_{N-1}) \in \mathcal{X}_f \\ J_N^*(x(N)) = F_{q(N)}(x_N) = F_{q(N)}(f_{q(N-1)}(x(N-1), u_{N-1})) \end{cases} \quad (10)$$

It is clear that the optimal control problem (9)-(10) is a multiparametric program problem, where $x(N-1)$ is a parametric vector. In terms of terminal region \mathcal{X}_f and the system equation (1), the feasible region \mathcal{X}_{N-1} at time $N-1$ is obtained. [7] discuss the discretized computation on the optimal control of hybrid systems, where the initial state and the terminal state are determined and the key point is to search the maximum lower bound of the value function. The parameter vector increases the complexity of computing the optimal control feedback law. Based on the algorithm in [7], the value function $V_q(x)$ is introduced, when $x = x_0, q = q_0, V_{q_0}(x_0)$ is a lower bound on the cost for optimally bring to the system from determined initial state (x_0, q_0) to the terminal state (x_{t_f}, q_{t_f}) . It should be noted that without the loss of the generality, we discuss the case where continuous state space is two-dimensional system.

Let $e_1 = [1 \ 0]^T$, $e_2 = [0 \ 1]^T$, $\forall x \in \mathcal{X}_{N-1}$, let

$$x_{N-1}^{jk} = x_{N-1} + jhe_1 + khe_2,$$

$$x_{N-1}^{jk} \in \mathcal{X}_{N-1}, \text{ and } j, k \in \mathbb{Z},$$

$$Y_{N-1}^{jk} \triangleq \{x : x = x_{N-1}^{jk} + \theta_1 he_1 + \theta_2 he_2, -1 \leq \theta_1 \leq 1, -1 \leq \theta_2 \leq 1\},$$

$$\left(\underline{f}_{q(N-1)}^{jk}\right)_i = \min_{x \in Y_{N-1}^{jk}, u \in U} \{f_{q(N-1)}(x, u)e_i\},$$

$$\underline{F}_{q(N-1)}^{jk} = \min_{x \in Y_{N-1}^{jk}, u \in U} \{F_{q(N-1)}(x, u)\}, i = 1, 2$$

$$V_{q(N-1)}^{jk} = V_{q(N-1)}(x_{N-1}^{jk}),$$

$$\Delta_i V_{q(N-1)}^{jk} = (V_{q(N-1)}(x_{N-1}^{jk} + he_i) - V_{q(N-1)}(x_{N-1}^{jk}))/h,$$

$$\Delta_{-i} V_{q(N-1)}^{jk} = (V_{q(N-1)}(x_{N-1}^{jk}) - V_{q(N-1)}(x_{N-1}^{jk} - he_i))/h, \quad i = 1, 2.$$

Introduce new vector variables, $\lambda_{q(N-1)}^{jk} \in \mathbb{R}^2$ for (j, k) at time $N-1$, construct the following inequalities:

$$\left\{ \begin{array}{l} 0 \leq \left(\lambda_{q(N-1)}^{jk}\right)_1 + \left(\lambda_{q(N-1)}^{jk}\right)_2 + \underline{F}_{q(N-1)}^{jk} \\ \left(\lambda_{q(N-1)}^{jk}\right)_{|i|} \leq \left(\underline{f}_{q(N-1)}^{jk}\right)_{|i|} \Delta_i V_{q(N-1)}^{jk}, i = -2, -1, 1, 2 \\ \left(\lambda_{q(N-1)}^{jk}\right)_{|i|} \leq \left(\overline{f}_{q(N-1)}^{jk}\right)_{|i|} \Delta_i V_{q(N-1)}^{jk} \\ 0 \leq V_{q(N)}^{jk} - V_{q(N-1)}^{jk} + G(x_{N-1}^{jk}, q(N-1), q(N)), x_{N-1}^{jk} \in \mathcal{S}_{q(N-1), q(N)} \\ 0 \geq V_{q(N)}^{xN}, x_N \in \mathcal{X}_f \end{array} \right. \quad (11)$$

If there exists $V_{q(N-1)}^{jk}$ such that inequalities (11) hold, which are Bellman type inequalities. It can be proved that that $V_{q(N-1)}^{jk}$ is the lower bound of the cost to go function $J_{N-1}(x_{N-1})$, and the proof is given in [7]. However, any function that meets the constraints is a lower bound on the cost to go function, thus to yield the useful bounds, it is necessary to find an maximum of all grid points in the feasible region \mathcal{X}_{N-1} ,

$$J^*(x(N-1)) \triangleq \max_{x_{N-1}^{jk} \in \mathcal{X}_{N-1}, j, k \in \mathbb{Z}} \left\{ V_{q(N-1)}^{jk}(x_{N-1}^{jk}) \right\} \quad (12)$$

Assuming that

$$V_{q(N-1)}^{j_0 k_0} = \max_{x_{N-1}^{jk} \in \mathcal{X}_{N-1}, j, k \in \mathbb{Z}} \left\{ V_{q(N-1)}^{jk}(x_{N-1}^{jk}) \right\} \quad (13)$$

when $j = j_0, k = k_0$, for $x = x_{j_0 k_0} + \theta_1 h e_1 + \theta_2 h e_2 \in Y_{N-1}^{j_0 k_0}$, define the interpolating function:

$$\begin{aligned} V_{q(N-1)}(x) &= (1 - \theta_1)(1 - \theta_2)V_{q(N-1)}^{j_0 k_0} + \theta_1(1 - \theta_2)V_{q(N-1)}^{(j_0+1)k_0} \\ &+ (1 - \theta_1)\theta_2 V_{q(N-1)}^{j_0(k_0+1)} + \theta_1\theta_2 V_{q(N-1)}^{(j_0+1)(k_0+1)} \end{aligned} \quad (14)$$

From (14), the optimal feedback control law can be calculated as

$$u_{N-1} = \arg \min_{u \in U} \left\{ \frac{\partial V_{q(N-1)}}{\partial x} f_{q(N-1)}(x, u) + F_{q(N-1)}(x, u) \right\} \quad (15)$$

so far, the optimal control law at the first step is finished.

From the second step $n = N - 2$ to the last one $n = 0$, the cost to go function is defined on the feasible region \mathcal{X}_{n+1} , we will solve the problem (5), which is still a multiparametric program problem, the computing process is analogous as the first step, which is presented as follows:

- (I) Divide the feasible region \mathcal{X}_n into evenly distributed grid points, and introduce $x_n^{jk}, Y_n^{jk}, \left(\underline{f}_{q(n)}^{jk} \right)_i, \left(\overline{f}_{q(n)}^{jk} \right)_i, \underline{F}_{q(n)}^{jk}, V_{q(n)}^{jk}, \Delta_i V_{q(n)}^{jk}, \Delta_{-i} V_{q(n)}^{jk}, i = 1, 2$;
- (II) Solve the linear program problem:

$$\begin{aligned} J^*(x(n)) &\triangleq \max_{x_n^{jk} \in \mathcal{X}_n, j, k \in \mathbb{Z}} \left\{ V_{q(n)}^{jk}(x_n^{jk}) \right\} \\ \text{s.t.} &\begin{cases} 0 \leq \left(\lambda_{q(n)}^{jk} \right)_1 + \left(\lambda_{q(n)}^{jk} \right)_2 + F_{q(n)}^{jk} \\ \left(\lambda_{q(n)}^{jk} \right)_{|i|} \leq \left(\underline{f}_{q(n)}^{jk} \right)_{|i|} \Delta_i V_{q(n)}^{jk}, \quad i = -2, -1, 1, 2 \\ \left(\lambda_{q(n)}^{jk} \right)_{|i|} \leq \left(\overline{f}_{q(n)}^{jk} \right)_{|i|} \Delta_i V_{q(n)}^{jk}, \quad i = -2, -1, 1, 2 \\ 0 \leq V_{q(n+1)}^{jk} - V_{q(n)}^{jk} + G(x_n^{jk}, q(n), q(n+1)), \quad x_n^{jk} \in S_{q(n), q(n+1)} \end{cases} \end{aligned} \quad (16)$$

(III) After solving the maximum value of $V_{q(n)}^{jk}$, define the interpolating function $V_{q(n)}(x)$, then calculating the optimal feedback input

$$u_n = \arg \min_{u \in U} \left\{ \frac{\partial V_{q(n)}}{\partial x} f_{q(n)}(x, u) + F_{q(n)}(x, u) \right\} \quad (17)$$

It should be noted that the dynamic program methodology to compute the optimal control feed back input in this paper is different from [6]. In [6], the cost function is quadratic and the optimal controller design is for the piecewise affine (PWA) system, if the hybrid system can not be modeled as a PWA system, and the methodology in computing the optimal controller needs to be further discussed. Also, in [7], the initial state and the terminal state are determined, thus there are no parameters in the optimal control problems. In this paper, the initial state is a vector parametric vector, the solution to optimal control must make an dynamic enumeration to search the maximum lower bound in every sample period, the problem is different from [7].

4 Simulation Example

We use the local area network in the laboratory to construct a networked control system, where the network contains Ethernet and the communication between nodes is done using TCP/IP sockets. The experiment setup is shown in figure 2.

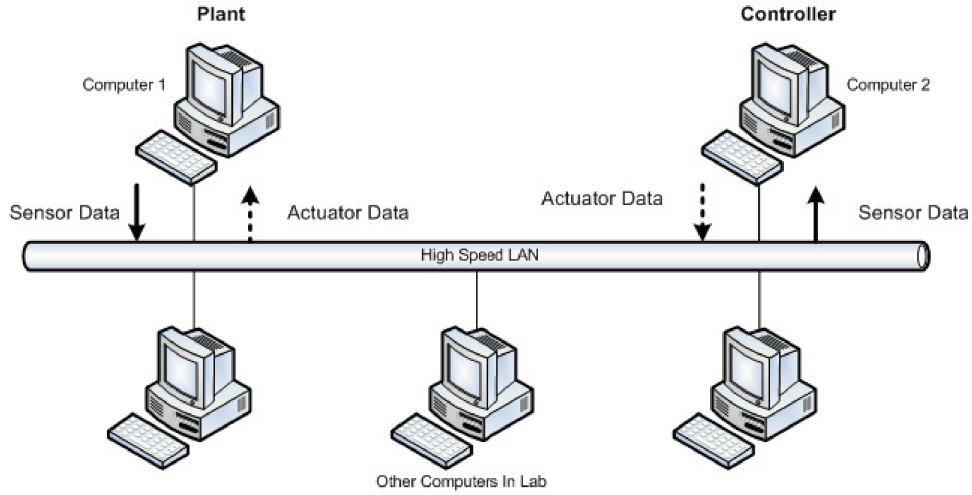


Figure 2: The networked control system experiment setup

In our experiment setup, one computer (Computer 1) works as a plant, and the other computer (Computer 2) works as a controller, these two computers and the other computers are connected over the local area net in the lab. Computer 1 simulate the dynamics of the plant, which can obtain the control signal from the net, make the output calculation, and send the computation results to the controller computer. Computer 2 obtains the plant output, and calculates the control signal, then send the control signals to the plant computer. Note that the networked control systems with multiple switching modes can be carried out in the experiment setup. Based on the hybrid system model of the networked control system, the different dynamics of the plant can be simulated in the plant computer, and the controller computer calculates the control results and sends them to the plant computer and control the dynamics of the plant in different modes.

Because TCP/IP is used in the Ethernet in the lab, the end to end data transmission is reliable, and the packets loss between the plant computer and the controller computer can not be considered. But the network-induced delay needs to be considered when the plant computer and the controller computer exchange data across the network. We test the delays between two computers in the network, it can be found that the time delay generally maintains a fixed value, in our experiment setup, the fixed value is much less than the sampling period. Therefore, it is reasonable that the networked-induced delay can not be considered in this paper, and the model and the solution to the optimal control can be validated in this simulation.

The networked control system simulated in the experiment setup is given as follows.

$$x(k+1) = A_{q_i}x(k) + Bu(k), i = 1, 2 \quad (18)$$

where

$$A_{q_1} = \begin{bmatrix} \frac{\sqrt{2}}{2} & -\frac{\sqrt{2}}{2} \\ \frac{\sqrt{2}}{2} & \frac{\sqrt{2}}{2} \end{bmatrix}, A_{q_2} = \begin{bmatrix} \frac{\sqrt{2}}{2} & \frac{\sqrt{2}}{2} \\ -\frac{\sqrt{2}}{2} & \frac{\sqrt{2}}{2} \end{bmatrix}, B = \begin{bmatrix} 0 \\ 1 \end{bmatrix},$$

$$S_{q_1, q_2} = \{x : [1 \ 0]x(k) < 0\},$$

$$S_{q_1, q_2} = \{x : [1 \ 0]x(k) \geq 0\}, \quad (19)$$

$$x(k) \in [-10, 10] \times [-10, 10],$$

$$u(k) \in [-1, 1],$$

define the cost function

$$J(U_N, x(0)) \triangleq x_N^T P x_N + \sum_{k=0}^{N-1} x_k^T Q x_k + u_k^T R u_k \quad (20)$$

where

$$P = Q = \begin{bmatrix} 700 & 0 \\ 0 & 700 \end{bmatrix}, R = 1,$$

Terminal region

$$\mathcal{X}_f = [-0.01, 0.01] \times [-0.01, 0.01],$$

$$N = 3.$$

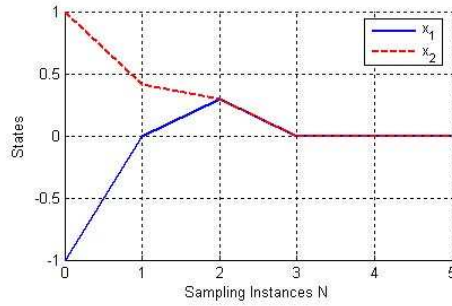


Figure 3: The optimal trajectory of the state variable x

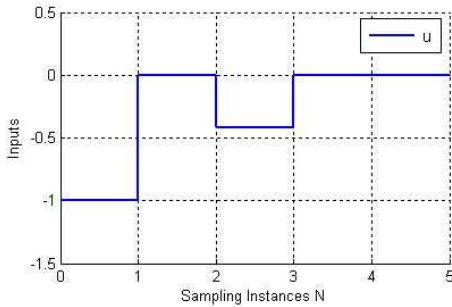


Figure 4: The optimal control input when $x = [-1 \ 1]^T$

The optimal control problem is minimizing the cost function and solving the optimal control feedback input. In terms of the steps presented in section 3 and some toolbox related with multiparametric programming [8] and optimal control [9], the solving program is designed, and then the optimal control can be obtained. When $x_0 = [-1 \ 1]^T$, the optimal trajectory of the state variable x is shown in Fig. 3, and the control input is shown in Fig. 4.

5 Conclusion

In networked control systems with multiple switching modes, it is necessary to calculate the optimal control feedback input, which can improve the system performance and save the cost. This paper models

the class of networked control systems as a hybrid system and addresses a optimal control problem, where initial state is a parametric vector. Consider switching modes and unknown initial states, the dynamic program techniques are proposed to solve the optimal control problem, where every step calculation need enumerate the grid points in feasible region to find a maximum lower bound of the cost function and solve the optimal feedback input. Finally, an example is given to illustrate the techniques. It should be noted that, the switching modes in networked control systems make the calculation of the optimal control input more complex, dynamic program can reduce the calculation complexity than the heuristic enumeration. In the future research, it is an important task to improve the computation efficiency and reduce the complexity. In addition, time delays are common in networked control systems, it is an interesting area to work into the optimal control problem with delay.

References

- [1] W. Zhang, M. S. Branicky , S. M. Phillips . Stability of networked control systems. *IEEE Control Systems Magazine*, Vol. 21, pp. 84-99, 2001.
- [2] H. Fujika, K. Ito. Performance optimization for a class of networked control systems with communication constraints. *Proceedings of the American Control Conference*, pp. 248-253, 2003.
- [3] L. Lu, L. Xie, M. Fu. Optimal control of networked systems with limited communication: a combined heuristic and convex optimization approach. *Proc. of 42th IEEE Int. Conf. on CDC*, pp. 1194-1199 2003.
- [4] A. van der Schaft, H. Schumacher, *An Introduction to Hybrid Dynamical Systems*, Berlin: Springer-Verlag, 2000.
- [5] R. Alur, C. Courcoubetis, T. A. Henzinger. Hybrid automata: an algorithmic approach to the specification and verification of hybrid systems. In: Grossman R L, Nerode A, Ravn A P, et al, eds. *Hybrid Systems, Lecture Notes in Computer Science*, Berlin: Springer-Verlag, Vol. 736, pp. 209-229, 1993.
- [6] F. Borrelli, *Constrained optimal control of linear and hybrid systems*, Berlin: Springer-Verlag, 2003.
- [7] S. Hedlund, A. Rantzer. Optimal Control of Hybrid Systems. *Proc. 38th IEEE Int. Conf. on CDC*, pp. 3972-3977, 1999.
- [8] M. Kvasnica, P. Grieder, M. Baotic, et al, Multi-Parametric Toolbox. ETH, Swiss Federal Institute of Technology, 2004.
- [9] S. Hedlund, A. Rantzer, CDP Tool: A Matlab tool for optimal control of hybrid systems. Department of Automatic Control, Lund Institute of Technology, 1999.

Authors: Gang Zheng, Wenli Zeng, Fanjiang Xu
Laboratory of Integrated Information Systems Technology
Institute of Software, Chinese Academy of Sciences
No.4 South Fourth Street, Zhongguancun, Beijing, China, 100080
E-mail: gangzhengcn@yahoo.com.cn

Received: November 6, 2006

Ant Colony with Dynamic Local Search for the Time Scheduling of Transport Networks

Salah Zidi, Salah Maouche, Slim Hammadi

Abstract: This article presents an ant colony optimization for the time scheduling of public transport traffic. In fact, the assistance of a decision support system becomes necessary for the real-time regulation of this transport networks since the size of the search space increases exponentially with the number of vehicles and stops. So, we propose an ant colony algorithm with dynamic local search, in the case of unpredictable disturbance. This approach consists in applying a local search window with increasing dimension according to the iterations. It treats the regulation problem as an optimization and provides the regulator with relevant decisions. A regulated timetable is proposed as solution aiming at minimizing the waiting time of passengers. We insure the three most important criteria of regulation which are the punctuality, the regularity and the correspondence.

Keywords: urban transportation systems, real-time scheduling, ant colony optimization.

1 Introduction

In real time, the transport system can be affected in an unpredictable way by incidents which cause a delay between these theoretical time schedules and the real time schedules. In these conditions, we have re-adjust the planning (time table) made at previous time to return quickly to the theoretical schedules. It is a real-time regulation.

Within this context we developed an algorithm of scheduling which allows us to ensure the most important three criteria: the punctuality, the regularity of passing of vehicles by stops as well as the correspondence between the lines of the different transport modes. It is an ant colony algorithm where the main goal is to find in every movement between two successive stops the delay which it is necessary to apply to concerned vehicles to optimize these three criteria of regulation.

At the beginning, our regulation algorithm encountered difficulties to escape from local optima. In fact, the optimization problem which we have to resolve is complicated and the research space is important. To manage these difficulties we propose the idea of the dynamic local search. It is the new method which consists in applying a local search window with increasing dimensions according to the iterations.

This article contains five parts. In the first, we will present the regulation problem. The second part is a presentation of the ant colony algorithm. In the third part we will detail our algorithm of regulation and we will also explain the simulation results of this approach in the urban transport network of Lille. We will finish by a conclusion.

2 Real-time regulation

The planning process of a public transport company is made by establishing different timetables that describe trips according to the lines, frequencies, transport demand, and travel times in the network. These trips are then transformed into blocks and assigned to vehicles. A crew scheduling process finally follows this vehicle scheduling [1]. Hence, the vehicle schedules are fixed for every timetable period. This type of vehicle scheduling is in fact called predictive scheduling. It is based on a periodic review

of demand and resource availability in order to create arrival and departure times for the vehicles at the different stops of the network.

However, in reality, travel times and transport demands are not fixed because of random external influences that affect the traffic within the network and cause disturbances. These disturbances can be, for example, caused by traffic jams, accidents, or strikes. Consequently, the theoretical schedules resulting from the planning process cannot be followed exactly, which compels trips to start late and makes customers wait longer.

Therefore, to reduce the effects of the disturbances, the theoretical schedules have to be adapted to the real traffic conditions through regulation, or rescheduling tasks [2]. This process is then called reactive scheduling. It consists in creating new schedules that increase the level of service by undertaking operational decisions, such as, the injection of an extra vehicle in the network, or the deviation of the routes of some vehicles. The real-time traffic management of an urban transport system is presented by the figure 1.

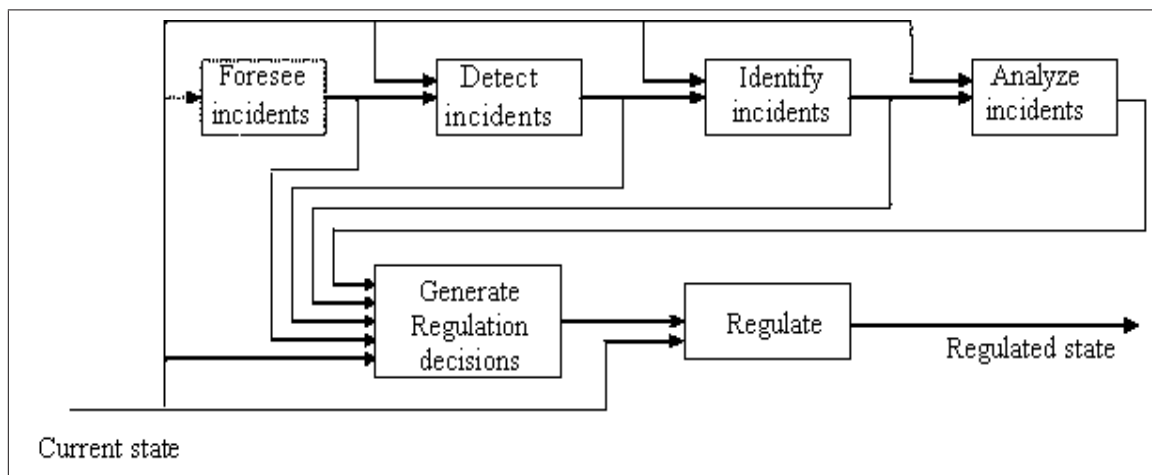


Figure 1: Process of real time management of public transport traffic

Presently, it's a human operator, regulator, who performs these real time tasks and controls the global network traffic by treating the information provided by the Automatic Vehicle Monitoring (AVM) system and the vehicle drivers. The level of service can be represented by different regulation criteria such as, the regularity, punctuality, and connection criteria. The choice of the criteria depends on the regulation objectives obtained from the nature of the disturbances. However, the regulator is usually overloaded with information, which complicates its decision-making task. In addition, despite the AVM system assistance, the regulator spends more than 50% of his work time in communication with the vehicle drivers. Hence, the regulator has to carry out difficult tasks that are often inaccessible for the human scale especially if many disturbances occur simultaneously, which involves the assistance of a decision support system [3].

Within this context, researchers began to think about the development of a computer system for the regulators by using different tools such as the fuzzy logic [4], the multi-agent system [5] and an evolutionary algorithm [6].

In our work we will apply an approach of ant colony optimization and we will introduce a new idea of dynamic local search.

3 Ant Colony Optimization (ACO)

Ant colonies are able to organize their foraging behavior in a seemingly efficient way without any centralized control[7]. This self-organizing structure is carried out via stigmergic communication, i.e. communication by changing the environment, in this case by laying down pheromone trails. Initially ants have no idea of where food is in the environment, so they wander randomly, leaving a pheromone trail. When an ant finds food it wanders back to the nest. Initially these paths will be arbitrary, but when an ant follows a shorter path it will be able to follow that path more often within the same time period than an ant following a longer path, so there is a positive reinforcement process whereby the shorter paths get stronger.

A simple version of this is illustrated in figure 2, where ants have two possible routes from a nest to a food source. If two ants set out at the same time, one taking route A and one route B, which is twice as long, then the ant taking A will have traveled back and forth between the food source twice in the same time that the other ant has traveled back and forth once. Therefore there will be a stronger pheromone trail on route A compared to route B. This idea can be effectively scaled up to solving route finding problems such as the TSP, with performance as good as or better than existing heuristics.

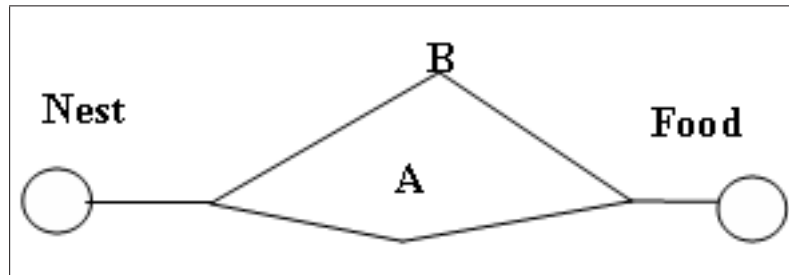


Figure 2: A simple ant foraging problem.

The natural ants inspired "ant colony algorithms" invented in 1992 by Marco Dorigo from Free Brussels University, in his Ph.D. thesis [8]. In an iteration of this algorithm, n ants build n solutions according to decisions based on heuristics criteria and on the quantity of pheromone. This quantity is updated by examining the solutions. It is strengthened for the decisions having given better solutions and decreased for the others. This mechanism allows to improve gradually the solutions during the iterations.

The ants colony optimization were applied to divers problems of optimization such as the salesman traveling problem [9], the problems of robotics [10], the industrial problems [11] as well as the CARP (Capacitated Arc Routing Problem) in [12] and the rucksack problem [13]. And there are several versions of the ants colony algorithm such as the Ant System [14], the Min-Max Ant System [15], the ASrank [16] and the Ant Colony System [9].

4 Rescheduling algorithm

4.1 Notation

We use even notations in the horizon of regulation.

S^H : Set of stops of the regulation horizon.

V^H : Set of the vehicles in the horizon of regulation.

S_k^r : k^{th} stop situated on the line r .

V_i^l : i^{th} vehicle in the line l .

$Veh(V_i^l, S_j^m, S_k^r)$: First successor of V_i^l at traveling S_j^m to S_k^r .

a_{ij}^{lm} : Stop variable of V_i^l at S_j^m .

X_{ijk}^{lmr} : Destination variable of V_i^l from S_j^m to S_k^r .

td_{ij}^{lm} : Arrival time of V_i^l at S_j^m .

td_{ij}^{lm} : Departure time of V_i^l from S_j^m .

$Nmont_{ij}^{lm}$: Number of persons who go aboard V_i^l in S_j^m .

$Ndesc_{ij}^{lm}$: Number of persons who come down of V_i^l in the stop S_j^m .

$\rho_{ii'}^{ll'm}$: Rate of correspondence from V_i^l to $V_{i'}^{l'}$ in S_j^m .

$\mu(\Delta t_i, S_j^m, S_k^r)$: Arriving rate of the passengers traveling between these stops during Δt_i .

$N_{ijk}^{l'mr}$: Number of passengers in $V_{i'}^{l'}$ traveling from S_j^m to S_k^r .

$Y_{ii'}^{ll'm}$: Variable of correspondence from V_i^l to $V_{i'}^{l'}$ in the stop S_j^m (equal 1 if a correspondence is possible and 0 otherwise).

$w_{ii'}^{ll'm}$: Number of transferring persons from V_i^l to $V_{i'}^{l'}$ at S_j^m .

C_{ij}^{lm} : Load of V_i^l at its departure from S_j^m .

AT: total time of waiting of the passengers in the regulation horizon.

AT_0 : Initial waiting time of passengers at the different stops of the regulation horizon according to the disturbed schedules.

TT: Total duration of transfers in the regulation horizon.

TT_0 : Initial transfer or connection time between the different vehicles of the regulation horizon according to the disturbed schedules.

RT: Total duration of Roads in the regulation horizon.

RT_0 : Initial route time for the different vehicles of the regulation horizon according to the disturbed schedules.

4.2 Criteria of regulation

To have a good quality of service in a transport network, several criteria must be assured during the off-line planning and the on-line regulation such as the safety, the regularity, and the punctuality. In the present problem, we chose the criteria of the regularity, the punctuality and the correspondence. They are the most important and the most used by regulators and researchers.

Regularity

This criterion expresses the preservation of the regularity of the time intervals which separate the successive passings of vehicles. It concerns the minimization of the passenger wait in stops.

The calculation of the traveler wait in a stop S_j^m depends on the interval separating two successive vehicles and the number of travelers at this stop.

We suppose that in a given period of the day, $V_{i'}^{l'}$ is the vehicle succeeding V_i^l in the stop S_j^m . The time interval which separates both passages is:

$$\Delta t = td_{i'j}^{l'm} - td_{ij}^{lm} \quad (1)$$

We consider the distribution of the passenger arrivals, $\mu_{S_j^m}(t)$, to the stop S_j^m . We can then calculate, according to the figure 3, the passenger wait, during t . (equation 2)

$$attente(\Delta t, S_j^m) = \int_0^{\Delta t} \mu_{S_j^m}(t)(\Delta t - t)dt \quad (2)$$

The distribution of the passenger arrivals to stops is often considered as a non-stationary process [6]. Besides, if we have reduced intervals (2 to 4 minutes) or situated in the homogeneous periods, we can consider a constant passenger flow, $\mu_{S_j^m}$. Consequently, the number of persons who arrive in S_j^m during Δt is $\mu_{S_j^m} \times \Delta t$ and the average wait becomes:

$$attente(\Delta t, S_j^m) = \mu_{S_j^m} \times \frac{\Delta t^2}{2} \quad (3)$$

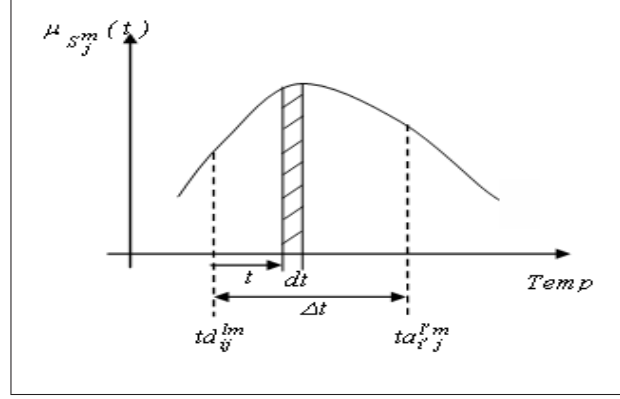


Figure 3: Distribution of the passenger arrivals to a stop

In the case of a wider interval not belonging to a homogeneous period, it can be divided into several reduced intervals to simplify the calculation of the traveler waits, $\Delta t = \bigcup_{I=1..N} \Delta t_I$. The number of persons arriving in S_j^m during Δt_I with a rate of arrival equal to μ_I is $\mu_I \times \Delta t_I$. Their average wait is then:

$$attente(\Delta t_I, S_j^m) = \mu_I \times \Delta t_I \times \left(\frac{\Delta t_I}{2} + \sum_{I'=I+1}^N \Delta t_{I'} \right) \quad (4)$$

Indeed, the averages wait of the travelers who arrived during Δt_I is $(\frac{\Delta t_I}{2} + \sum_{I'=I+1}^N \Delta t_{I'})$. We can so calculate the average wait during t at the stop S_j^m :

$$attente(\Delta t, S_j^m) = \sum_{I=1}^N \mu_I \times \Delta t_I \times \left(\frac{\Delta t_I}{2} + \sum_{I'=I+1}^N \Delta t_{I'} \right) \quad (5)$$

We can now formulate, in the following equation, the total wait, at the stop S_j^m , of the travelers who go to S_k^r during the interval Δt which separates the successive passages of both vehicles V_i^l and V_i^r ($V_i^r = Veh^+(V_i^l, S_j^m, S_k^r)$).

$$attente(\Delta t, S_j^m, S_k^r) = \sum_{I=1}^N \mu(\Delta t_I, S_j^m, S_k^r) \times \Delta t_I \times \left(\frac{\Delta t_I}{2} + \sum_{I'=I+1}^N \Delta t_{I'} \right) \quad (6)$$

The duration of the wait of all the passengers at S_j^m is then the sum of the waits for all the vehicles which pass by this stop, as described below:

$$attente(S_j^m) = \sum_{V_i^l \in V^h} (a_{ij}^{lm} \times \sum_{S_k^r > S_j^m} attente(t_{a_{ij}^{rm}} - t_{a_{ij}^{lm}}, S_j^m, S_k^r)) \quad (7)$$

Finally, because the criterion of regularity is concerning the total wait, AT, of passengers at stops in the regulation horizon, this AT is then formulated in equation 8 and 9 by adding the wait at the different concerned stops.

$$AT = \sum_{S_j^m \in S^h} attente(S_j^m) \quad (8)$$

$$AT = \sum_{S_j^m \in S^h} \sum_{V_i^l \in V^h} (a_{ij}^{lm} \times \sum_{S_k^r > S_j^m} attente(t_{a_{ij}^{rm}} - t_{a_{ij}^{lm}}, S_j^m, S_k^r)) \quad (9)$$

Correspondence

The correspondence criterion is associated to the duration of transfers between vehicles in the disrupted zone. We can suppose that the number of persons in transfer at stop S_j^m is proportional to the passenger number who go to this stop with the rate $\rho_{i'j}^{l'm}$ so $w_{i'j}^{l'm} = \rho_{i'j}^{l'm} \times Ndesc_{ij}^{lm}$.

We can deduct the total duration of transfers, TT , who is equal to a sum of the durations of the correspondences between the various vehicles at the concerned stops of the network (equation 10).

$$TT = \sum_{V_i^l \in V^h} \sum_{V_{j'}^{l'} \in V^h} \sum_{S_j^m \in S^h} Y_{i'j}^{l'm} \times w_{i'j}^{l'm} \times (td_{ij}^{l'm} - ta_{ij}^{lm}) \quad (10)$$

Punctuality

The punctuality criterion deals with the route duration of the different vehicles. It is computed after an estimation of the vehicle loads via the arrival rates of the passengers at the stops, and also the initial real loads that are assumed known. Hence,

$$RT = \sum_{V_i^l \in V^h} \sum_{S_j^m \in S^h} a_{ij}^{lm} \times C_{ij'}^{lm'} \times (td_{ij}^{lm} - td_{ij'}^{lm'}) \quad (11)$$

In fact, the loads are determined by the number of the alighting and boarding persons, according to the arrival rates or to the origin destination matrix. It can be written as

$$C_{ij}^{lm} = C_{ij'}^{lm'} - Ndesc_{ij}^{lm} + Nmont_{ij}^{lm} \quad (12)$$

4.3 Principle of the rescheduling algorithm

At first, we have a set of stops and routes of the disrupted zone. We add for every inter-stop (route chosen between two successive stations) a set of fictitious arcs which don't have a physical existence but we consider them as delays to be applied to this road. In the figure 4, for example, we dispose of 5 arcs between every two successive stops. The first arc presents the real arc with 0 minutes of delay and the others possess 1, 2, 3 or 4 minutes of delay which we can consider in one of both stops or in a route between these stops.

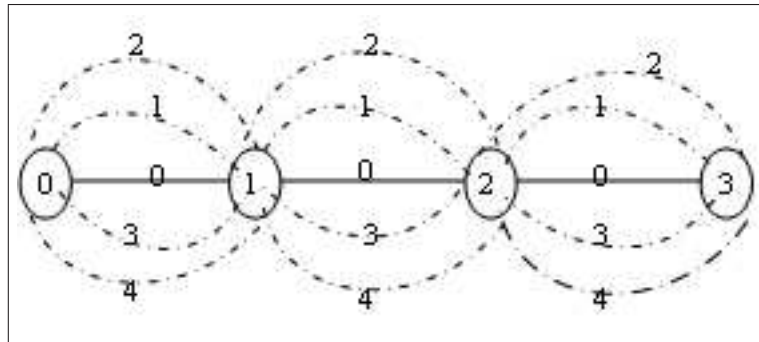


Figure 4: Graphic presentation of the decision arcs

The objective of the ant colony algorithm is to find the delay to be applied for every vehicle, with the aim to finding the schedules that satisfy the different criteria then propose a regulated timetable. So, for every vehicle ants move between stops and search the best arcs (delay) to be taken, until the arrival terminus. An ant has to propose all the delays which it is necessary to apply between the departure and the arrival.

4.4 Objective function

The Objective Function to optimize is an aggregation of three criteria representing the total travel time, total waiting time, and total transfer time. This aggregation relies on weight parameters representing the relative importance of the criteria according to the disturbances and the regulator objectives. For instance, if no connection is involved in the disturbance, the weight parameter associated with the transfer criterion would be surely null. Hence, the objective function to maximize is written as

$$f = \sum_{c=1}^{c=3} \alpha_c Cr_c \quad (13)$$

Where

$Cr_1 = (AT_0 - AT)$: for the regularity,

$Cr_2 = (TT_0 - TT)$: for the transfer (correspondence),

$Cr_3 = (RT_0 - RT)$: for the punctuality, α_1, α_2 and α_3 weight parameters for the regularity, transfer and punctuality criteria, respectively and $\sum -1^3 \alpha_c = 1$.

4.5 Generation of a new solution

From a stop s and with the probability P , an ant uses the first method witch chooses an arc i with the probability P_1 described by the equation (14). In that case we give the same probability to the k arcs (in our case $k=5$) to be chosen. This choice allows us a better exploration of the research space.

$$P_1 = \begin{cases} \frac{1}{k} & \text{if } i \in \Omega_s \\ 0 & \text{otherwise} \end{cases} \quad (14)$$

With the probability $1-P$, the ant uses the second method, more intelligent than the first. That is by regard to the pheromone trail, $\tau(t)$. And it chose an arc according to the probability given by the equation (15).

$$P_1 = \begin{cases} \frac{[\tau_i(t)]}{\sum_{j=1}^k [\tau_j(t)]} & \text{if } i \in \Omega_s \\ 0 & \text{otherwise} \end{cases} \quad (15)$$

Where Ω_s is a set of arcs witch have a stop s as departure.

4.6 Update of pheromone trail

By analogy with the nature, every ant leaves a quantity of pheromone on every chosen arc. We reinforce the pheromone trail on the chosen arcs by taking into account vaporization. That is represented by the equation (16), which includes a term of persistence ρ and a term of strengthening $\Delta\tau_a$, it is a quantity added by an ant a .

$$\tau_i(t+1) = \rho \tau_i(t) + \sum_{allants} \Delta\tau_a \quad (16)$$

Where $\Delta\tau_a = f_a$ is the objective function of the solution proposed bay the ant a .

4.7 Algorithm structure

Every ant moves from a stop to the other, by using the method of generation of solution described previously, and it adds this arc to its road, until the terminus stop, then the ant begins again from the departure stop for all the vehicles of the disrupted zone. As soon as the ant chose the regulation decision (the delay) to apply to every vehicle, we build the new regulated timetable and we calculate the three criteria: the regularity, the punctuality and the transfer then the objective function which we compare

with those found by the previous ants and we keep the best (maximal). When all the ants treat all the transport services we update the pheromone trail on every arc. The algorithm structure is presented by the figure 5.

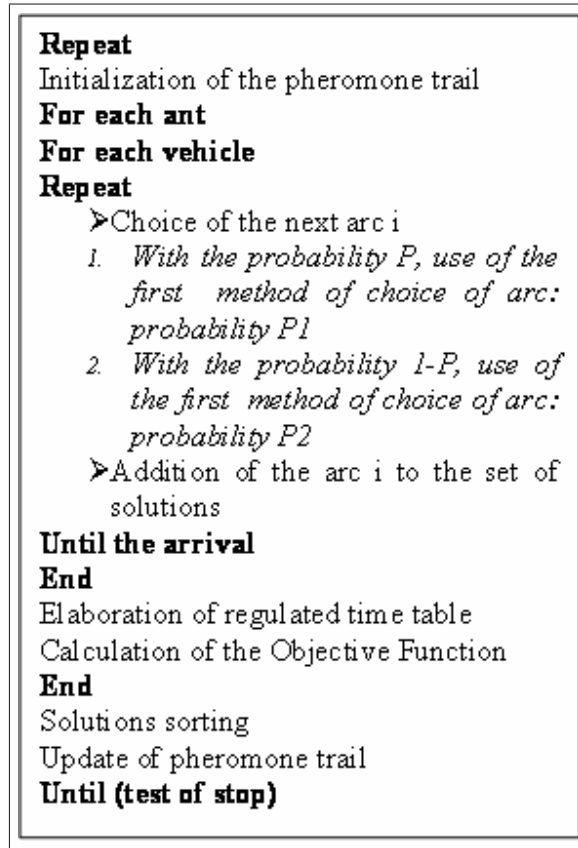


Figure 5: Ants colony Algorithm for the regulation

We stop the algorithm when the best solution found by ants is unchanged since a number of iteration I1 or a maximum number of iteration I2 is attained.

4.8 Dynamic local search

To escape from local optima, the metaheuristic algorithms showed an important efficiency. But, many difficulties persist for the more intricate problems and the wide research areas. We proposed in the first algorithm, in the paragraph IV, the second solution based on research idea. According to our early execution tests related to the second algorithm, in the paragraph V. C, we noticed that the unequal decisions to zero (the delays to be applied) are always located in a part of the disrupted spatiotemporal zone. So, we adopted another way based on local research, which is one of the most applied ideas with ant colony algorithms [12] as well as other heuristics such as the genetic algorithms [17]. This idea, which shows promising results, is based on a procedure that aims to improve the found solutions. In fact, this idea deals with a restricted research area, where the early solutions are located. Nevertheless, we still have the problem of bumping into local optimums areas, which leads us to poor quality solutions. So, we used a new idea of dynamic local research.

This idea aims at restricting the research area by means of spatiotemporal windows with increasing dimension according to the iterations. We begin the investigation in a small zone of the research space and we look for decisions, which can be different from zero on this zone, but we apply only the zero

```

Repeat
Initialization of the pheromone trail
For each ant
For each vehicle
Repeat
If (( $s < s1$  ||  $s > s2$ ) && ( $t < t1$  ||  $t > t2$ ))
    Delay = 0
End if
Else
    ➤ Choice of the next arc  $i$ 
    1. With the probability  $P$ , use of the first method of choice of arc: probability  $P1$ 
    2. With the probability  $1 - P$ , use of the first method of choice of arc: probability  $P2$ 
    ➤ Addition of the arc  $i$  to the set of solutions
End else
Until the arrival
End
Elaboration of regulated time table
Calculation of the Objective Function
End
Solutions sorting
Update of pheromone trail
After some iteration:
 $S1--$ 
 $S2++$  Increase of the spatiotemporal
 $T1--$  zone
 $T2++$ 
Until (test of stop)

```

Figure 6: Rescheduling ant colony algorithm with dynamic local search

decision delay on the rest of the research space. After some iteration, we increase the spatiotemporal dimensions of this zone and we investigate the research space for new solutions. After that, we compare the results and we continue to increase the local search zone, after some iteration, until we get a dimension equals to the complete space.

The figure 6 shows our improved algorithm comparing to the one illustrated in figure 5. This algorithm includes the research process with increase of the zone. In fact, we try to look for optimal decisions included between s1 and s2 stations (spatial limitation), and t1 and t2 times (temporal limitation). We affect the decision zero outside of this zone. After some iteration, we decrease a station for s1 and we add a station for s2 to increase the spatial zone and we make same for the temporal window. Without initializing the pheromone trails, the solutions of the first zone will be more strengthened than the others and therefore they will have more chance to be chosen.

5 Simulation and result

We applied this work to scenarios inspired from a real transportation system existing in Lille, in the north of France. We used an algorithm with 100 ants and two maximal number of iteration I1=10 and I2=500 and a probability P=10%.

5.1 Scenario1

In the line 0 which has a frequency of one bus every 10 minutes. A disturbance, caused by the vehicle V_3^0 , is detected at t_{pert}=12:01am, at its departure from the stop S_2^0 . The incident consists of a traffic accident between two cars, what slows down vehicles. The delay of the disrupted vehicle at its arrival in S_3^0 is estimated to 5 minutes. We suppose that no correspondence is involved in the disturbance. So, we are only interested in the criteria of regularity and punctuality. We assume that the studied horizon is included in a homogenous period of the day. Then, we can have a constant arrival rate of passengers at all the stations. Let $\mu = 2$ passengers per minute.

	S_0^0	S_1^0	S_2^0	S_3^0	S_4^0	S_5^0	S_6^0	S_7^0
V_0^0	0	0	0	0	0	0	0	0
V_1^0	0	0	0	0	0	0	0	0
V_2^0	0	0	0	0	0	0	0	0
V_3^0	0	0	0	0	0	0	0	0
V_4^0	0	0	0	0	0	0	0	0
V_5^0	0	0	0	0	0	0	0	0
V_6^0	0	0	0	0	0	0	0	0
Example 1: $\alpha_1 = \alpha_2 = 0$ and $\alpha_3 = 1$ $f = 0$								
V_0^0	0	0	0	0	0	0	0	0
V_1^0	0	0	0	0	0	0	0	0
V_2^0	0	0	0	0	0	2	1	0
V_3^0	0	0	0	0	0	0	0	0
V_4^0	0	0	0	3	0	0	0	0
V_5^0	0	0	0	1	0	0	0	0
V_6^0	0	0	0	0	0	0	0	0
Example 2: $\alpha_1 = 1$ and $\alpha_2 = \alpha_3 = 0$ $f = 160$								

Table 1: Results of the monocriterion regulation

The table 1 shows the delays to be applied to the vehicles of the regulation horizon. They involve decisions proposed by our ant colony algorithm for a regulation. For the first two examples, we consider a monocriterion regulation where we optimize only the punctuality in the first and the regularity in the second.

In the example1, the optimal solution for the punctuality can correspond only to null decisions in all the compartments of table. So, we had a null objective function f . In the example 2 the algorithm can allow to delay vehicles to adjust the intervals which separate them. We notice that vehicles V_2^0 and V_4^0 , before and after the disrupted vehicle, were delayed 3 minutes and V_5^0 was delayed 1 minute.

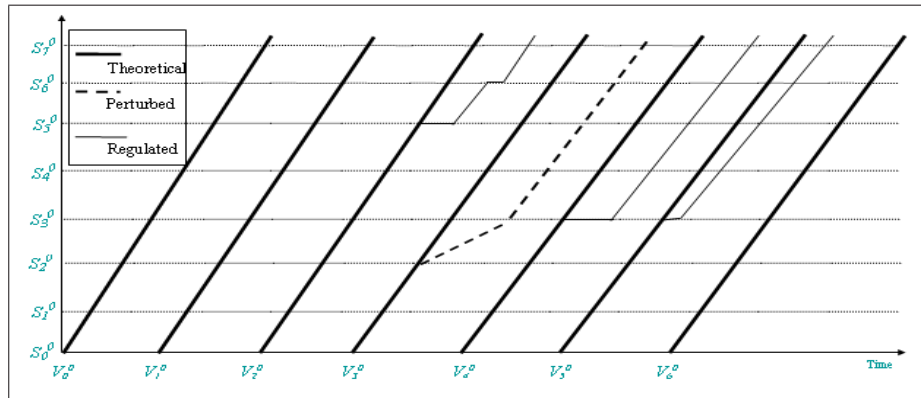


Figure 7: Vehicles schedules representation for the example 2 scenario 1

The figure 7 shows the efficiency of the scheduling algorithm to insure the regularity of vehicles in the perturbed zone.

	S_0^0	S_1^0	S_2^0	S_3^0	S_4^0	S_5^0	S_6^0	S_7^0
V_0^0	0	0	0	0	0	0	0	0
V_1^0	0	0	0	0	0	0	0	0
V_2^0	0	0	0	0	1	0	0	0
V_3^0	0	0	0	0	0	0	0	0
V_4^0	0	0	0	1	0	0	0	0
V_5^0	0	0	0	0	0	0	0	0
V_6^0	0	0	0	0	0	0	0	0
Exp 3: $\alpha_1 = 0.9\alpha_2 = 0\alpha_3 = 0.1f = 20.89$								
V_0^0	0	0	0	0	0	0	0	0
V_1^0	0	0	0	0	0	0	0	0
V_2^0	0	0	0	0	3	0	0	0
V_3^0	0	0	0	0	0	0	0	0
V_4^0	0	0	0	3	0	0	0	0
V_5^0	0	0	0	1	0	0	0	0
V_6^0	0	0	0	0	0	0	0	0
Exp 4: $\alpha_1 = 0.98\alpha_2 = 0\alpha_3 = 0.02f = 132.78$								

Table 2: Results of the multicriteria regulation

The example 3 favors the punctuality criterion, although $\alpha_1 < \alpha_3$. We notice a difference with the example 2 in the number of treated decisions. Indeed, only vehicles V_2^0 and V_4^0 have to be delayed 1 minute and we find an objective function $f = 20,89$. In the example 4 the result is very similar to the

example 2. Indeed, V_2^0 and V_4^0 were delayed 3 minutes as in the example 2, but for the vehicle V_2^0 the delay is applied in S_4^0 instead of and because the passenger number in these stops is more important thus a delay in is more interesting for the punctuality. We had $f=132.78$. In this first scenario the time of execution is always between 7 and 8 seconds.

5.2 Scenario2

The disturbance is detected at $t_{pert}=12:24$. It is caused by a technical problem at the tram line T, obliging the tram V_3^T to stand still 7 min at stop S_2^T . This tram-line has a frequency of one vehicle per 10 min. The stop is situated at 10 min from a connection node, N, where a connection is planned at 12:40 with a bus from line B, which has a frequency of one bus every 20 min. However, because of the disturbance, it would arrive at 12:43 at N, so the connection would not occur.

We assume that the studied horizon is included in a homogenous period of the day. Then, we can have a constant arrival rate of passengers at all the stations ($\mu = 2$). Additionally, we assume that the connection rates between the two concerned lines are constant. Hence, we suppose that the number of passengers in the tram arriving at the node and willing to take a bus on line is proportional to the load of the tram with a rate of 10%. and, the connection rate from the buses to the trams is 20%.

We applied our algorithm for a first example which takes into account the regularity criterion (table 3). The best solution is obtained within 20 s with a maximal value of the objective function $f=362$ passengers-minute, that is a decrease of wait of 10 minutes for more than 36 passengers. We notice the important number of decisions (delays) for the disrupted line (T) to adjust the intervals before and after the disrupted vehicle.

Line T									
	S_0^T	S_1^T	S_2^T	S_3^T	N	S_5^T	S_6^T	S_7^T	S_8^T
V_0^T	0	0	0	0	0	0	0	0	0
V_1^T	0	0	0	3	0	0	3	0	0
V_2^T	0	0	0	0	0	0	0	0	0
V_3^T	0	0	3	2	0	0	0	1	0
V_4^T	0	0	0	3	0	0	1	0	0
V_5^T	0	0	0	0	0	0	0	2	2
V_6^T	0	0	0	0	0	0	0	0	0
Line B									
	S_0^B	S_1^B	S_2^B	S_3^B	N	S_5^B	S_6^B	S_7^B	S_8^B
V_0^B	0	0	0	0	0	0	0	0	0
V_1^B	0	0	0	0	0	0	0	0	0
V_2^B	0	0	0	0	0	0	0	0	0
V_3^B	0	0	0	0	0	0	0	0	0
V_4^B	0	0	0	0	0	0	0	0	0
$\alpha_1 = 1 \alpha_2 \text{ and } \alpha_3 = 0$									

Table 3: Results of example1 for scenario 2

The second example concerns the transfer criterion (table 4). So, the delays were applied before the stop N and we had an objective function $f=208$.

The figure 8 shows the efficiency of the scheduling algorithm to insure the correspondence in the perturbed zone.

We executed the algorithm also in other multicriteria example where $\alpha_1 = 0.4$, $\alpha_2 = 0.58$ and $\alpha_3 = 0.02$. We had a decrease of the decisions number (not equal to zero) because the punctuality criterion

Line T									
	S_0^T	S_1^T	S_2^T	S_3^T	N	S_5^T	S_6^T	S_7^T	S_8^T
V_0^T	0	0	0	0	0	0	0	0	0
V_1^T	0	0	0	0	0	0	0	0	0
V_2^T	0	0	0	0	0	0	0	0	0
V_3^T	0	0	0	3	3	0	0	0	0
V_4^T	0	0	0	0	0	0	0	0	0
V_5^T	0	3	0	3	0	0	0	0	0
V_6^T	0	0	0	0	0	0	0	0	0
Line B									
	S_0^B	S_1^B	S_2^B	S_3^B	N	S_5^B	S_6^B	S_7^B	S_8^B
V_0^B	0	0	0	0	0	0	0	0	0
V_1^B	0	0	0	0	0	0	0	0	0
V_2^B	0	0	0	2	0	0	0	0	0
V_3^B	0	0	0	0	0	0	0	0	0
V_4^B	0	0	0	0	0	0	0	0	0
$\alpha_1 = 0, \alpha_2 = 1 \text{ and } \alpha_3 = 0$									

Table 4: Results of example 2 for scenario 2

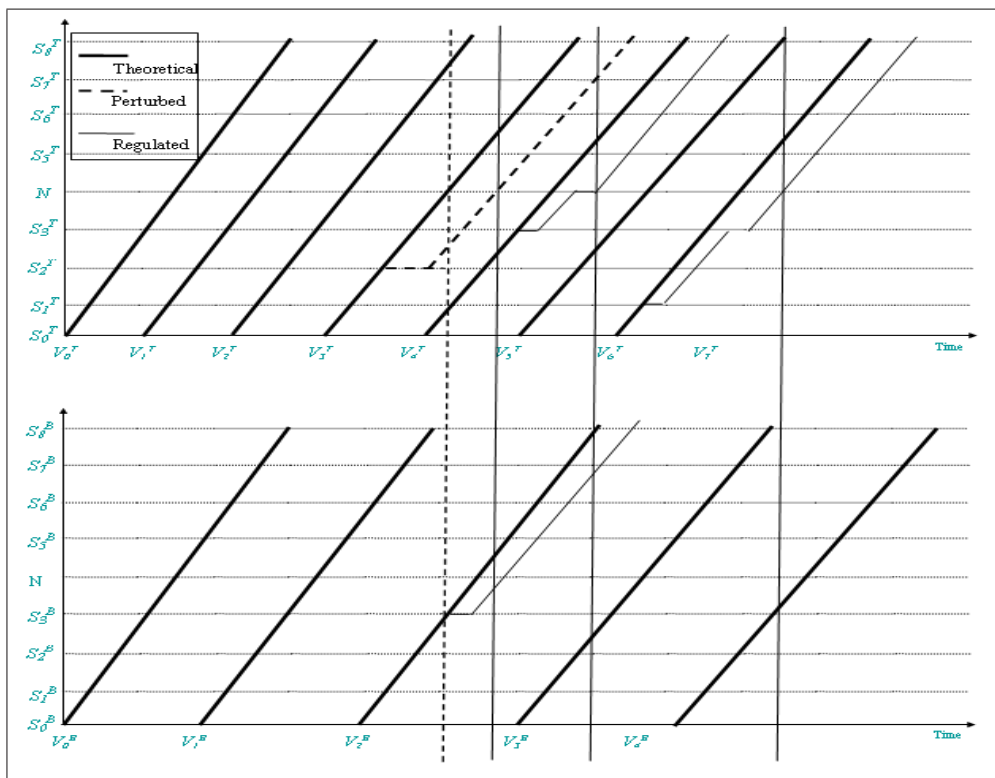


Figure 8: Vehicles schedules representation for the example 2 scenario 2

and we had $f=104$.

5.3 Comparison between both rescheduling ant colony algorithms

We applied both rescheduling algorithms, without local search and with dynamic local search, for real transport scenarios. We present in the table 5 the results of these simulations. We notice that the algorithm with dynamic local search is faster. Its execution time is always lower than the first algorithm, with same number of iteration. The ant colony algorithm with the dynamic local search space proposes an important improvement of solutions with regard to the algorithm without local search.

		Ant Colony Algorithm (ACA)		ACA with dynamic local search	
Scenario	Example	f	Execution time (ms)	f	Execution time (ms)
1	1	0	7390	0	7390
	2	160	7157	182	6922
	3	20.89	7047	20.89	6890
	4	132.78	7468	132.94	6860
2	1	192	10094	212	10000
	2	526.4	10150	533.99	8290
	3	394	10000	391.956	9370
3	1	362	28000	362	29000
	2	208	31000	232	22800
	3	104.88	28930	104.88	28060
	4	114.39	28.31	115.23	26040
4	1	192	10500	192	7828
	2	290	10109	310	8578
	3	0	5000	0	5000
	4	74.8	8700	74.8	8672

Table 5: Results of the both rescheduling ant colony algorithms

For the found optima, we notice that it is also effective. In fact, the results of the algorithm with dynamic local search are better than the author 7 times on 15 examples. The local search allows us to win in execution times and in search space exploitation. In fact, it is easier and faster to look for optima in a smaller zone. This parameter time is very important for our real time problem of regulation. But also the idea of the dynamic dimension allows us more investigation than the idea of the classic local search.

6 Conclusion

The disturbance of a transport system affects, first of all, the vehicle schedules. In this article we presented an ant colony algorithm for the time-based regulation of a multimodal transport network, in real-time. The results of this algorithm applied to real scenarios of transportation system existing in Lille, showed the efficiency of our approach. The execution time is also important. Indeed our objective consists in proposing quickly a solution before the propagation of the disturbance.

For a set of five stops, for example, for every vehicle there are $4^4 = 254$ possible solutions. So it is a complex problem. And we also noticed problems of convergence of our algorithm because of the important dimension of the research space. The idea of the dynamic local search allowed us to win in the execution times but also the improvement of the solutions without decreasing the search space exploration and exploitation.

References

- [1] D. Huisman, R. Freling, and A. P. M. Wagelmans, "A dynamic approach to vehicle scheduling," *Econometric Inst., Erasmus University, Rotterdam, The Netherlands, Rep. EI2001-17*, 2001. begin comment
- [2] S. Maouche, H. Laichour, S. Hayat, "amélioration de la qualité de correspondances dans les réseaux de transport", rapport final GRRT, avril 2001.
- [3] P. Borne, B. Fayeche, S. Hammadi and S. Maouche, "Decision Support System for Urban transportation networks", *IEEE SMC Part C: Applications and Reviews, Special Issue on Decision Technologies in honour of Prof Madan Singh, Vol.33, No.1*, pp.67-77, 2003.
- [4] A. Soulhi, "Contribution de l'intelligence artificielle à l'aide à la décision dans la gestion des systèmes de transport urbain". Thèse de doctorat, université des sciences et technologies de Lille, France, 2000.
- [5] H. Laichour, "Modélisation multi-agent et aide à la décision : Application à la régulation des correspondances dans les réseaux de transport urbain". Thèse de doctorat, université des sciences et technologies de Lille, France, 2002.
- [6] B. Fayeche, "Régulation des réseaux de transport multimodal : systèmes multi-agent et algorithmes évolutionnistes", Thèse de doctorat, université des sciences et technologies de Lille, France, 2003.
- [7] J. D. Moss and C. G. Johnson, "An ant colony algorithm for multiple sequence alignment in bioinformatics", In David W. Pearson, Nigel C. Steele, and Rudolf F. Albrecht, editors, *Artificial Neural Networks and Genetic Algorithms*, pages 182-186. Springer, April 2003.
- [8] M. Dorigo, "Optimization, Learning and Natural Algorithms". Ph.D.Thesis, Politecnico di Milano, Italy, in Italian, 1992.
- [9] M. Dorigo and L. M. Gambardella, "Ant Colonies for the Traveling Salesman Problem". *BioSystems*, 43:73-81. Also Technical Report TR/IRIDIA/1996-3, IRIDIA, Université Libre de Bruxelles, 1997.
- [10] N. Monmarché, "Algorithme de fourmis artificielles : application à la classification et à l'optimisation", Thèse à l'université de François Rabelais Tour, 2000.
- [11] C. Gagné and W. L. Price, "Optimisation par colonie de fourmis pour un problème d'ordonnancement industriel avec temps de réglages dépendants de la séquence". 3e Conférence Francophone de MOdélisation et SIMulation MOSIM01, Troyes (France), 2001.
- [12] P. Lacomme, C. Prins, A. Tanguy, "Optimisation par colonies de fourmis pour les tournées sur arcs". 4e Conférence Francophone de MOdélisation et SIMulation MOSIM03, Toulouse (France), 2003.
- [13] I. Alaya, C. Solnon and K. Ghédira, "Algorithme fourmi avec différentes stratégies phéromonales pour le sac à dos multidimensionnel", MHOSI'05, Hammamet, Tunisie, 2005.
- [14] M. Dorigo, V. Maniezzo, and A. Colorni. The ant system: Optimization by a colony of cooperating agents. *IEEE Transactions on Systems, Man and Cybernetics, Part B*, 26(1):2941, 1996.
- [15] T. Stutzle and H. Hoos. MAX-MIN Ant system and local search for combinatorial optimization problems. In S. Vos, S. Martello, I.H. Osman, and C. Roucairol, editors, *Meta-Heuristics: Advances and Trends in Local Search Paradigms for Optimization*, pages 137-154. Kluwer, Boston, 1998.

- [16] B. Bullnheimer, R. F. Hartl, and C. Strauss. "A new rank-based version of the ant system: a computational study". Technical Report POM-03/97, Institute of Management Science, University of Vienna, Accepted for publication in the Central European Journal for Operations Research and Economics, 1997.
- [17] P. Lacomme, C. Prins and W. Ramdane-Chérif "Competitive genetic algorithms for the Capacitated Arc Routing Problem and its extensions", in E.J.W. Boers and al. (ed.), Applications of evolutionary computing, pp. 473-483, Lecture Notes in Computer Science 2037, Springer, 2001.

acknowledgement:

the authors want to acknowledge the support of the EU thought the FEDER grant # OBJ2-2005/3-4.1-253PRESRGE-7820

Salah ZIDI, Salah MAOUCHE and Slim HAMMADI
Université des Sciences et Technologies de Lille and Ecole centrale de Lille
UFR I.E.E.A.
Bâtiment P2, Bureau 308 UFR I.E.E.A. Cité Scientifique 59655 Villeneuve d'Ascq Cedex France
E-mail: salah.zidi@ed.univ-lille1.fr, salah.maouche@univ-lille1.fr, slim.hammadi@ec-lille.fr

Received: November 11, 2006

Generic Modeling and Configuration Management in Product Lifecycle Management

Souheil Zina, Muriel Lombard, Luc Lossent, Charles Henriot

Abstract: The PLM (Product Lifecycle Management) is often defined as a set of functions and procedures which allows one to manage and to exploit the data defining at the same time the products and the processes implemented for their developments. However, the installation of a PLM solution remains a difficult exercise taking into account the complexity and the diversity of the customer requirements as well as the transverse utilization of this solution in all the company's' functions. The issues faced by both editors and integrators of PLM applications arise from the specific aspect of customers' projects, even though most functional needs are often generic.

In this paper we are focused on product modeling in PLM applications, more particularly on configuration management that traces product evolutions throughout its life-cycle. We will insist on the links between the configuration needs and the multi-view approach models and we release problems related to PLM applications deployment. Our work concerns the PLM generic solutions based on the concept of generic models. This generic model takes into account the configurations specification associated to the managed product and can be extended to cover specific needs.

Keywords: PLM, Configuration management, Generic modeling.

1 Introduction

Monitoring the technical information is one of the main preoccupation of the companies. Indeed, the increasingly constraining regulations and the higher competition level require being more rigorous and reactive to the customers' requests. The product quality improvement and the reduction costs cycles require applying technical data management rules and means.

The PLM (Product Lifecycle Management) appeared to answer the need of managing growing volumes of data in more and more complex environments. The PLM covers product life cycle integrality, without stopping itself at the design stages; it extends today to a wide scope of fields such as the Aerospace-Defense, Food, Drugs, Public Sector, Engineering, Manufacturing, etc. Product term thus indicates diverse entities in very varied trades.

The product life cycle management by a PLM solution allows including, not only all the necessary elements to ensure its traceability, like modeling, document management, numerical analysis, know-how capitalization, etc. but all the information system components making it possible to ensure the product monitoring from its manufacture to its marketing until its disappearance or likely its recycling.

In PLM applications, the technical data are organized within configurations. The configuration management is used to manage products complexity and knowledge diversity resulting from various business cases in the company. Indeed, the growing number of PLM applications users, the technical data volume and the various evolutions associated to these data require:

- controlling and checking the exchanged technical data consistency, unicity and safety,
- taking into account data evolutions and all their effects on the product and its components.

This is why the configuration management is a fundamental component in PLM applications, making it possible to control and manage complexity related to the data.

In the literature, several researches treat various types of problems around the PLM. This work is especially interested in the problems related to the data exchange and sharing [32, 26], the process management problems [19, 12, 33] and the product configuration management problems [20, 21, 18, 4].

In this paper, we are centered on technical data management and particularly on configuration management. In the first part of this document, we present problems related to the configurations modeling and a treatment example on given configurations. In the second part, we will show why the PLM solution deployment in a company remains a difficult exercise with the showing off of first problems.

The study carried out at LASCOM¹ consisted, starting from existing PLM applications, to set up a step of reverse engineering which made it possible to formalize the concepts used in PLM applications within a UML meta-model. This fundamental stage made it possible to validate the handled concepts at the conceptual level, then to underline the advantages of working on this modeling level to capitalization.

2 The product modeling in PLM applications

A technical object is thus a business object on which data management requirements are expressed in regard to the management and the handling of complex objects. The technical data concerns the design, the manufacture, the maintenance, the recycling and the marketing [3]. The definition of various business or technical objects and the links between them strongly depends on the company needs, organization and working methods.

The diversity of PLM applications (diversity related to the customer's specificities), the data increasing complexity and the need for evolving and flexible systems (due to the evolution of the needs as time goes by) implies that there is not an universal PLM application model being able to meet all the customers conflicting needs.

In the literature several research tasks are interested in product modeling with different approaches and technologies: use RDF (Resource Description Framework) [17], Topic Maps [16], or the oriented-object approaches [9] which aim to model and implement PDM (Product Data Management) systems using UML (Unified Modeling Language).

2.1 Configuration Management in PLM applications

Research works are interested in methods and tools development for managing the product configuration; they deal especially with generic product modeling. In the literature, several methods, based on artificial intelligence techniques, propose solutions to solve the products configuration problems [29]. These methods are based on rules and constraints [1, 31, 10].

The product configuration is based on a configuration model (often called product generic structure); the model describes the components (called also configuration elements or objects members of a configuration) that can be included in the product configuration. The configuration model also includes the combination rules between these components.

Various tools, called configurators (e.g. EngCon [14], WeCoTin [2]), make it possible to obtain a precise product description, which satisfies the needs and which is validated by the compliance with the rules of constraints defined in the configuration model. These tools can be integrated in PLM applications to

¹LASCOM (www.lascom.com) is an editor of life cycle management solutions concerning company product and processes.

contribute to configure the product.

In our work we are centered particularly on the configuration management. Like configuration tools, the configuration management tools are also based on product models making it possible to formalize technical objects, links and constraints which express managed and traced needs. Indeed, the configuration management is a discipline of management which consists in applying technical and administrative rules to the development, the production and maintenance, in all configuration article life cycle. It consists in managing the technical description of a system (and its different components), like managing the whole of the modifications made during the system evolution.

The configuration management finds out an interest when it concerns a product management that have a lot of variants and a long lifecycles or unit complex products like the production system itself or special machines [22]. Figure 1 presents a configuration example of a production site composition modeled in a PLM application. This configuration follow the evolution of the productions lines and their adaptability to the product.

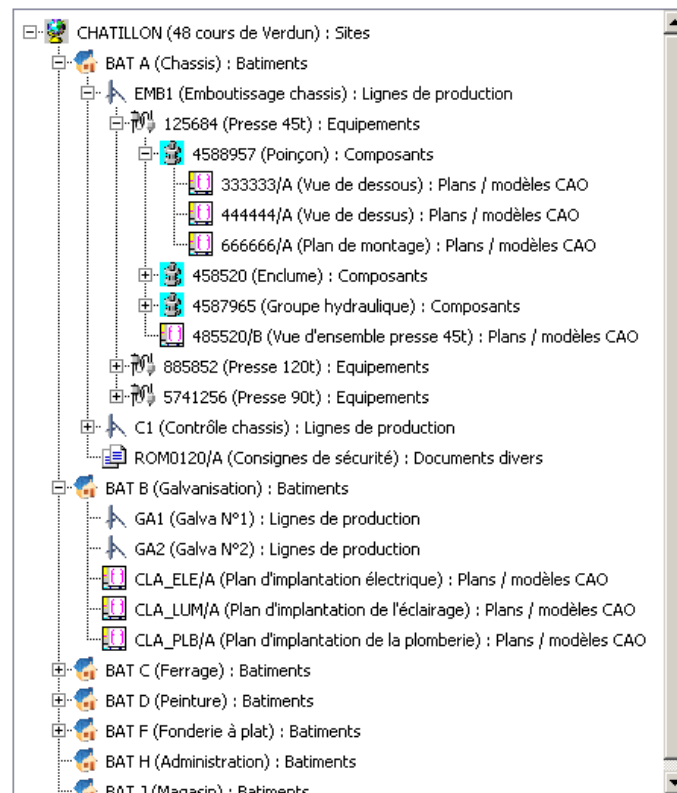


Figure 1: Example of a production site configuration.

The configuration management consists in controlling information of product structure, especially its decomposition in elementary subsets, parts and addition to the whole of this information, functional and physics characteristics. The standard [15] presents recommendations for using configuration management in industry. It provides the detailed process, organization and procedures of management. According to this standard, the configuration management is an integral part of the PLM; it provides a clear vision of the configuration state, associated to products or projects, as well as theirs evolutions by guaranteeing a total traceability.

Configuration management tools integrate functions and mechanisms allowing audit and control of all actions carried out on the product configuration.

2.2 Product multi-point of view modeling

The concepts of view and point of view were studied in several fields related to the data processing: databases, analyzes and design, programming languages, etc. In the literature several research tasks integrated the concepts of view and point of view in products modeling [24, 23, 13, 25, 28], these views are generally used to express different trades' needs on the product. Figure 2 presents an example of different business views around a product.

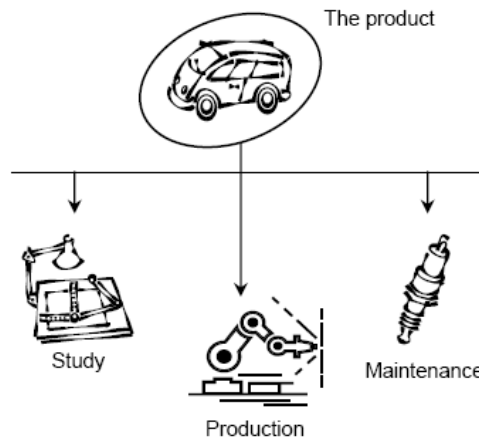


Figure 2: Various business views associated with a product.

The notion of point of view, classically used in the literature, has for main goal the description of a complex entity having several facets. The points of view make it possible to structure information starting from various criteria related with trade or product. This make it more representative and understandable and so easier to exploit. Each actor of the company handles particular view of the product that corresponds to his specific needs: functional view, technical view, industrial view, etc. There are two principal approaches which were used to take into account the actors points of view in the product model: Multi-view and Multi-model approaches.

The multi-view approach is based on the development of a single model starting from different views. This unique model is accessible according to several points of view. The main advantage of the use of a single model is that modifications made on a sub-model are reflected in the other sub-models. Consequently, the problems of inconsistency due to the division of the data between the partial models are avoided [24, 23]. This approach is very much used in works to product representation in CAD (Computer-Aided Design) systems. Research of Million [23] relates to the problem of designing technical information systems in an industrial multi-actors context in order to visualize information according to various views. The suggested method, called VIM (Viewpoints Information Modeling), makes it possible to build up, by successive adjustments, a total data model starting from an initial model centered on the technical object according to the points of view considered.

The principal interest of the multi-view approach lies in the fact that there is a unique model to manage, which facilitates the exchanges management and information sharing. However, it leads to a static product representation because the models handled by the various actors are fixed and do not vary at the same time as the product representation [8].

The multi-model approach consists in creating a model associated with each actor's view on the

product. Thus, there as exist many models as of different points of view on the product. Each model contains the technical objects and the relations which correspond to the given point of view. The management of the relations between these various models imposes using a whole of coherence rules which must apply to the models whole.

The Multi-models approach makes possible to structure the data following specific models to each point of view on the product. These separated models can evolve independently. However, coherence maintenance and information sharing between these models are much more difficult to ensure. The problem of coherence is attenuated by the use of rules of coherence, but their identification and their formalization remain difficult.

2.3 Configuration models and data processing

To be coherent with the different actors needs on the product, the configuration models must take into account these concepts of view and points of view associated to the product. According to the application needs, Advitium™, software package developed by the LASCOS company, define several types of configuration for a product (a given technical object). We define, for example, design configuration, documentary configuration, configuration carried out according to the stages reached in the project, etc. These configuration types correspond to different points of view on the product.

Each configuration is based on its own model and can evolve independently of the other types of configuration associated with the product. These configurations structure the data necessary to the product definition. Thus, each actor will gather, treat on a hierarchical basis and complete the technical objects according to his own needs. It is for this purpose that various structures of the product are managed. Each one corresponds to a particular configuration type.

We defined the concept of “context” related to the configuration elements in order to take into account the specific use of context data. The application of a context allows defining contextual views on the configuration [34].

Starting from existing PLM applications, the study carried out at LASCOS consisted in setting a step of reverse engineering (step 1) which made it possible to formalize the concepts (step 2 & 3) used in Advitium™ within an UML meta-model [27] (this meta-model is not presented in this paper). The employed methodology is illustrated by figure 3, the PLM applications deployment (step 4 & 5) is described by figure 7 section 3.1.

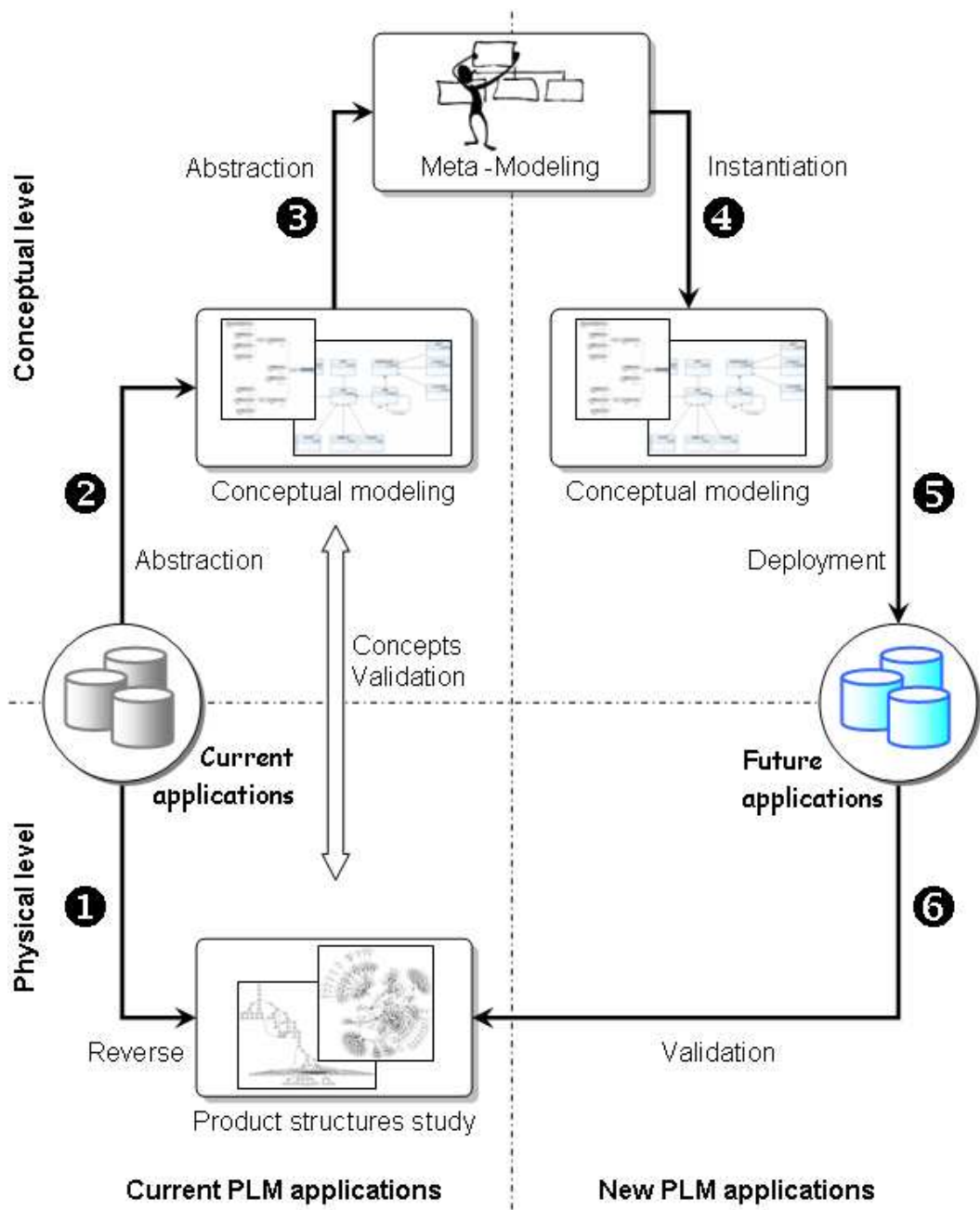


Figure 3: The employed methodology.

We developed tools for PLM applications retro-modeling, these tools allow formalizing configuration links between various technical objects classes. Our problematic is located in the formalization of the technical objects and links existing between them to answer:

- a technical data presentation matter to user,
- optimization of existing links in data base considering semantic studies produced according to customers requirements,
- easy access to configuration data and an optimization of the treatments on the configuration elements.

Our tool allows, from Advitium™ relational databases, to generate an XSD (Xml Schema Definition) of configurations definition. Figure 4 represents the hierarchical structure of classes in an example of a technical object (OT01_SITE) configuration model. An example of this class instance is given by figure 1.

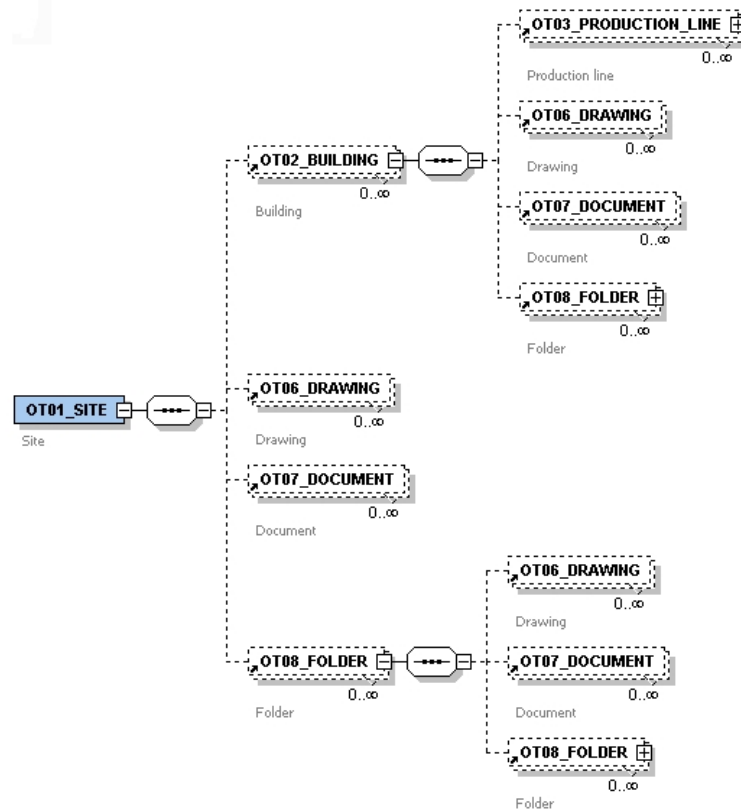


Figure 4: Example of configuration XML Schema.

In this model, configuration elements (Buildings, Drawings, Documents, Folders, etc.) are linked between them and organized to form configurations.

Technical objects can be related for various reasons: to express a composition link, to make a specialization, membership, etc. Links between the technical objects can be *static* (specific to a technical object instance) or *dynamic* (evolve with the technique objects versions) [4]. Majority of configuration models are recursive. It is noted, in figure 4, that the class “Folder” is re-used at various places in the hierarchy. This led, at the physical level, to infinite hierarchical structures. Our tool, associated with Graphviz [11], allows the visualization of configuration links graph of an existing PLM application. This representation informs us about the configuration structure and characteristics (depth, degree of objects re-uses, etc.).

Figure 5 presents the graph of product study configuration. We noted that the whole of the technical objects which constitute the product structure can be represented using a DAG (Directed Acyclic Graph). Each graph consists of nodes set (technical objects); these nodes are connected by links. Links have properties (link type, beginning and expired dates, etc.) allowing to describe more precisely relationships among the objects and authorizing, thus, the configuration traceability evolutions.

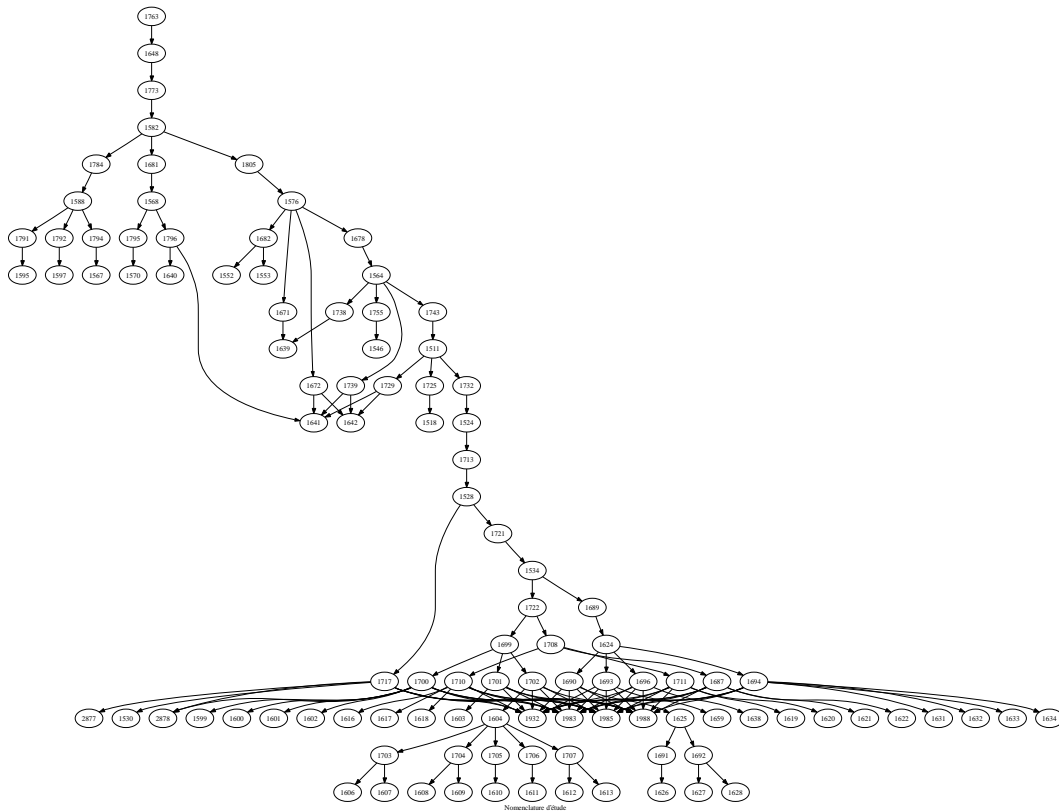


Figure 5: Example of study configuration graph in existing PLM applications.

The nodes can contain additional informations (order, descriptions, etc.), which lead the need for defining an entity node as presented at figure 6.

In order to implement applications according to customer requirements, this model includes a set of basic concepts (figure 6.a) independent of any applicability use (e.g. Part, Configuration, User, Group, etc.). These concepts can be specialized to complet the model according to application needs (figure 6.b). The derivation of this conceptual model gives a part of the physical model (relational model) currently implemented in the Advitium™ software package.

Data treatments related to the configurations can be inspired from techniques and methods resulting from the graphs theories. Indeed, in the configurations handling and management, certain basic user's functions are commonly used:

- Search, in a given technical object configuration, the whole of descendants of this object (to obtain the configuration elements).
- Search, in a given technical object configuration, the whole of the ascending of this object (to obtain the employment cases).
- Make search with criteria related on technical objects and their links properties (e.g. validity dates). In certain research, the criteria on links properties must be checked for the whole links constitute the way between the starting and arrival technical object.

In order to improve application performances related to configurations management (in particular search and navigation functions in configurations), we studied certain technical solutions which aim im-

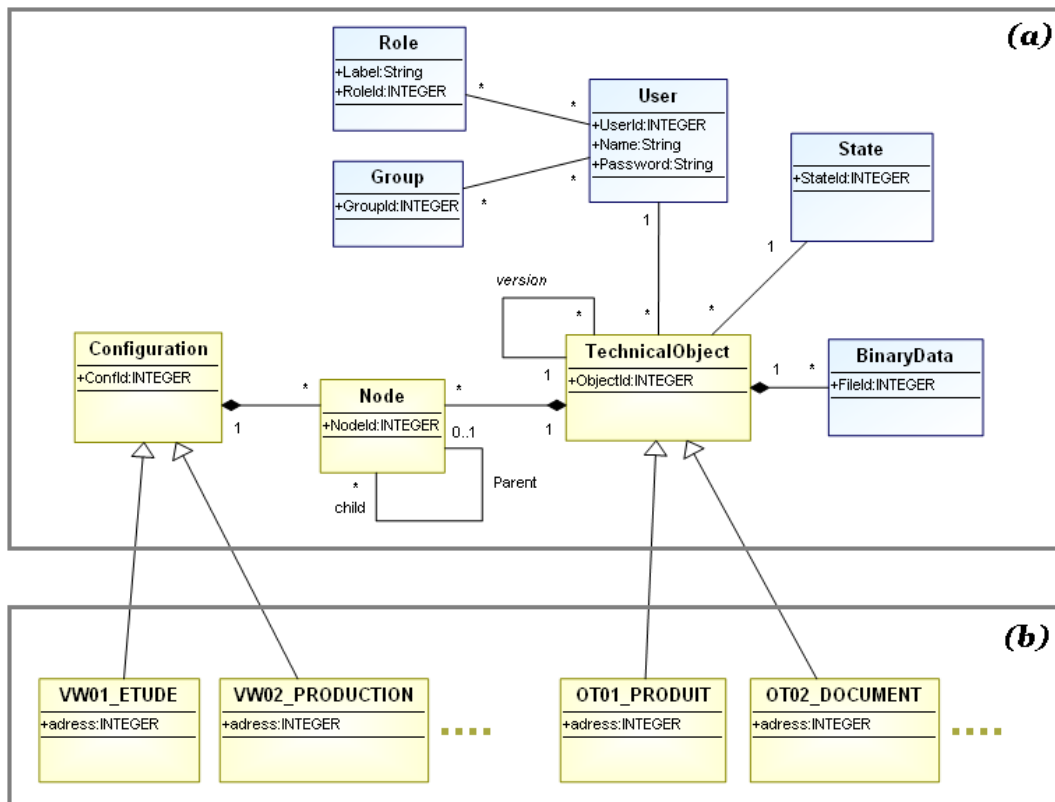


Figure 6: A part of generic model.

plementing hierarchical structures in relational databases. Among these solutions, we quote the “Nested Sets” method [5] (well adapted to handle the trees structures in the relational databases). Other research tasks are interested in the resolution of this problems type which consists in managing hierarchical data structures in relational databases [7, 30].

3 The reference model construction

PLM applications are based on complex and evolving product structures. The issues faced by both editors and integrators arise from the specific aspect of customers’ projects. As company’s needs are often specific, a PLM solution implementation requires heavy investments mainly regarding development aspects. These developments require huge implementation timetables and massive resources. One explanation lays on the fact that developments are very specific, and stress applied by PLM solution integrators on physical aspect rather than on conceptual aspect.

However, the consideration of the needs at the conceptual level, by PLM applications editors, permit to capitalize knowledge related to their products engineering and to rationalize the design and development teams working methods. Indeed, the knowledge capitalization helps to preserve, to share and above all to re-use know-hows generated through customers’ projects. This re-use thus allows:

- offering a better times control of engineering and a more flexible software offer,
- limiting PLM applications maintenance costs,
- facilitating the evolution PLM applications and allowing a greater users autonomy.

3.1 The generic models

So as to capitalize, it is recommended to study a set of reference models by sector or trade, in order to have a base of standard models or generic models. In fact, it is rather easier to particularize a model dedicated to a sector of activity than to reinvent it each time.

Thereby, we reveal two levels of trade:

- **Generic level:** in this level a person is in charge of creating generic models, by studying certain number of similar cases already encountered and modeled in reference models. These models can be enriched, if necessary, with generic specificities even if these specificities are not used till now but they are useful regarding the preceding businesses.
- **Particular level:** in this level a person is particularizing this generic level suited to trade to obtain the particular desired model. This model is particularized according to the specification elements. Thus, this person will have to particularize a partially defined model existing, and will have only to complete this initial model so as to provide the model to be implemented in the company, consequently making a gain of time.

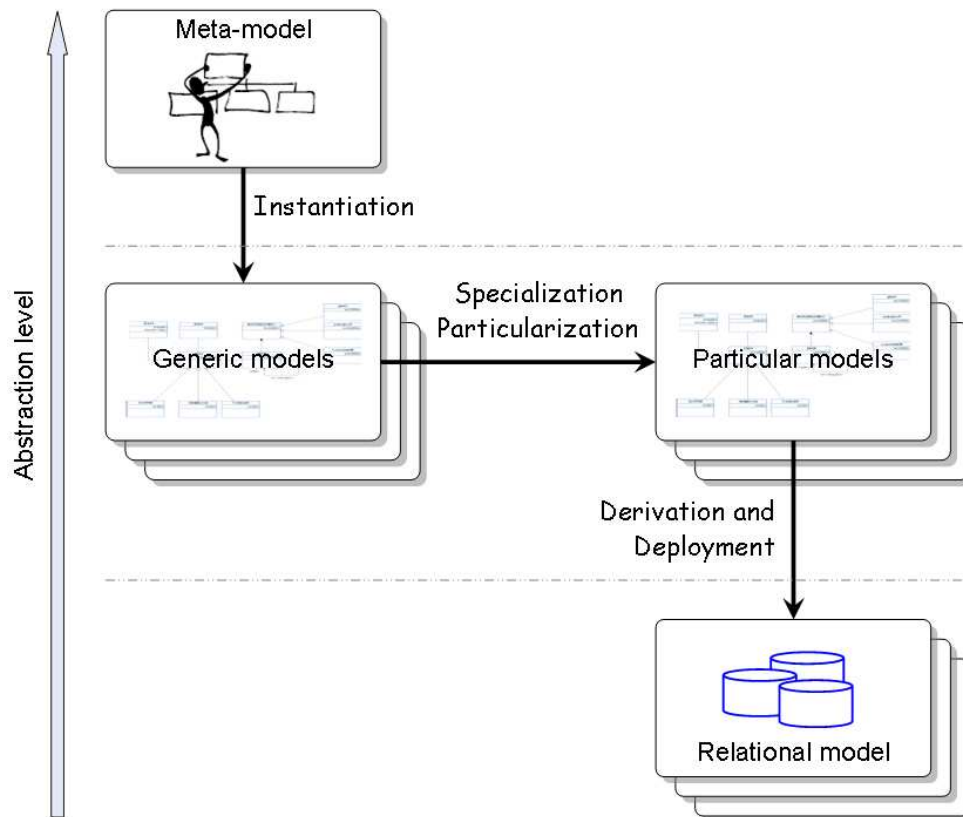


Figure 7: Process of model instantiation.

Figure 7 represents the interest that can be disposed by generic models per activity sector to simplify the work of PLM solutions integrators or developer.

3.2 Functions deployment

It has already been showed, compared to database modeling approaches, that a good data organization (coherent models and adapted to the needs) allows to considerably simplify the treatments and

thus to improve the performances of the concerned applications. Indeed, a generic implementation is often too general when it is used in a specific situation; this generalization often causes an ineffective execution. To increase the performances, this implementation must be adapted in order to keep preserving only the necessary functionalities in a specific situation.

It is thus suitable to define and associate elementary functions to the generic models. These functions can be combined and organized to meet the specific needs expressed during models particularization. Otherwise, for better PLM application appropriation by users, a “trade translation” of the functions is also necessary.

4 Summary and Conclusions

The product life cycle management is a recent field, the perimeter of PLM applications is in constant evolution. This evolution implies that there is not a data model able to meet all the customer requirements.

Our work concerns the generic solutions of technical data management based on the concept of generic model. This generic model takes into account the configuration specification associated to technical objects.

Disposing of generic models by sector or by trade permits to facilitate the work of the PLM solutions integrators or developers. This work can be done through an audit to extract the modeling invariants. It is advisable to well determine the trade sectors. Thus, in the objective of the PLM tools appropriation by the users, this classification propose solutions practically ready-made for its deployment in term of modeling of the technical data. This dimension allows decreasing or eliminating the specific developments. In these models, the terminology thus is well taken into account, since particularized with a given industrial sector.

References

- [1] M. Aldanondo, H. Fargier, and M. Véron. *Configuration, configureurs et gestion de production*, Hermès Science, Traité IC2 Productique, pp.179-209, 2001.
- [2] T. Asikainen, T. Männistö, and T. Soininen. Using a Configurator for Modelling and Configuring Software Product Lines Based on Feature Models, *WSVMPD*, 2004.
- [3] A. Bernard. Modèles et approches pour la conception et la production intégrées. Productique, méthodes et outils, CPI'99, numéro spécial de la revue *JESA*, Vol.37, Issue 2-3, 2000.
- [4] T. W. Carnduff and J. S. Goonetillake, Configuration management in evolutionary engineering design using versioning and integrity constraints, *Advances in Engineering Software*, Vol.35, Issue 3-4, pp.161-177, 2004.
- [5] J. CELKO. *Joe Celko's Trees and Hierarchies in SQL for Smarties*. Morgan Kaufmann, 2004.
- [6] P.Y. Chao and T.D. Chen. Analysis of Assembly through Product Configuration, *Computers in Industry*, Vol.44, pp.189-203, 2001.
- [7] Y. Chen, *On the computation of recursion in relational databases*. In *Effective Databases For Text & Document Management*, S. A. Becker, Ed. Idea Group Publishing, Hershey, PA, pp.263-277, 2003.

-
- [8] I. El Khalkhali. *Système intégré pour la modélisation, l'échange et le partage des données de produits*. Institut National des Sciences Appliquées de Lyon, 2002.
- [9] B. Eynard, T. Gallet, P. Nowak, and L. Roucoules. UML based Specifications of PDM Product Structure and Workflow. *Computers in industry*, Vol.55, Issue 3, pp. 301-316, 2004.
- [10] H. Fargierh and L. Henocqueh. Configuration à base de contraintes. *Information Interaction Intelligence*, Actes des 2ième Assises nationales du GdR I3, pp.141-159.
- [11] AT&T Labs, 2005. Graphviz.
Available from: <http://www.research.att.com/sw/tools/graphviz/>.
- [12] D. Grigori, F. Casati, M. Castellanos, U. Dayal, M. Sayal, and M.-C. Shan. Business Process Intelligence, *Computers in Industry Journal*, special issue on workflow mining, Vol.53, Issue 3, pp.321-343, 2004.
- [13] Y. Harani. *Une approche multi-modèles pour la capitalisation des connaissances dans le domaine de la conception*. PhD thesis, Institut National Polytechnique de Grenoble, 1997.
- [14] O. Hollmann, T. Wagner and A. Günter. EngCon Ő A Flexible Domain-Independent Configuration Engine. *Workshop Configuration at ECAI-2000*, 2000.
- [15] ISO 10007:2003. Quality management systems Ő Guidelines for configuration management, 2003.
- [16] ISO/IEC 13250:2003. Information technology - SGML applications - Topic maps (2nd edition), 2003.
- [17] H-B. Jun, D. Kiritsis, and P. Xirouchakis. Product lifecycle information modeling with RDF, *International Conference on Product Lifecycle Management*, pp.44-54, 2005.
- [18] E. Kasper and J. Riis. Expected and Realized Costs and Benefits when Implementing Product Configuration Systems, *International Design Conference - Design 2004*, Dubrovnik, Croatia, 2004.
- [19] A K A de Medeiros, WMP van der Aalst, AJMM Weijters. workflow mining: current status and futur directions. *Coops/DOA/ADBASE*, LNCS 2888, pp.389-406, 2003.
- [20] T. Männistö, R. Sulonen. Evolution of Schema and Individuals of Configurable Products, in Proc. of ECDM'99 - *Workshop on Evolution and Change in Data Management*, Versailles, France, Springer Verlag, November 15-18, 1999.
- [21] T. Männistö. *A conceptual modelling approach to product families and their evolution*. PhD thesis, Helsinki University of Technology, 2000.
- [22] P. Martin, L. Lossent, L. Abt and F. Brassset. Conception de machines spéciales: méthodologie d'élaboration de cahier des charges. *Mécanique & Industries* Vol.5, pp.305-316, 2003.
- [23] O. Million, M. Lombard, G. Ris. Analysis and modeling of a technical information system: A modular approach. Proceedings of IDMMME'1998 *Integrated Design and Manufacturing in Mechanical Engineering*, UTC, Compiègne (France), Vol.4, pp.1245-1252, May 27-29, 1998.
- [24] M. Nassar. VUML: A Viewpoint oriented UML Extension. In the *18th IEEE International Conference on Automated Software Engineering (ASE'2003)*, Montreal, Canada, 2003.
- [25] F. Noël. A Dynamic multi-view product model to share the product behaviours among designers. *International Conference on Product Lifecycle Management*, pp.113-120, 2005.

- [26] P. Nowak, B. Rose, L. Saint-Marc, B. Eynard, L. Gzara, M. Lombard. Towards a design process model enabling the integration of product, process and organisation, *5th International Conference on Integrated Design and Manufacturing in Mechanical Engineering*, IDMME 2004, Bath (United Kingdom), April 5-7, 2004.
- [27] OMG. OMG Unified Modeling Language Specification v1.5: Revisions and recommendations, Version 1.5. Object Management Group Document formal/03-03-01, 2003.
- [28] A. Saucier, *Un modèle multi-vues du produit pour le développement et l'utilisation de systèmes d'aide à la conception en ingénierie mécanique*, Thèse Ecole Normale Supérieure de Cachan, France, 1997.
- [29] T. Soinenen, and M. Stumptner. Introduction to Special Issue on Configuration. Artificial Intelligence for Engineering Design, *Analysis and Manufacturing*, Vol.17, Issue 1-2, 2003.
- [30] S. Subbarayan and H.R. Andersen. Linear Functions for Interactive Configuration Using Join Matching and CSP Tree Decomposition. *IJCAI-2005 Configuration Workshop*, 2005.
- [31] M. Véron. *Modélisation et résolution du problème de configuration industrielle: utilisation des techniques de satisfaction de contraintes*. PhD thesis, Institut National Polytechnique, Tarbes, November 2001.
- [32] L. Yesilbas, B. Rose, M. Lombard. Specification of a repository to support collaborative knowledge exchanges in IPPOP project. *Computers in Industry*, Vol.57, Issue 8-9, pp.690-710.
- [33] H. Zhuge : A process matching approach for flexible workflow process reuse, *Information and software technology*, Vol.44, pp.445-450, 2002.
- [34] S. Zina, M. Lombard, L. Lossent. Integration of contextual views in configuration management for PLM applications. *9th IFAC Symposium on Automated Systems Based on Human Skill And Knowledge*, 2006.

Souheil ZINA ^{1,2}, Muriel LOMBARD ¹, Luc LOSSENT ¹, Charles HENRIOT ²
E-mail: s.zina@lascom.com

¹ Centre de Recherche en Automatique de Nancy - UMR 7039
Université Henri Poincaré, Nancy I
Faculté des Sciences - B.P. 239
54 506 Vandoeuvre-lès-Nancy, France

² LASCOM
Burospace - Antélie 4, Route de Gisy
91 571 Bièvres Cedex, France

Received: November 11, 2006

Author index

Benrejeb M., 9, 61
Borne P., 7, 9, 73
Bouzaouache H., 21
Braiek N.B., 21
Béarée R., 35

Colas F., 35
Craye E., 53, 61

Dangoumau N., 53
Dieulot J.Y., 35
Donnelly D., 45
Dutilleul S.C., 61

Hamani N., 53
Hammadi S., 110
Henriot C., 126

Jerbi N., 61

Lescher F., 73
Li P., 85
Li Q., 93
Li S., 85
Lombard M., 126
Lossent L., 126
Lu Y., 85

Maouche S., 110

Sakly A., 9
Soudani D., 9
Sun F.C., 93

Thimoumi I., 35

Wei H., 85

Xu F., 101

Zeng W., 101
Zhao J.Y., 73
Zheng G., 101
Zidi S., 110
Zina S., 126

Description

International Journal of Computers, Communications & Control (IJCCC) is published from 2006 and has 4 issues per year, edited by CCC Publications, powered by Agora University Editing House, Oradea, ROMANIA.

Every issue is published in online format (ISSN 1841-9844) and print format (ISSN 1841-9836). We offer free online access to the full content of the journal (<http://journal.univagora.ro>). The printed version of the journal should be ordered, by subscription, and will be delivered by regular mail.

IJCCC is directed to the international communities of scientific researchers from the universities, research units and industry.

IJCCC publishes original and recent scientific contributions in the following fields:

- Computing & Computational Mathematics,
- Information Technology & Communications,
- Computer-based Control

To differentiate from other similar journals, the editorial policy of **IJCCC** encourages especially the publishing of scientific papers that focus on the convergence of the 3 “C” (Computing, Communication, Control).

The articles submitted to **IJCCC** must be original and previously unpublished in other journals. The submissions will be revised independently by two reviewers.

IJCCC also publishes:

- papers dedicated to the works and life of some remarkable personalities;
- reviews of some recent important published books.

Also, **IJCCC** will publish as supplementary issues the proceedings of some international conferences or symposiums on Computers, Communications and Control, scientific events that have reviewers and program committee.

The authors are kindly asked to observe the rules for typesetting and submitting described in *Instructions for Authors*.

There are no fees for processing and publishing articles. The authors of the published articles will receive a hard copy of the journal.

Instructions for authors

Papers submitted to the International Journal of Computers, Communications & Control must be prepared using a LaTeX typesetting system. A template for preparing the papers is available on the journal website <http://journal.univagora.ro>. In the template file you will find instructions that will help you prepare the source file. Please, read carefully those instructions.

Any graphics or pictures must be saved in Encapsulated PostScript (.eps) format.

Papers must be submitted electronically to the following address: ccc@univagora.ro.

The papers must be written in English. The first page of the paper must contain title of the paper, name of author(s), an abstract of about 300 words and 3-5 keywords. The name, affiliation (institution and department), regular mailing address and email of the author(s) should be filled in at the end of the paper. Manuscripts must be accompanied by a signed copyright transfer form. The copyright transfer form is available on the journal website.

The publishing policy of IJCCC encourages particularly the publishing of scientific papers that are focused on the convergence of the 3 “C” (Computing, Communications, Control).

Topics of interest include, but are not limited to the following:

- Applications of the Information Systems
- Artificial Intelligence
- Automata and Formal Languages
- Collaborative Working Environments
- Computational Mathematics
- Cryptography and Security
- E-Activities
- Fuzzy Systems
- Informatics in Control
- Information Society - Knowledge Society
- Natural Computing
- Network Design & Internet Services
- Multimedia & Communications
- Parallel and Distributed Computing

Order

If you are interested in having a subscription to “Journal of Computers, Communications and Control”, please fill in and send us the order form below:

ORDER FORM		
I wish to receive a subscription to “Journal of Computers, Communications and Control”		
NAME AND SURNAME:		
Company:		
Number of subscription:	Price Euro	for issues yearly (4 number/year)
ADDRESS:		
City:		
Zip code:		
Country:		
Fax:		
Telephone:		
E-mail:		
Notes for Editors (optional)		

1. Standard Subscription Rates (2006)

- Individual: One Year (4 issues) 70 Euro
- Institutional: One Year (4 issues) 90 Euro

2. Single Issue Rates

- Individual: 20 Euro
- Institutional: 25 Euro

For payment subscription rates please use following data:

HOLDER: Fundatia AGORA, CUI: 12613360

BANK: EUROM BANK ORADEA

BANK ADDRESS: Piata Unirii nr. 2-4, Oradea, ROMANIA

IBAN ACCOUNT for EURO: RO02DAFB1041041A4767EU01

IBAN ACCOUNT for LEI/ RON: RO45DAFB1041041A4767RO01,

Mention, please, on the payment form that the fee is “for IJCCC”.

EDITORIAL ADDRESS:

CCC Publications

Piata Tineretului nr. 8

ORADEA, jud. BIHOR

ROMANIA

Zip Code 410526

Tel.: +40 259 427 398

Fax: +40 259 434 925

E-mail: ccc@univagora.ro, Website: www.journal.univagora.ro

Copyright Transfer Form

To The Publisher of the International Journal of Computers, Communications & Control

This form refers to the manuscript of the paper having the title and the authors as below:

The Title of Paper (hereinafter, "Paper"):

.....

The Author(s):

.....

.....

.....

.....

The undersigned Author(s) of the above mentioned Paper here by transfer any and all copyright-rights in and to The Paper to The Publisher. The Author(s) warrants that The Paper is based on their original work and that the undersigned has the power and authority to make and execute this assignment. It is the author's responsibility to obtain written permission to quote material that has been previously published in any form. The Publisher recognizes the retained rights noted below and grants to the above authors and employers for whom the work performed royalty-free permission to reuse their materials below. Authors may reuse all or portions of the above Paper in other works, excepting the publication of the paper in the same form. Authors may reproduce or authorize others to reproduce the above Paper for the Author's personal use or for internal company use, provided that the source and The Publisher copyright notice are mentioned, that the copies are not used in any way that implies The Publisher endorsement of a product or service of an employer, and that the copies are not offered for sale as such. Authors are permitted to grant third party requests for reprinting, republishing or other types of reuse. The Authors may make limited distribution of all or portions of the above Paper prior to publication if they inform The Publisher of the nature and extent of such limited distribution prior there to. Authors retain all proprietary rights in any process, procedure, or article of manufacture described in The Paper. This agreement becomes null and void if and only if the above paper is not accepted and published by The Publisher, or is withdrawn by the author(s) before acceptance by the Publisher.

Authorized Signature (or representative, for ALL AUTHORS):

.....

Signature of the Employer for whom work was done, if any:

Date:

Third Party(ies) Signature(s) (if necessary):